# ABSTRACT

Title of Thesis: THE CHARACTERISTICS AND IMPACTS OF IMPERVIOUSNESS FROM A GIS-BASED HYDROLOGICAL PERSPECTIVE

Sunghee Kim, Master of Science, 2005

Thesis Directed By: Associate Professor, Glenn E. Moglen,
Department of Civil and Environmental Engineering

With the concern that imperviousness can be quantified differently depending on data sources and methods, regression equations to translate between imperviousness estimates using land use and land cover were developed. In addition, this study examined how quantitatively different imperviousness estimates affect the prediction of hydrological response. The regressions between indicators of hydrological response and imperviousness-descriptors were evaluated by examining goodness-of-fit measures such as explained variance or relative standard errors.

The results show that imperviousness estimates using land use are better predictors of hydrological response than imperviousness estimates using land cover. Also, this study reveals that flow variability is more sensitive to spatially distributed models than lumped models, while thermal variability is equally responsive to both models. The findings from this study can be further examined from a policy perspective with regard to policies that are based on a threshold concept for imperviousness impacts on the ecological and hydrological system.

# THE CHARACTERISTICS AND IMPACTS OF IMPERVIOUSNESS

# FROM A GIS-BASED HYDROLOGICAL PERSPECTIVE

by

Sunghee Kim

Thesis submitted to the Faculty of the Graduate School of the
University of Maryland, College Park in partial fulfillment
Of the requirements for the degree of
Master of Science
2005

Advisory Committee:

Professor Glenn E. Moglen, Chair
Professor Kaye Brubaker
Professor Richard H. McCuen

***In the memory of my father-in-law***

## DEDICATION

**To my brave mother who is in her fight against a brain tumor**

## ACKNOWLEDGEMENTS

I would like to thank my advisor, Dr. Glenn Moglen for his guidance and constant encouragement. My gratitude goes to my committee members, Dr. Richard McCuen and Dr. Kaye Brubaker for their academic mentorship. The support provided by Dr. John Townshend and Paul Davis from the Global Land Cover Facility at the University of Maryland Institute for Advanced Computer Study (GLCF/UMICACS) is gratefully acknowledged. My special thanks go to my three children, Sangduk, Shinduk, and Jungduk. They have been my great source of joy and emotional support. My deepest appreciation goes to my husband, DJ for holding my hands through all of my rough times.

## TABLE OF CONTENTS

## LIST OF TABLES

## LIST OF FIGURES

# CHAPTER ONE

# INTRODUCTION

## 1.1 Background

### 1.1.1 Importance of imperviousness

The importance of imperviousness (hereafter IMP) on the environment has been recognized for many years (Klein, 1979; Schueler, 1994; US EPA, 1997; Paul and Meyer, 2001; Krause et al., 2004). These studies claim that IMP is an excellent indicator of land use/land cover change, since it can be easily recognized and monitored. According to the US EPA report (1997), increased IMP leads to increased runoff volumes and peak flows, while baseflow decreases. Due to its profound effects on hydrological response, IMP is an important predictor in rainfall-runoff modeling.

In addition, IMP is a key variable for water quality modeling, due to strong relationships between IMP and stream health. For instance, IMP has a direct effect on stream temperature (Vought et al., 1998). As IMP increases, sedimentation and pollutant loads also increase, which degrades water quality (Schueler, 1994). Many hydrological models have been developed such that IMP is a variable used in predicting the hydrological response due to land use/ land cover change.

As a planning and management tool, IMP has drawn much attention. It is relatively simple both to calculate and to monitor changes. Schueler (1994) described IMP as one of the few variables that could be explicitly quantified, managed, and controlled at each stage of land development. For this reason, researchers have claimed that IMP is an excellent tool in planning and regulatory applications (Schueler, 1994;

Arnold and Gibbons, 1996). Arnold and Gibbons (1996) suggested that IMP be considered in community /regional planning, neighborhood/site planning, and even regulation. The role of IMP will continue to grow as an environmental indicator, a predictor of the hydrological response, and as a planning tool.

### 1.1.2 Existence of threshold-imperviousness

As an environmental indicator, IMP has been shown to have a strong relationship with stream health. Numerous studies have suggested that the ecological system as well as the hydrological system undergoes negative impacts when IMP exceeds a certain threshold (Klein, 1979; Carlson and Arthur, 2000; Bird et al., 2002). Research outcomes are so consistent that land planners and decision-makers tend to implement IMP thresholds into their policies to limit land development and to protect water resources (Kauffman and Brant, 2000; Yeager and Swamikannu, 2001; O'Brien, 2005).

A challenge to integrating such threshold approaches is the sensitivity of IMP to measuring/estimating methods as well as data sources (Capiella and Brown, 2001; Bird et al., 2002; Brabec and et al., 2002; Dougherty et al., 2004). All measures/estimates of IMP present different values, depending on methods and data sources. Considering the role of IMP in the hydrological modeling, significant questions arise: how do IMP estimates from different data sources affect hydrological modeling and the prediction of hydrological response? Which measures are better for designing hydrological infrastructures? Is there a true threshold value of IMP that one can apply to anticipate certain levels of hydrological impacts?

In order to answer these questions, this study investigates the sensitivity of hydrological response to IMP estimates. IMP is quantified by two different approaches: (1) IMP based on coefficients assigned to unique land use categories; and (2) IMP based on satellite-derived land cover. The primary difference between these two approaches is the data sources: land use versus land cover. Throughout this study, the IMP estimated using land use is abbreviated as IMP-LU, while IMP-LC is the abbreviation for IMP derived from land cover. Although land use and land cover are fundamentally different, they are often mapped together and the confusion of their usages is still high. From a hydrological perspective, it is unclear whether land use and land cover are equally effective in predicting hydrological impacts.

### 1.1.3 Imperviousness from land use and land cover

Land use reflects human activities on the landscape. For instance, agricultural lands, forestry lands, or recreational lands are categorical types of land use. Land cover focuses on the land surface. Deciduous trees, wetlands, grass, or roads are examples of land cover. Land use requires additional spatial information such as boundaries of zoning districts or parcel sizes, while land cover can be determined by remotely observed landscape features.

Most often, land use and land cover do not have a 1-to-1 relationship. A single land use category may contain the multi-components from land cover categories or vice versa. For instance, the land use category of “open urban land” applies to golf courses, which typically contain several land cover categories such as evergreen trees, grass, and/or water. Figure 1-1 is a view of the University of Maryland. The left side of the

State Highway 193 is a golf course, while the main campus is located on the right side of the highway. Figures 1-2 (a) and (b) are land use and land cover for the same spatial extent as the area shown in Figure 1-1, respectively. According to Figure 1-2, land use indicates that people use the right side of the highway as an institution, while land cover presents the nature of the surface such as deciduous trees, evergreen trees, developed open space and others.


Figure 1-1. A view of the University of Maryland from about 5058 ft above, using Google Earth. A golf course appears on the left side and main campus is located on the right side.

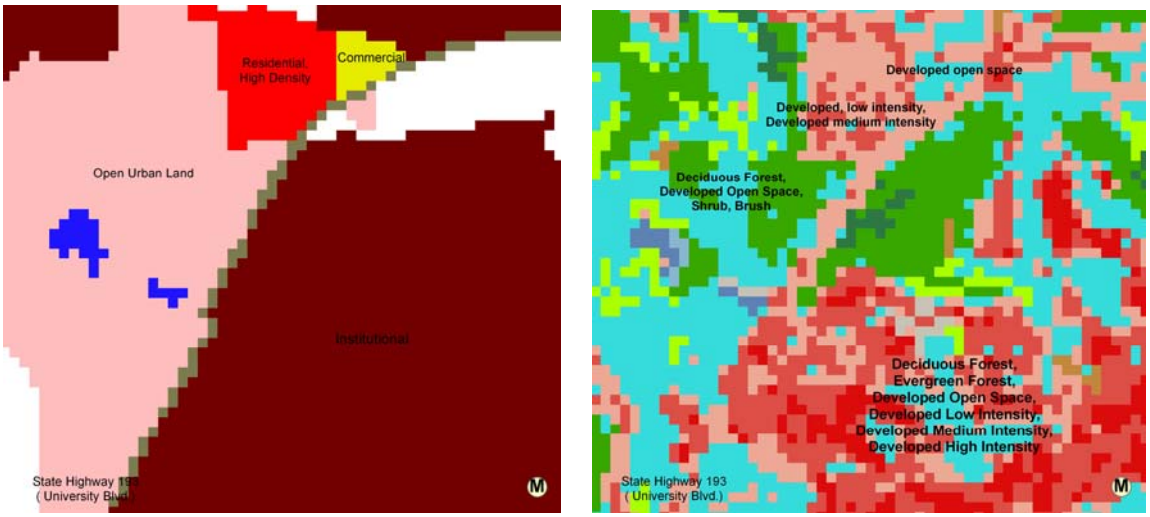


(a) (b)

Figure 1-2. (a) Land use presentation of the area shown in Figure 1-1. Water appears in blue. Some land use categories are shown in white-color in order to simplify color-coded presentation in this figure. (b) Land cover presentation of the area shown in Figure 1-1.

Due to the difference of land use and land cover, IMP estimates using these data sources are quantified differently from each other as seen in Figure 1-3. However, these estimates are highly correlated, because of describing the same phenomenon. It is crucial for hydrologists and engineers to understand that IMP as a predictor in a hydrological model should be obtained in the same way as the data with which the model has been calibrated. Due to either the lack of consistent data availability or poor documentations on the model development, the potential exists to misapply hydrological models simply by using inappropriate measures of IMP.

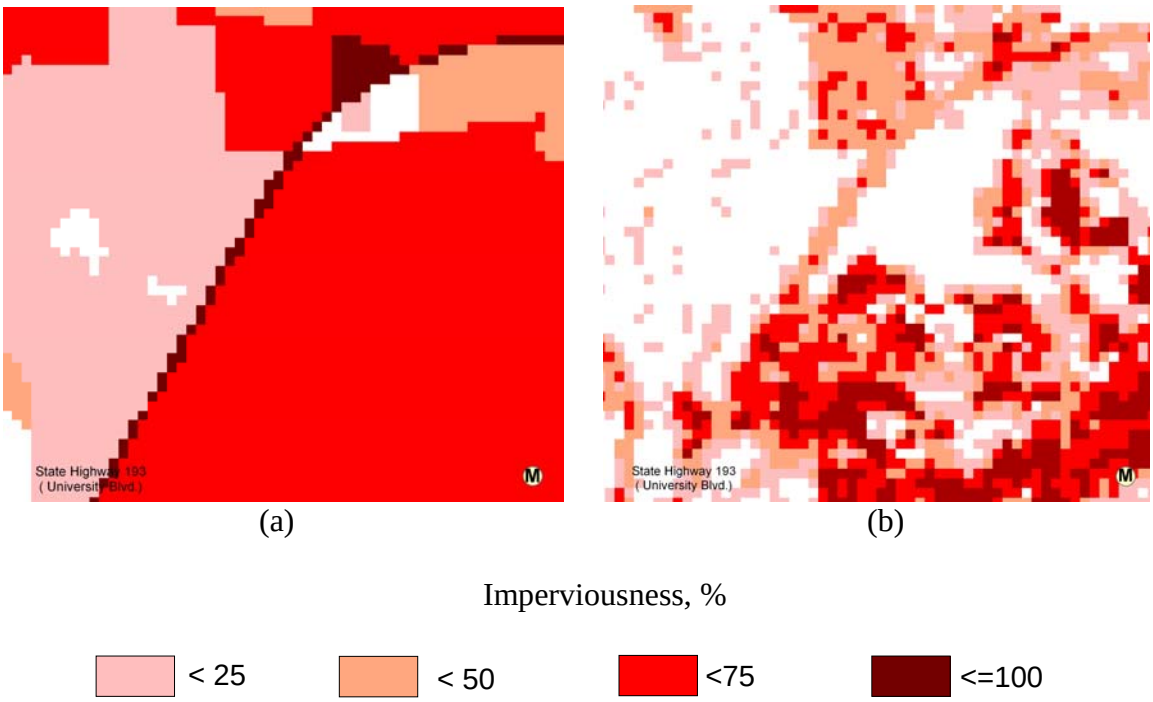


Figure 1-3. (a) IMP-LU: Imperviousness based on land use shown in Figure 1-2(a). (b) IMP-LC: Imperviousness based on land cover shown in Figure 1-2(b). IMP-LU tends to produce higher IMP than IMP-LC.

### 1.1.4 Spatially lumped and spatially distributed imperviousness

To predict the hydrological response due to IMP change, IMP is used as a variable in hydrological models that can be divided into two distinct categories: spatially lumped and spatially distributed. The spatially lumped model uses aggregate IMP, which is an averaged IMP over individual study basins. It does not take into account the spatial distribution of IMP within a given basin. On the other hand, the spatially distributed model accounts for the spatial variability within the basin. While spatially distributed models require extensive computations, they capture characteristics of landscape organization and hopefully translate them into more accurate predictions.

In this study, comparisons of lumped and spatially distributed hydrological models, using both IMP-LU and IMP-LC, will be performed. Also, the sensitivity of the

hydrological response to these models will be compared. Within the scope of this study, the hydrological response refers both to flow variability and to thermal variability.

### 1.2 Objectives

The goal of this study is to examine characteristics of IMP and its impact on hydrological response. To achieve the goal, specific objectives will be investigated:

1. The first objective is **to identify relations and to develop equations to translate between IMP using land use (IMP-LU) and IMP derived from land cover (IMP-LC)**.

   The differences in IMP estimated from land use and land cover will be examined, resulting in regression equations that allow for the transformation between IMP from one data source to its equivalent value using the other data source.

2. The second objective is to **determine whether IMP using land use (IMP-LU) or IMP derived from land cover (IMP-LC) is better at predicting hydrological response** in terms of flow variability and thermal variability.

   Goodness-of-fit measures for regression models using IMP-LU and IMP-LC will be compared to assess which data source serves as a more effective predictor of hydrological response.

3. The third objective is **to determine whether spatially lumped or spatially distributed IMP is a better predictor of hydrological response** in terms of flow variability and thermal variability.

   This objective will determine if hydrological response are more sensitive to simple aggregate IMP or to spatial distribution of IMP.

### 1.3 Summary

This study will provide tools for converting IMP from one data source to the other. Data sources, IMP-LU or IMP-LC will be identified as an effective predictor of hydrological response. Also, it will be decided whether the spatial distribution of IMP is a better predictor than an average IMP. The value of these accomplishments is twofold. This study develops a good understanding of the difference between data sources, land use and land cover, and the impact of IMP from the hydrological perspective. Also, land use planners and policy makers can use the results of this study to guide defining and implementing IMP thresholds into their policies.

# CHAPTER TWO

# LITERATURE REVIEW

## 2.1 Overview

This chapter is to discuss the work of others related to IMP and the hydrological response. The chapter consists of four sections. The first section presents others' work pertaining to the impact of IMP on the hydrological and ecological system. The second section discusses studies on indicators of hydrological response due to land use change. In the third section, various methods for IMP measurement are compared. The final section is for the studies on hydrological methods to evaluate the impact of IMP.

## 2.2 Impact of imperviousness on hydrological and ecological systems

It has been well documented that the impact of IMP is multi-dimensional. It affects not only stream hydrology but also stream morphology (Booth, 1990 for channel stability; U.S. EPA, 1997 for channel widening; Scholz and Booth, 2001 for bank erosion; Awasthi et al., 2002 for soil erosion). Furthermore, it has an impact on stream water quality (Old et al., 2003 for sediment transport; Galli, 1990 cited in Schueler, 1994; James and Verspagen, 1996 cited in Van Buren et al., 2000 for thermal impacts; Schueler, 1994 for nutrient loads and bacterial contamination), and stream ecology (Klein, 1979 for diversity of aquatic insects and fish; Limburg and Schmidt, 1990 for fish spawning; Larson et al., 2001 for habitat features; Kaufman and Marsh, 1997 for habitat fragmentation; Mitchell, 1999 and Sweeney, 1992 for the effect of riparian canopy; Finkenbine et al., 2000 for stream rehabilitation; numerous studies compiled in Schueler,

1994 for stream diversity). Cappiella and Brown (2001) include their comprehensive literature review on studies on the relationship of urbanization with ecological system and the physical impact of urbanization on hydrology, geomorphology, and habitats.

From a hydrological standpoint, IMP affects every component in the hydrological cycle. For example, as IMP increases, evaporation decreases (Dow and DeWalle, 2000). Figure 2-1 depicts increased IMP which causes infiltration to decrease. The decrease in infiltration and evapo-transpiration allows an increase in runoff. The change in hydrological processes leads to the following hydrological response as seen in Figure 2-2; (a) increased flow volume, (b) increased peak flow (c) increased peak flow duration, and (d) decreased base flow (US EPA, 1997; Stewart et al., 1999; Rose and Peters, 2001; Booth, 2002).

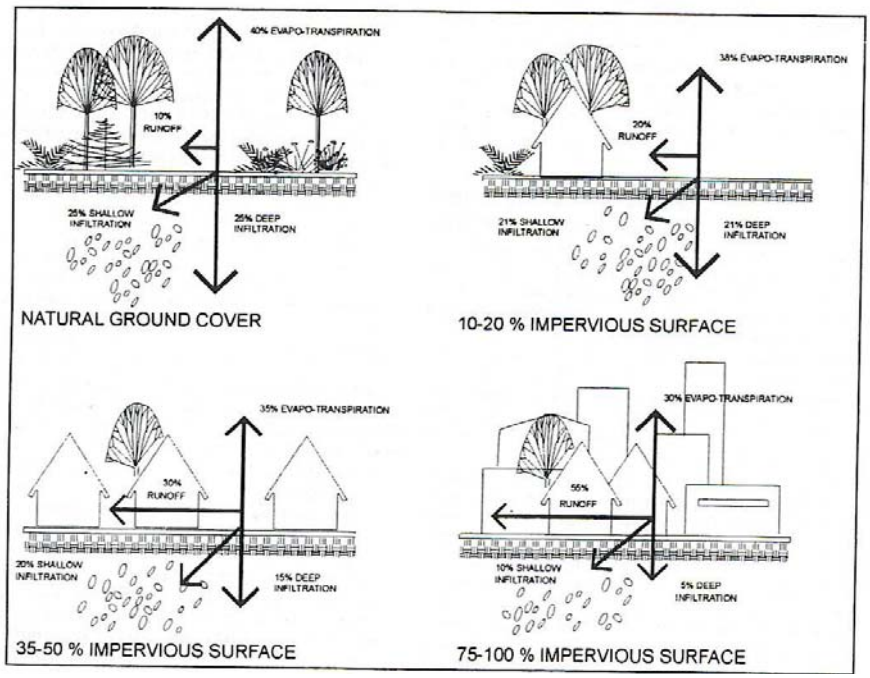


Figure 2-1. Relationship between IMP and the hydrological response (Arnold and Gibbons, 1996)

One recent study was conducted on the impact of IMP on the hydrological cycle at a given basin from a historical perspective (Jennings and Jarnagin, 2002). Jennings and Jarnagin stated that the same effect has been observed as one based on a contemporary comparison across different study basins: as IMP increased from 1949 to 1994, mean daily streamflow increased significantly and so did the frequency of daily streamflow at given volumes.

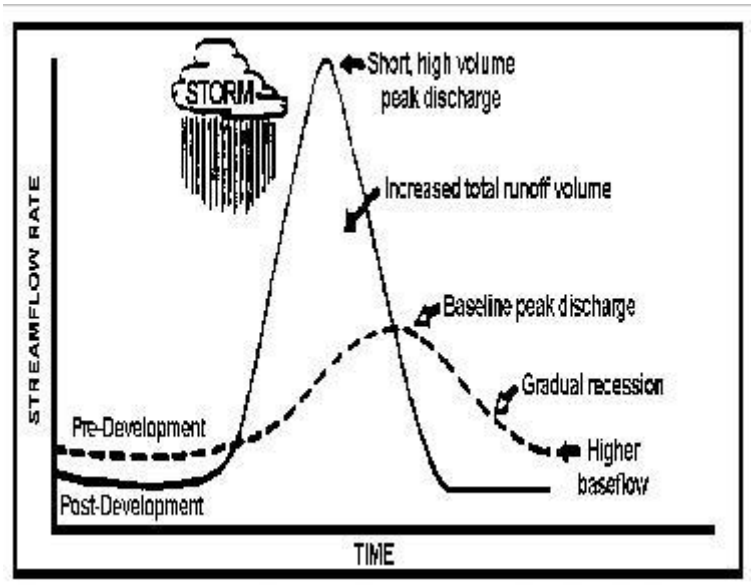


Figure 2-2. Impact of urbanization on stream flow (US EPA, 1997)

**2.3 Indicators of the hydrological response due to land use change**

In order to indicate hydrological response, many researches have focused on two regimes: flow regime and thermal regime. Richter et al. (1996) suggested that indicators be able to monitor five characteristics of the flow regime. Those five characteristics are monthly average magnitudes, magnitude and duration of annual extreme conditions, timing of annual extreme conditions, frequency and duration of high and low pulses, and rate and frequency of change in flow conditions. According to Poff et al. (1997),

magnitude of discharge, frequency of occurrence, duration, timing, and the rate of change should be considered for the ecological consequences of human activities. Among those characteristics, Archer and Newson (2002) claimed in their paper that indices of flow variability provide more comprehensive information of hydrological regime changes due to land use change than any other indices. According to Archer and Newson, flow variability is not only a good indicator of land use change but also is an important control on river ecology (Newson and Newson, 2000, cited in Archer and Newson's paper). For example, Scoggins (2000) claimed that the general hydrological-stream-character indicating flow variability has a significant relationship to the benthic macroinvertebrate community. Clausen and Biggs (1997) made a similar conclusion in that flow variability was significantly related to most of the biological variables.

In order to monitor the thermal regime change due to land use change, studies have been conducted with their focus on air temperature change (Bartholow, 2000), on surface radiant temperature change (Carlson and Arthur, 2000), and on stream temperature change. According to Coutant (1976), stream temperature is the most pervasive among all environmental indicators in the aquatic system. Stream temperature can act as a lethal agent that kills the fish directly, as a stressing agent that destroys the fish indirectly, as a controlling actor that sets the pace of metabolism and development, and as a limiting factor that restricts activity and distribution.

Nonetheless, studies on the variability in the thermal regime due to IMP through abiotic measurements have not been well documented compared to the variability in the flow regime. Among some studies found for this literature review chapter, Klein (1979) claimed that the widening of the channel due to increased runoff results in shallower

water depths, in turn, contributes to greater temperature fluctuations. According to Krause et al. (2004), stream temperature is elevated due to increased solar input from channel widening, diminished vegetative shading, or thermally enhanced runoff that passes over a heated impervious surface. Stream temperature fluctuation gets exacerbated with impeded base flow which might play a role as a temperature buffer. The rapid rise in stream temperature can occur as a heated summer storm flushes into a stream. A literature review authored by Paul and Meyer (2001) reported that a study on Long Island urban streams showed mean summer temperatures 5-to-8 degree Celsius warmer and winter temperatures 1.5- to-3 degree Celsius cooler than forested streams. Also, temperature pulses were observed during summertime storm runoff.

Such temperature disturbance is detrimental to the stream biota. For instance, Vought et al.'s (1998) findings included a significant difference in the total accumulated degree-day between channelized streams without riparian vegetation and natural woodland. Furthermore, the average temperature for the channelized streams was warmer than the one for natural streams by 1-degree Celsius. Such thermal enhancement, Vought et al. showed, has a critical effect on the life cycles of invertebrates, limiting their abundant distribution. A similar effect of stream temperature change was observed by Sweeney (1993). According to him, warming stream by 2 to 5 degree Celsius affects growth rate, survivorship, adult size and fecundity, and timing of reproduction greatly.

Based on many researches including the studies described above, it is evident that a strong correlation exists between IMP and stream health. Arnold and Gibbons (1996) developed threshold values that characterize stream health as summarized in Table 2-1.

Table 2-1. Relationship between stream health and imperviousness. (Arnold and Gibbons, 1996)

| Stream health | Imperviousness |
|---|---|
| protected | <10% |
| impacted | <30% |
| degraded | Over 30% |

Even though Arnold acknowledged that thresholds are controversial and are subject to change, many studies agree that stream degradation occurs around 10% of IMP (Klein, 1979; Limburg and Schmidt, 1990; Arnold and Gibbons, 1996; Carlson and Arthur, 2000; Paul and Meyer, 2001; Bird et al., 2002). These threshold values become reliable when the measurements of IMP show their consistency and accuracy in estimating IMP. One study shows that levels of accuracy in estimating IMP affect hydrological response (Lee and Heaney, 2003). The study estimated IMP in five different levels of accuracy and compared the effect of those different IMP estimates on the predicted runoff hydrograph from a single precipitation event. Based on hydrological simulations using SWMM, they found a 265% difference in peak discharge and a 275% difference in total runoff volume depending on levels of accuracy in estimating IMP. The following section reviews studies on methods for measuring IMP.

**2.4 Measurements of imperviousness**

The accuracy in quantifying IMP is known to depend on measurement methods as well as data sources. According to Brabec et al. (2002), IMP has been measured in the following ways: (1)identify impervious area on aerial photos and use a planimeter to measure each area; (2)overlay a grid on an aerial photo and count the number of intersections that overlaid impervious area; (3)classify satellite images; (4) estimate IMP

from widely available census data (Gluck & McCuen, 1975 cited in Brabec et al.'s paper); (5)develop relations between the percentage of urbanization in a region and the percentage of IMP. With the development of technologies, the methods described above continue to evolve using GIS and remote sensing.

While adopting new technologies, research efforts have been made to compare studies between classical methods and technology-aided methods. For example, Capiella and Brown (2001) measured IMP with four different methods such as direct measurement, estimates of IMP based on land use, estimates based on road density, and estimate based on population. The study found that the most accurate method was a direct measurement method. However, estimating IMP based on land use was the most feasible, considering cost, accuracy and time. The study concluded that the process of selecting a measurement method should consider not only accuracy, but also criteria such as resources, and the ability of future forecasting.

Knowing that remotely sensed data has a certain limit in recognizing features on the ground, the interest in comparing results from using remotely sensed data and using ground truth has grown. In the study conducted by Jennings et al. (2004) the estimate of IMP based on NLCD 92 (National Land Cover Dataset 92) was compared with the estimate measured from the planimetric ground truth. The regression analysis indicates a strong relationship between IMP extracted using NLCD 92 and the ground truth. However, the regression equation implies that the measurement using NLCD 92 underestimates IMP compared to the planimetric ground truth. According to Bird et al. (2002), using multiple data source such as block-level census data combined with road

networks provide improved accuracy compared to using NLCD 92 alone. The following section describes how IMP estimates are utilized to assess the hydrological response.

### 2.5 Hydrological methods to evaluate the impact of imperviousness

The impact of IMP on the hydrological system has been assessed largely by using the rainfall-runoff relation, since the most sensitive process to IMP in the hydrological cycle is runoff as seen in Figure 2-1. To predict the change in the rainfall-runoff relation due to IMP change, methods for the calculation of runoff should have parameters that are a function of IMP. For instance, one widely used method for estimating peak runoff is the Rational method. The method contains a runoff coefficient, C, that can be expressed as a function of IMP (Schueler, 1994; Tan et al., 2000; Hill, 2000; Becciu and Paoletti, 2000). The study conducted by Tan shows that the increase of IMP resulted in a large value of runoff coefficient, hence, a large peak discharge.

On the other hand, the SCS-CN method developed by NRCS (formerly SCS) is widely used for estimating runoff depth for a given storm event. It contains a curve number that can be expressed as a function of IMP as well as other properties (McCuen, 1998). Since the SCS-CN method considers most of factors which affect runoff in the hydrological cycle, it is a widely used method to evaluate the cause and effect between land use change and hydrological response (Weng, 2001; Moglen and Beighley, 2002; Melesse et al., 2003; Melesse and Graham, 2004). Being widely used, it has been implemented into hydrological models such as HEC-1, TR-55, and TR-20, which were developed by federal agencies and are expected to be used continuously. Bhaduri et al. (2001) stated that models such as HEC-1, TR-55, TR-20 had been routinely used in

assessing the impact of proposed land use changes on runoff changes to prevent flooding problems. The following quote from Melesse and Graham's (2004) paper projects the future of the SCS-CN method.

> "Dingman (2001) concluded that the NRCS(SCS)-CN approach will continue to be used since (1) it is computationally simple, (2) it uses readily available watershed information, (3) it has been packaged in readily available tables, graphs, and computer programs, (4) it appears to give reasonable results under many conditions, and (5) there are few other practicable methodologies for obtaining a priori estimates of runoff that are known to be better."

Nonetheless, it has been recognized that the SCS-CN method is a representative lumped parameter model that applies an averaged single value to each hydrologic computation unit being modeled. Therefore, it is known that the SCS-CN method using lumped parameters cannot effectively reflect the spatial variability of physical characteristics of a basin. On the other hand, a spatially distributed parameter model uses parameters that are determined based on each grid cell within a basin. Recently, there have been research efforts to integrate the SCS-CN method into a spatially distributed modeling process, so that the SCS-CN method reflects the spatial variability of basin characteristics which may affect runoff (Melesse and Shih, 2002; Rainis, 2004). They focused on describing a process of applying SCS-CN methods to individual mapping units, at 30-meter resolution. Furthermore, numerous studies have been conducted to evaluate hydrological response due to land use change using the SCS-CN method which parameters are spatially distributed (Corbett et al., 1997; Mohan and Shrestha, 2000; Shrestha, 2003).

As studies on spatially distributed parameter models continue to emerge, so do comparison studies with lumped parameter models. Goodrich and Kepner (2000) cited

Wood et al.'s (1988) findings based on his experiment with averaging runoff over different sub-basin areas by aggregating. The variance of mean runoff decreased until the process of aggregation reached a 1km x 1km sub-basin scale. Vieux (2001) examined the effect of using lumped parameters compared to using spatially distributed parameters. In his book, he concluded that spatial variability should be incorporated into a model presentation. The conclusion was supported by his observations that using spatially distributed parameters allowed a hydrologic model to be more responsive, rather than being delayed and attenuated. In spite of those advantages in using spatially distributed parameter models, it was considered to be impracticable due to extensive computing time and the enormous quantity of needed data. With the advent of GIS and improved computer power, however, constraints on handling and computing vast spatial data sets have been significantly reduced. In the next section, hydrological modeling in a GIS environment with remote sensing data is discussed.

**2.6 GIS-based hydrological model**

In the hydrology-related community, GIS has been considered a useful tool for storing data derived from a soil map, a digital elevation map, a land cover map, a land use map and others that are characterized in the GIS-environment. It overlays different types of geo-referenced maps and extracts necessary information for hydrological modeling in a time-efficient manner. As a result, the computing time for the parameterization of spatially distributed hydrological models has been reduced substantially. Furthermore, the GIS capability in coupling with remotely sensed data allows hydrological models to reflect the nature of physical characteristics of a basin more efficiently.

Taking into account the quantity of input data and the spatial pattern of land use/land cover change, the GIS with remote sensing technique is the most suitable and the most powerful tool to evaluate hydrological response due to IMP change. For example, Brun and Band (2000) assessed the effects of land use change in urbanizing watersheds on the hydrological response, using GIS coupled with HSPF and BASIN. The study concluded that the runoff ratio increased as IMP increased for any percent soil saturation. Through this study, Brun and Band (2000) demonstrated that simulating a variety of land use scenarios at ease is one of the advantages of using hydrologic modeling coupled with GIS. This is consistent with Stuebe and Johnston's work (1990). It shows that the GIS-based SCS-CN method is much more advantageous to the manual SCS-CN method, especially when the study area is large and different scenarios are explored.

Within the scope of this study, hydrological methods such as water-balance or SCS-CN method are modified and compared. Interfacing those hydrological models and parameterization are performed in GIS environment. GIS also facilitates identifying hydrological response units with a basin-delineation tool. GIS is used as a tool for mapping and displaying hydrological variables and spatial distribution of the hydrologic process. Remotely sensed data is integrated into a GIS-based parameterization process to obtain spatial information in a time-, and cost-efficient way. The following chapter describes data sources, methods, and model structures.

# CHAPTER THREE

# METHODOLOGY

## 3.1 Overview

The goal of this study is to examine characteristics of IMP and the impact of IMP on hydrological response. This chapter presents the methodology used to accomplish the goal. It includes data collection, a description of study sites, and hydrological models to examine the relationship between imperviousness and the hydrological response. Indicators of the hydrological response are defined. Within the scope of this study, the hydrological response refers both to flow variability and to thermal variability.

## 3.2 Data collection

This section describes data collection in two categories: spatial data and non-spatial data. Spatial data are geographically referenced data and are needed for this study since a geographic information system (GIS) is utilized as a tool for the parameterization of hydrological models, storing and displaying data. They are stored in two primary forms in a GIS environment: vector and raster. Vector data are comprised of points, lines, and polygons, whereas raster data are represented by grid cells or pixels. In this study, all spatial data were collected and converted into raster formats, since the hydrological models used in this study are easily parameterized using raster data. Any one piece of spatial data represented either by vector or by raster, is referred to as a layer in a GIS-environment. Collecting a topographic layer, a pollution layer, and a property layer and putting them together creates thematic maps.

### 3.2.1 Spatial data for GIS-analysis

#### 3.2.1.1 Land use layer

The land use 2000 layer developed by Maryland Department of Planning (MDP) is obtained in a vector format. It is in the Maryland State Plane Coordinate System and each polygon represents a land usage predominant within the polygon based on a modified version of an Anderson Level II classification system. Table 3-1 is the description of individual land use classes according to Anderson et al.

Table 3-1. Anderson Level II land use classification system (Anderson et al., 1976).

| Code | Land cover class | Description |
|---|---|---|
| 11 | Residential | Residential and land uses ranges from high density to low density on the periphery of urban expansion. |
| 12 | Commercial and Services | Areas used predominantly for the sale of products and services. |
| 13 | Industrial | A wide array of land uses from light manufacturing to heavy manufacturing plants. It includes surface structures associated with mining operations. |
| 14 | Transportation, Communications, and Utilities | Include highways, railroads, airport and their facilities. Communications and utilities are those involved in processing, treatment, and transportation of water, gas, oil, and electricity and areas used for airwave communications. |
| 15 | Industrial and Commercial Complexes | Include industrial and commercial land uses that typically occur together or in close functional proximity. They commonly are labeled with terminology such as “Industrial Park” |
| 16 | Mixed Urban or Built-up land | A mixture of Level II Urban or Built-up uses where individual uses cannot be separated at mapping scale. |
| 17 | Other Urban or Built-up land | Golf driving ranges, zoos, urban parks, cemeteries, waste dumps, water-control structures and spillways. |

Table 3-1(continued). Anderson Level II classification system.

| | | |
|---|---|---|
| 21 | Cropland and Pasture | Include cropland harvested, cultivated summer fallow and idle cropland, land on which crop failure occurs, cropland used only for pasture in rotation with crops, pasture on land more or less permanently used for that purpose. |
| 22 | Orchards, Groves, Vineyards, Nurseries, and Ornamental Horticultural Areas | Orchards, groves and vineyards produce the various fruit and nut crops. Nurseries and horticultural areas are used perennially for those purposes. Tree nurseries which provide seedlings for plantation forestry also are included here. |
| 23 | Confined Feeding Operations | Large, specialized livestock production enterprises, chiefly beef cattle feedlots, dairy operations with confined feeding, and large poultry farms. |
| 24 | Other Agricultural Land | Includes farmsteads, holding areas for livestock and training facilities on horse farms, farm lanes and roads, ditches and canals, small farm ponds. |
| 31 | Herbaceous Rangeland | Lands dominated by naturally occurring grasses and forbs. It also includes the palmetto prairie areas which consist mainly of dense stands of medium length and tall grasses. |
| 32 | Shrub and Brush Rangeland | It can be found in arid and semiarid regions characterized by xerophytic vegetative types. It also includes a dense mixture of broadleaf evergreen shrubs, and the occurrences of mountain mahogany and scrub oaks. |
| 33 | Mixed Rangeland | Area with more than one-third intermixture of either herbaceous or shrub and brush rangeland species. |
| 41 | Deciduous Forest Land | All forested areas having a predominance of trees that lose their leaves at the end of the frost-free season or at the beginning of a dry season. |
| 42 | Evergreen Forest Land | All forested areas in which the trees are predominantly those which remain green throughout the year. |
| 43 | Mixed Forest Land | All forested areas where both evergreen and deciduous trees are growing and neither predominates. |
| 51 | Streams and Canals | They include rivers, creeks, canals, and other linear water bodies. |
| 52 | Lakes | Nonflowing naturally enclosed bodies of water. |
| 53 | Reservoirs | Artificial impoundments of water used for irrigation, flood control, municipal water supplies, recreation, hydroelectric power generation |

Table 3-1(continued). Anderson Level II classification system

| | | |
|---|---|---|
| 54 | Bays and Estuaries | Inlets or arms of the sea that extend inland. |
| 61 | Forested Wetland | Wetland dominated by woody vegetation. |
| 62 | Nonforested Wetland | Wetland dominated by wetland herbaceous vegetation or nonvegetated. |
| 71 | Dry Salt Flats | It occurs on the flat-floored bottoms of interior desert basins which do not qualify as wetland. |
| 72 | Beaches | The smooth sloping accumulations of sand and gravel along shorelines. |
| 73 | Sandy Areas other than Beaches | They are composed of dunes accumulations of sand transported by the wind. |
| 74 | Bare Exposed Rock | It includes areas of bedrock exposure, desert pavement, scarps, talus, slides, volcanic material, and other accumulations of rock without vegetative cover. |
| 75 | Strip Mines Quarries, and Gravel Pits | Extractive mining activities that have significant surface expression. Vegetative cover and overburden are removed to expose such deposits as coal, iron ore, limestone, and copper. |
| 76 | Transitional Areas | Areas which are in transition from one land use activity to another. |
| 77 | Mixed Barren Land | A mixture of Barren land features occurs and the dominant land use occupies less than tow-thirds of the area. |
| 81 | Shrub and Brush Tundra | Various woody shrubs and brushy thickets found in the tundra environment. |
| 82 | Herbaceous Tundra | Various sedges, grasses, forbs, lichens, and mosses, all of which lack woody stems. |
| 83 | Bare Ground Tundra | Tundra occurrences which are less than one third vegetated. |
| 84 | Wet Tundra | It usually found in areas having little topographic relief. |
| 85 | Mixed Tundra | A mixture of the Level II Tundra occurrences where any particular type occupies less than two-thirds of the area of the mapping unit. |
| 91 | Perennial Snowfields | Accumulations of snow and firn that did not entirely melt during previous summers. |
| 92 | Glaciers | It originates from the compaction of snow into firn and finally to ice under the weight of several successive annual accumulations. |

#### 3.2.1.2 Impervious surface layer

An impervious surface layer, one of three layers in the National Land Cover Dataset (NLCD) 2001 may be downloaded from the USGS website (USGS, 2004 a). It is in a GeoTIFF format with a spatial resolution of 30-meter. Each pixel has a value which represents the percent-IMP over a pixel. It will be referred to as IMP-LC in this study.

#### 3.2.1.3 Land cover 2001 layer

From the same USGS website mentioned above, the land cover layer may be downloaded in a GeoTIFF format with 30-meter resolution. Each pixel has a value representing one of 21 land cover classes which are listed and described in Table 3-2.

#### 3.2.1.4 Digital Elevation Model (DEM) layer

The USGS National Elevation Dataset (NED) over Maryland may be downloaded from the USGS website from where NLCD (National Land Cover Dataset) 2001 appears. It has 1 arc second of spatial resolution in the Geographic projection which corresponds to an individual cell size of 0.00028 degree, approximately 30-meter resolution. Each grid cell contains a single value which represents the elevation over each cell in the vertical units of meters above sea level.

Table 3-2. Land cover classes and their descriptions for National Land Cover Dataset (NLCD) 2001 (Homer et al., 2004).

| Code | Land cover class | Description |
|---|---|---|
| 11 | Open Water | All areas of open water, generally with less than 25 % cover of vegetation or soil. |
| 12 | Perennial Ice/snow | All areas characterized by a perennial cover of ice /snow, generally greater than 25 % of total cover. |
| 21 | Developed, Open Space | Includes areas with a mixture of some constructed materials, but mostly commonly include large-lot single-family housing units, parks, golf courses, and vegetation planted in developed settings for recreation, erosion control, or aesthetic purpose. |
| 22 | Developed, Low Intensity | Includes areas with a mixture of constructed materials and vegetation. Impervious surfaces account for 20-49 % of total cover. |
| 23 | Developed, Medium intensity | Includes areas with a mixture of constructed materials and vegetation. Impervious surfaces account for 50-79 % of total cover. |
| 24 | Developed, High Intensity | Includes highly developed areas where people reside or work in high numbers. Examples include apartment complexes, row housed, and commercial/industrial. Impervious surfaces account for 80 to 100% of total cover. |
| 31 | Barren Land | Barren areas of bedrock, desert pavement, scarps, talus, slides, volcanic material, glacial debris, sand dunes, strip mines, other accumulations of earthen material. Generally, vegetation accounts for less than 15 % of total cover. |
| 32 | Unconsolidated Shore | Unconsolidated material such as silt, sand, or gravel that is subject to inundation and redistribution due to the action of water. Characterized by substrates lacking vegetation except for pioneering plants that become established during brief periods when growing conditions are favorable. Erosion and deposition by waves and currents produce a number of landforms representing this class. |
| 41 | Deciduous Forest | Areas dominated by trees generally greater than 5 meters tall, and greater than 20 % of total vegetation cover. More than 75 % of the tree species shed foliage simultaneously in response to seasonal change. |

Table 3-2 (continued). Land cover classes and their descriptions for National Land Cover Dataset

| | | |
|---|---|---|
| 42 | Evergreen Forest | Areas dominated by trees generally greater than 5 meters tall, and greater than 20 % of total vegetation cover. More than 75 % of the tree species maintain their leaves all year. Canopy is never without green foliage. |
| 43 | Mixed Forest | Areas dominated by trees generally greater than 5 meters tall, and greater than 20 % of total vegetation cover. Neither deciduous nor evergreen species are greater than 75 % of total tree cover. |
| 51 | Dwarf Scrub | Alaska only areas dominated by shrubs less than 20 centimeters tall with shrub canopy typically greater than 20 percent of total vegetation. This type is often co-associated with grasses, sedges, herbs, and non-vascular vegetation. |
| 52 | Shrub/Scrub | Areas dominated by shrubs; less than 5 meters tall with shrub canopy typically greater than 20 % of total vegetation. |
| 71 | Grassland/ Herbaceous | Areas dominated by grammanoid or herbaceous vegetation, generally greater than 80 % of total vegetation. These areas are not subject to intensive management such as tilling, but can be utilized for grazing. |
| 72 | Sedge/Herbaceous | Alaska only areas dominated by sedges and forbs, generally greater than 80 % of total vegetation. |
| 73 | Lichens | Alaska only areas dominated by fruticose or foliose lichens generally greater than 80 % of total vegetation. |
| 74 | Moss | Alaska only areas dominated by mosses, generally greater than 80 % of total vegetation. |
| 81 | Pasture/ Hay | Areas of grasses, legumes, or grass-legume mixtures planted for livestock grazing or the production of seed or hay crops, typically on a perennial cycle. Pasture/ hay vegetation accounts for greater than 20 % of total vegetation. |
| 82 | Cultivated Crops | Areas used for the production of annual crops, such as corn, soybeans, vegetables, tobacco, and cotton and also perennial woody crops such as orchards and vineyards. Crop vegetation accounts for greater than 20 % of total vegetation. This class also includes all land being actively tilled. |
| 90 | Woody Wetlands | Areas where forest or shrubland vegetation accounts for greater than 30 % of total vegetative cover and the soil or substrate is periodically saturated with or covered with water. |
| 95 | Emergent Herbaceous Wetlands | Areas where perennial herbaceous vegetation accounts for greater than 80 % of total vegetative cover and the soil or substrate is periodically saturated with or covered with water. |

### 3.2.1.5 Soil layer and hydrologic soil group (HSG) layer

The soil layers over Maryland are obtained from the NRCS (Natural Resources Conservation Service) website. It is downloaded in a vector format and converted into raster with the spatial resolution of 30-meter.

According to NRCS (SCS, 1986), soils are classified into four hydrologic soil groups (HSG) to indicate the minimum rate of infiltration obtained after prolonged wetting. Group A soils have the highest infiltration rate among four groups as seen in Table 3-3 which summarizes the relationship between the HSGs and minimum infiltration rates.

Table 3-3. Minimum infiltration rate by hydrologic soil groups (SCS, 1986).

| HSG (Hydrologic Soil Group) | Minimum infiltration rate (inch / hr) | Mean Minimum infiltration rate (inch / hr) |
|---|---|---|
| A | 0.3-0.45 | 0.375 |
| B | 0.15 – 0.3 | 0.225 |
| C | 0.05 – 0.15 | 0.1 |
| D | 0-0.05 | 0.025 |

### 3.2.1.6 Curve number (CN) layer

Depending on HSG and land use categories, curve numbers are assigned to individual grid cells. Table 3-4 (a) summarizes curve numbers based on HSG from SCS (1986) and MDP land use categories. Table 3-4 (b) shows curve numbers based on HSG and NLCD land cover categories.

Table 3-4 (a). Curve number based on hydrologic soil group and land use. Land use 2000 layer developed by Maryland Department of Planning (MDP) is used for land use categories. For the antecedent moisture condition, AMC II is assumed in this study.

| LU code | Description | Curve Number | | | |
|---|---|---|---|---|---|
| | | HSG A | HSG B | HSG C | HSG D |
| 11 | Low Density Residential | 54 | 70 | 80 | 85 |
| 12 | Medium Density Residential | 61 | 75 | 83 | 87 |
| 13 | High Density Residential | 77 | 85 | 90 | 92 |
| 14 | Commercial | 89 | 92 | 94 | 95 |
| 15 | Industrial | 81 | 88 | 91 | 93 |
| 16 | Institutional | 81 | 88 | 91 | 93 |
| 17 | Open Urban Land | 49 | 69 | 79 | 84 |
| 21 | Cropland | 72 | 81 | 88 | 91 |
| 30 | Urban Herbaceous | 72 | 81 | 88 | 91 |
| 41 | Deciduous Forest | 36 | 60 | 73 | 79 |
| 42 | Evergreen Forest | 36 | 60 | 73 | 79 |
| 43 | Mixed Forest | 36 | 60 | 73 | 79 |
| 44 | Brush | 35 | 56 | 70 | 77 |
| 50 | Water | 100 | 100 | 100 | 100 |
| 60 | Wetland | 100 | 100 | 100 | 100 |
| 73 | Bare Ground | 77 | 86 | 91 | 94 |
| 171 | Highway Corridors | 98 | 98 | 98 | 98 |
| 172 | Railroad Corridors | 98 | 98 | 98 | 98 |
| 242 | Agricultural Buildings | 72 | 81 | 88 | 91 |

Table 3-4 (b). Curve number based on hydrologic soil group and land cover. National land cover dataset (NLCD)2001 is used for land cover categories. In order to assign curve numbers to individual land covers, land cover classes are mapped into Land use categories to utilize the relationship between land use and curve number shown in Table 3-4(a).

| Land cover classification | Land use Corresponding to land cover classification | Curve Number | | | |
|---|---|---|---|---|---|
| | | HSG A | HSG B | HSG C | HSG D |
| Open Water | Water | 100 | 100 | 100 | 100 |
| Developed, Open Space | Low Density Residential | 54 | 70 | 80 | 85 |
| Developed, Low Intensity | Medium Density Residential | 61 | 75 | 83 | 87 |
| Developed, Med | Institutional | 81 | 88 | 91 | 93 |
| - | High Density Residential | 77 | 85 | 90 | 92 |
| Developed, High | Urban, Commercial | 89 | 92 | 94 | 95 |
| Barren Land (rock, sand) | Barren Land (developing urban ) | 77 | 86 | 91 | 94 |
| Deciduous Forest | Deciduous Forest | 36 | 60 | 73 | 79 |
| Evergreen Forest | Evergreen Forest | 36 | 60 | 73 | 79 |
| Mixed Forest | Mixed Forest | 36 | 60 | 73 | 79 |
| Pasture/Hay | Pasture | 49 | 69 | 79 | 84 |
| Cultivated Crops | Cropland, Agriculture | 72 | 81 | 88 | 91 |
| Woody Wetland | Wetlands | 100 | 100 | 100 | 100 |
| Emergent Herbaceous Wetland | Wetlands | 100 | 100 | 100 | 100 |

### 3.2.2 Stream temperature

At the beginning of this study, measured stream temperature over several basins has been already collected from different studies. According to Nelson, the stream temperature is recorded at 30-minute time intervals, starting in 2002 (Nelson, submitted). The stream temperature was measured with the temperature loggers named Optic Stowaway Model WTA. They were placed below the water surface (Nelson, submitted). Due to significant seasonal variation, this study uses only stream temperature recorded during the summer, from May to September. The recorded temperature over the time period of 2002-2004 is plotted in Appendix A.

### 3.2.3 Stream flow

Mean daily stream flow datasets for each gauge station are downloaded from the USGS website (USGS, 2004 b). The time period of the interest for the study is six years centered on 2000, from the water year 1997 to the water year 2003. The stream flow is recorded in units of cubic-feet per-second (cfs). The plots of stream flow data over the study period are provided in Appendix B.

## 3.3 Study site

### 3.3.1 Selection of study basins

The study basins for the flow regime and thermal regime analysis are different as seen in Figure 3-1. Study basins for the flow regime analysis are selected primarily based on the availability of spatial data sets as well as historical stream flow data. For the thermal regime analysis, study basins are chosen primarily based on physical characteristics of basins such as historical land use change, IMP, size and location. Each selection is described below.

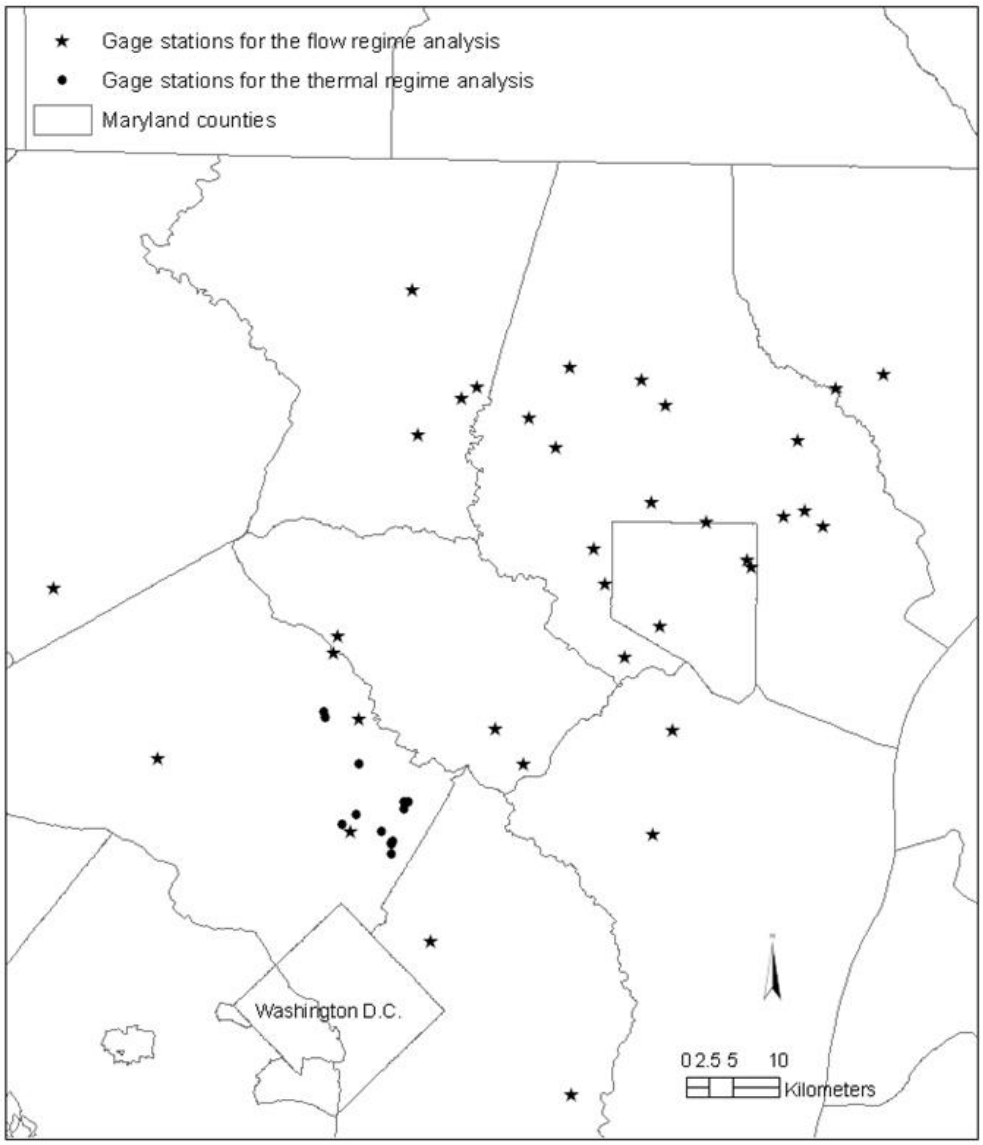


Figure 3-1. Study sites for the flow regime analysis are different from those for the thermal regime analysis, since the latter were already chosen for other research purposes (Palmer et al. 2002; Moglen 2004).

For the flow analysis, 35 basins where outlets are located at USGS gauging stations were chosen for this study. The criteria used to identify study gauges was the following: gauge must be currently active; its drainage area must be contained in the extent of other spatial data sets used in this study as well as within Maryland. The

locations of the study sites are shown in Figure 3-2 and Table 3-5 summarizes the USGS gauging station number and the size of each basin.

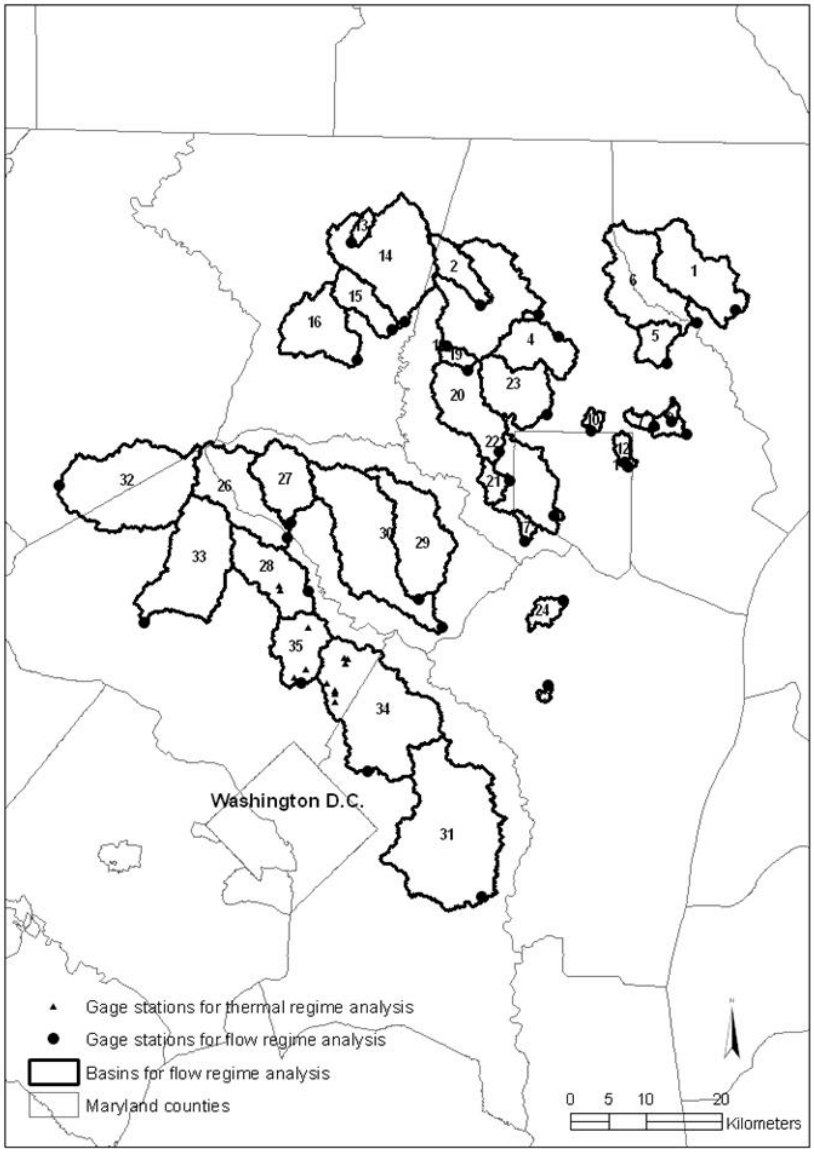


Figure 3-2. Study basins for the flow regime analysis.

Table 3-5. USGS gauge station number and size of each study basin selected for the flow regime analysis.

| No. | USGS gauge station number | Size, $mi^2$ |
|---|---|---|
| 1 | 1581700 | 34.80 |
| 2 | 1583100 | 12.30 |
| 3 | 1583500 | 59.80 |
| 4 | 1583600 | 20.90 |
| 5 | 1584050 | 9.40 |
| 6 | 1584500 | 36.10 |
| 7 | 1585090 | 2.73 |
| 8 | 1585095 | 1.34 |
| 9 | 1585100 | 7.61 |
| 10 | 1585200 | 2.13 |
| 11 | 1585225 | 0.21 |
| 12 | 1585230 | 3.52 |
| 13 | 1585500 | 3.29 |
| 14 | 1586000 | 56.60 |
| 15 | 1586210 | 14.00 |
| 16 | 1586610 | 28.00 |
| 17 | 1589100 | 2.47 |
| 18 | 1589180 | 0.23 |
| 19 | 1589197 | 4.23 |
| 20 | 1589300 | 32.50 |
| 21 | 1589330 | 5.52 |
| 22 | 1589352 | 65.90 |
| 23 | 1589440 | 25.20 |
| 24 | 1589500 | 4.97 |
| 25 | 1589795 | 1.00 |
| 26 | 1591000 | 34.80 |
| 27 | 1591400 | 22.90 |
| 28 | 1591700 | 27.00 |
| 29 | 1593500 | 38.00 |
| 30 | 1594000 | 98.40 |
| 31 | 1594526 | 89.70 |
| 32 | 1643500 | 62.80 |
| 33 | 1644600 | 50.70 |
| 34 | 1649500 | 72.80 |
| 35 | 1650500 | 21.10 |

The basins selected for the thermal analysis are the Paint Branch, Northwest Branch, and Hawlings River as shown in Figure 3-3(a). Figure 3-3(b) shows sub-basins within the Paint Branch study basin. Table 3-6 summarizes sizes of individual study sites. These study areas were already chosen for other research purposes (Palmer et al. 2002; Moglen 2004). These basins drain into the Potomac and Patuxent Rivers. The land pattern in these basins results from the wide development of the residential area around Washington, DC. Among the three basins, the Paint Branch is the most urbanized basin, whereas the Hawlings River basin is forested the most as seen in Table 3-7.

Table 3-6. Size of each study basin selected for the thermal regime analysis. There are three basins and each has two to eight sub-basins.

| ID | Basin Name | | Size, $mi^2$ |
|---|---|---|---|
| 1 | Hawlings River | HR18 | 2.15 |
| 2 | | HR19 | 1.03 |
| 3 | Northwest Branch | NW05 | 1.19 |
| 4 | | NW13 | 1.30 |
| 5 | | NW18 | 3.56 |
| 6 | Paint Branch | PB01 | 2.04 |
| 7 | | PB02 | 1.27 |
| 8 | | PB03 | 3.82 |
| 9 | | PB07 | 9.19 |
| 10 | | PB08 | 1.62 |
| 11 | | PB09 | 10.90 |
| 12 | | PB13 | 1.05 |
| 13 | | PB20 | 0.32 |

Table 3-7. Pattern of land use within each basin selected for the thermal regime analysis (Moglen, 2004).

| Basin | Residential, % | Agricultural, % | Forest, % | Other, % |
|---|---|---|---|---|
| Hawlings River (Hr) | 20 | 41 | 32 | 6 |
| Northwest Branch (Nwb) | 48 | 9 | 28 | 14 |
| Paint Branch (Pb) | 61 | 9 | 23 | 6 |

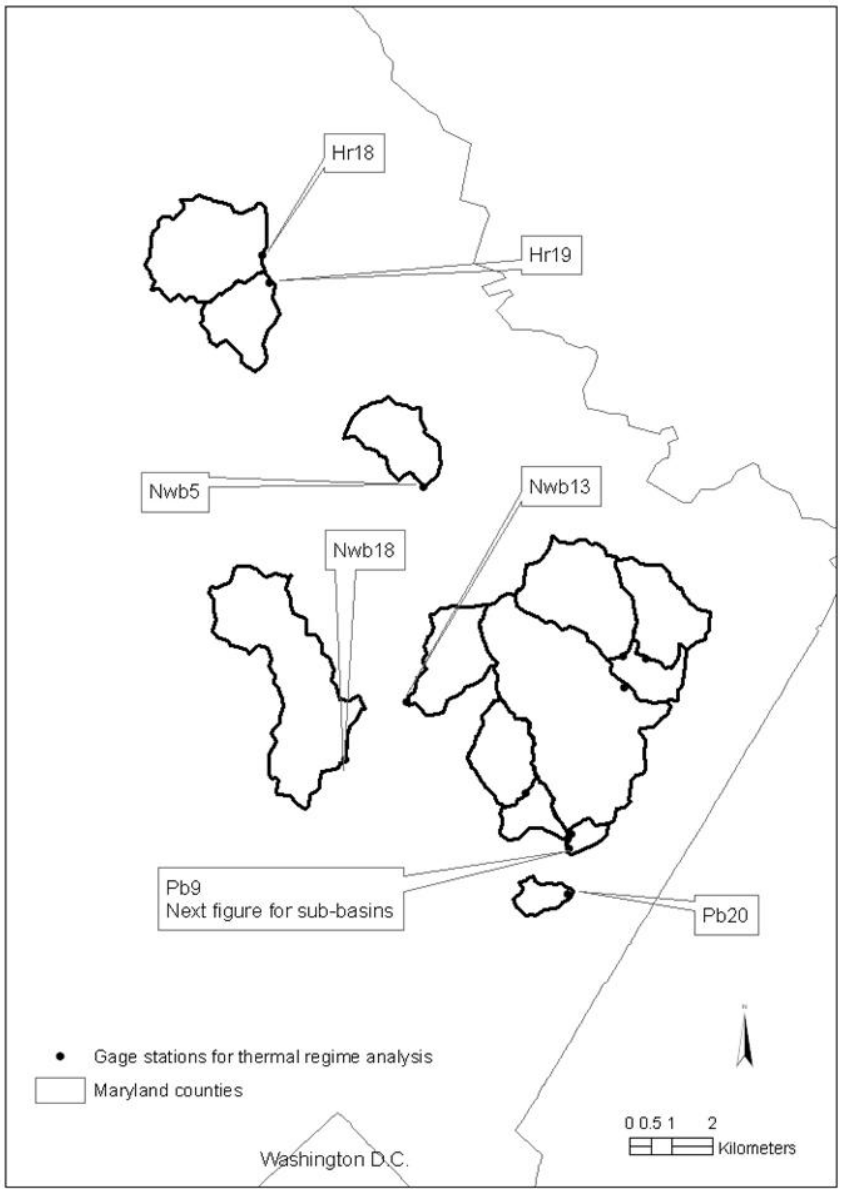


Figure 3-3(a). Study basins for the thermal regime analysis.

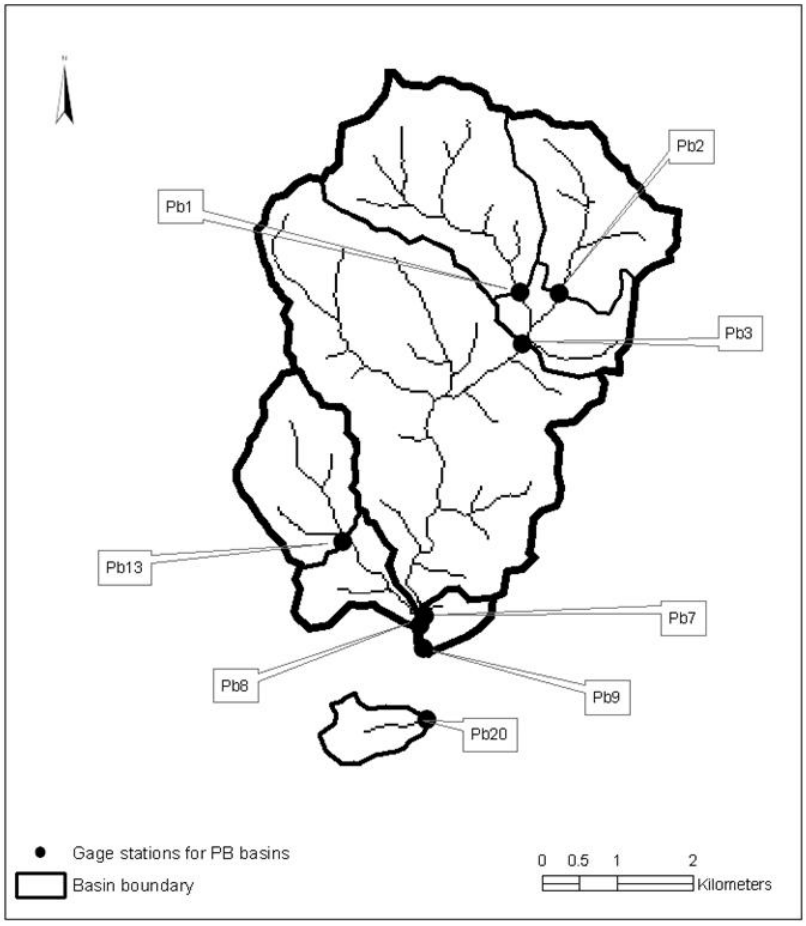


Figure 3-3(b). Sub-basins of the Paint Branch, one of basins selected for the thermal regime analysis.

### 3.3.2 Pre-processing for GIS-based hydrological analysis

In this study, all processes such as DEM pre-processing, the creation of a flow direction grid layer and flow accumulation grid layer, the delineation of basins, and the creation of a flow length grid layer are performed using ArcMap 8 and ArcView 3.3 with Spatial Analyst Tools. The process starts with the reprojection of digital elevation model (DEM) which is the primary data source for the GIS-based hydrological analysis. DEMs downloaded from the USGS website are reprojected to WGS84 UTM zone 18N

coordinate system, having 30-meter horizontal resolution. Then, it is processed to eliminate depressions which will hinder flow routing (Jenson and Domingue, 1988).

In order to delineate a basin and stream network, a value indicating flow direction needs to be assigned to each grid cell. Flow direction at a given grid cell is determined by the steepest downward slope among eight-adjacent neighbor cells (Jenson and Domingue, 1988). The value for flow accumulation can also be calculated from flow direction. Flow accumulation indicates the number of upstream grid cells flowing into a given grid cell. These methodologies have been well integrated into the GIS-environment.

Once the grid layer of flow direction is generated, the delineation of a basin can be performed based on the assigned flow direction in each grid cell. Furthermore, other information such as a basin size at a given outlet location and the longest flow length within a basin can be extracted. For example, to compute the flow length from a given grid cell to the outlet within a basin, a GIS-based hydrology tool is utilized so that it assigns a value for the flow length of 1 multiplied by spatial resolution, if the flow direction is cardinal at a given grid cell. If the direction is diagonal, the flow length becomes $\sqrt{2}$ * spatial resolution.

### 3.4 Comparison of imperviousness estimates

#### 3.4.1 Measurement of imperviousness

In this study, two IMP estimates will be compared: (1) IMP based on coefficients assigned to unique land use categories (IMP-LU); (2) IMP based on satellite-derived land cover (IMP-LC). Coefficients used in IMP-LU refer to an average percent IMP estimates

for each land use category. IMP-LU represents IMP based on land use which reflects anthropological activities as well as surface features, while IMP-LC represents IMP based on the reflectance from the land surface.

#### 3.4.1.1 IMP from land use

According to the metadata for land use from MDP, land cover types are initially classified using satellite-derived land cover (MDP, 2004). Then, urban land use categories were identified using individual parcel information. In other words, the urban land use classification from MDP differs from the urban land cover classification shown in Table 3-2, in that the former takes direct knowledge of human activities into account.

In order to determine the coefficient for a given land use category, this study employs the assumed IMP in developing curve numbers, one of hydrologic parameters in the SCS-CN method (SCS, 1986). Such a coefficient represents an assumed imperviousness fraction for individual land use categories. However, land use categories used in the SCS method are slightly different from those used in the MDP land use: mapping land use categories between different sources is needed prior to assigning the assumed IMP to a given land use category. Table 3-8 summarizes the relationship between the coefficients and land use categories. These coefficients are referred to as "SCS-coefficient".

Table 3-8. SCS-coefficients by land use categories (SCS, 1986).

| MDP Land use | SCS Land use | SCS-Coefficient |
|---|---|---|
| Urban | urban districts: commercial and business | 85 |
| Low Density Residential | residential, 1/2 acre | 25 |
| Medium Density Residential | residential, 1/4 acre | 38 |
| High Density Residential | residential, 1/8 acre or less | 65 |
| Commercial | urban districts: commercial and business | 85 |
| Industrial | Industrial | 72 |
| Institutional | N/A | 50 |
| Open Urban Land | less than 2 acre | 11 |
| Miscellaneous Transportation | N/A | 75 |
| Agricultural Buildings | less than 2acre | 10 |

#### 3.4.1.2 IMP from satellite-derived land cover

This study utilizes an impervious surface layer, one of the data products from the National Land Cover Dataset (NLCD) 2001. It is worthwhile to investigate the procedures for producing the IMP from the remotely sensed data to understand that the product is derived from land cover. Using 1-meter high resolution images such as IKONOS from Space Imaging and the digital orthophoto quadrangles(DOQ) of the USGS, a large number of training data are collected representing spectral and spatial variability of impervious areas(Yang et al., 2003). These are classified as one of five land cover classes which are impervious surface, forest, grass, water, and shadow. According to Yang et al., all 1-meter pixels classified as impervious surface are counted using a 30-meter grid based on 30-meter-resolution Landsat ETM+ imagery to compute IMP for each 30-meter grid cell. The purpose of this procedure is to calibrate the

relationships between percent IMP and Landsat spectral data so that the calibrated models are applied to all pixels in a mapping zone (Homer et al., 2004).

Following the procedures described in Sections 3.4.1.1 and 3.4.1.2, values of IMP-LU and IMP-LC are available for every 30-meter pixel. These values will be compared in an experiment described in Section 3.4.2.

### 3.4.2 Experiment for converting between IMP-LU and IMP-LC

The first objective in this study is to examine IMP-LU and IMP-LC and to provide conversion equations between these two. Figure 3-4 shows that the study area is imposed with a grid layer, 10km x 10km in this figure. The study area was chosen so that the most urbanized counties were included. According to Maryland NRI (National Resource Inventory) run by NRCS (NRCS, 2005), Maryland is one of the U.S.'s most rapidly growing areas, making it the sixth most urbanized state in the country. In 1997, the counties that had the highest percentage and greatest acreage of urban land were within the Baltimore-Washington-Annapolis population triangle. This triangle area includes Montgomery, Prince George's, Baltimore, and Howard counties.

The experiment is designed such that the study area is divided into numerous regular square boxes (hereinafter grid sampling cells) as seen in Figure 3-4. The cell size varies from 0.25x0.25 $km^2$ to 10x10 $km^2$. Each grid sampling cell contains a number of 30-meter grid cells which are mapping units of IMP-LU and IMP-LC. At a given grid sampling cell size, an aggregate IMP for each grid sampling cell is calculated by averaging all IMP values from 30-meter grid cells within a grid sampling cell. By this procedure, each grid sampling cell has two aggregate IMP, one from IMP-LU and the other from IMP-LC. Under the different aggregating scales, these quantities are used to

calibrate a set of regression equations. The reliability of the regression equations will be evaluated by examining goodness-of-fit measures.

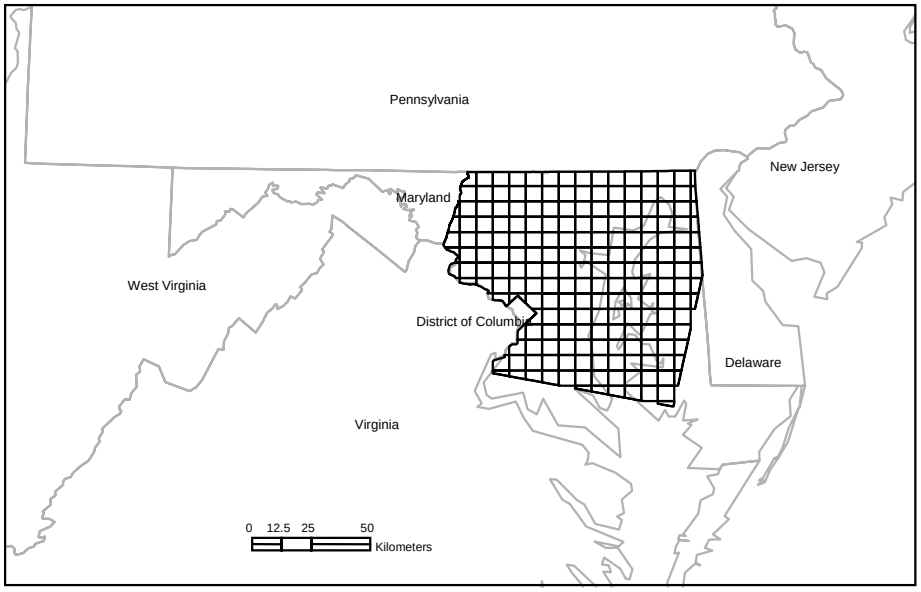


Figure 3-4. Study area for the comparison of IMP estimates based on different data sources: land use and land cover. The figure shows the study area gridded with the sampling cell size of 10 km x 10 km. Each sampling cell contains 30-meter grid cells which will be used to calculate an aggregate IMP at a given grid sampling cell.

## 3.5 GIS-based models reflecting imperviousness: IMP-descriptor

In order to examine IMP from various perspectives, models reflecting IMP are designed in this section. For this study, models are based on two approaches as presented in Figure 3-5: (a) lumped and no hydrological processes involved; (b) spatially distributed with hydrological processes considered. A GIS-based average IMP (aggregate IMP) within each basin is used for the case of (a), whereas GIS-based hydrological models are employed for the latter case, (b). Since these models generate indices of IMP, they are referred to as IMP-descriptors in this study.

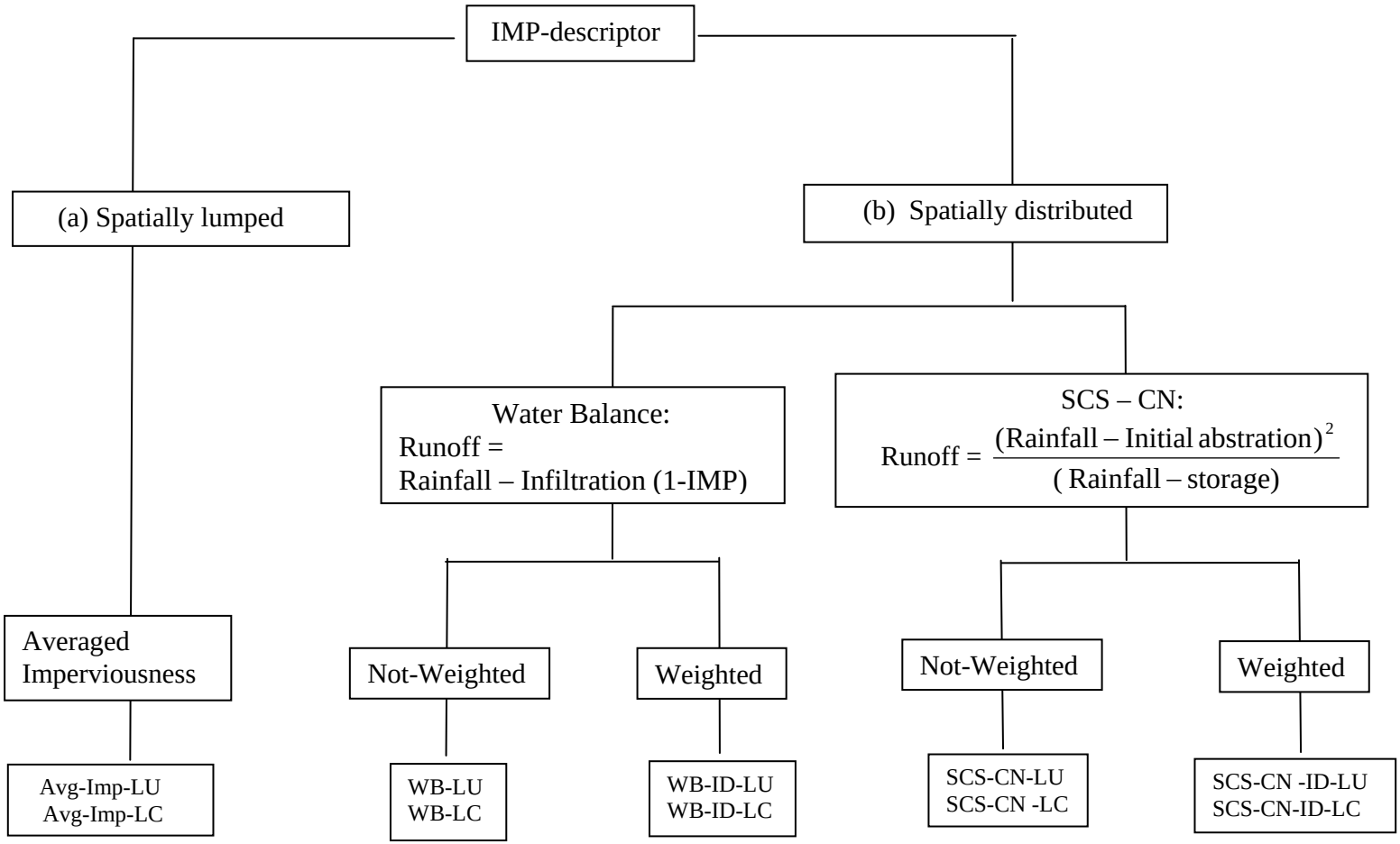


Figure 3-5. Imperviousness descriptors (IMP-descriptors) and their symbols used in this study. Names carrying "LU" at the end indicate that IMP-LU is used as an IMP dataset. Names carrying "LC" at the end indicate that IMP-LC is used as an IMP dataset.

### 3.5.1 IMP-descriptor: Spatially lumped model

A single lumped value of IMP over each study basin was determined within a GIS-environment. Although it is not related to hydrological process, this study is to evaluate the correlation of this lumped IMP with indicators of the hydrological response in the flow regime as well as the thermal regime.

### 3.5.2 IMP-descriptor: Spatially distributed model

Figure 3-5 illustrates that GIS-based hydrological methods calculating runoff volumes are derived from two ideas, either a water balance or the Soil Conservation Service – curve number (SCS – CN) method. The latter (the SCS – CN method) requires more input parameters, hence, more assumptions are involved compared to the former method. However, these methods are similar in that they are to be applied to individual grid cells in a GIS-raster environment and generate estimates of hypothetical downstream runoff, in order to account for spatial variability in IMP within each study basin. Also, modified approaches using weighted/not-weighted methods are applied to explore the effect of the proximity of IMP to the outlet of each study basin. These methods are described in the following section.

#### 3.5.2.1 Water balance approach

Water balance is an analysis based on the conservation of mass (McCuen, 1998). It assumes that the water volume leaving a basin or a computing unit equals the water

volume entering the basin or the computing unit after the abstraction such as infiltration or evapotranspiration as expressed mathematically in Equation 3-1,

$$I = O + E + F_{(1\text{-}IMP)} \tag{3-1}$$

where $I$= inflow in inches
$O$ = outflow in inches
$E$ = evapotranspiration in inches
$F$ =infiltration in inches

The infiltration ($F$) with the subscript of (*1-IMP*) indicates that water infiltrates only into the non-impervious area: $F_{(1\text{-}IMP)} = F - \alpha F$ where $\alpha$ is the IMP fraction. If this method is applied to the individual grid cells following the draining network, not only rainfall falling into the downstream-grid cell, but also cumulative runoff volume from upstream-grid cells becomes inflow to the downstream-grid cell. Hence, Equation 3-1 becomes

$$(P_{DS} + O_{US}) = O_{DS} + E_{DS} + (1 - \alpha_{DS}) F_{DS} \tag{3-2}$$

where $P_{DS}$ = rainfall at a downstream grid cell, 3.2 grid cell inches is used in this study which roughly corresponds to 2-year, 24-hour storm depth in Montgomery County, MD
$O_{US}$ = cumulative upstream grid cell runoff in grid cell-inches
$O_{DS}$ = outflow or downstream grid cell runoff in grid cell-inches
$E_{DS}$ = evapotranspiration in grid cell-inches
$F_{DS}$= infiltration at the downstream grid cell in grid cell-inches
$\alpha_{DS}$=fraction of IMP at a given grid cell
= 0.01 *(IMP extracted from land cover or land use layer)

Assuming evapotranspiration $E_{DS}$ in Equation 3-2 is negligible during a storm event, it was not quantified. This study focuses primarily on a comparison of storm runoff response.

On the other hand, infiltration significantly affects the runoff process depending on soil properties that vary widely from place to place and in time (Beven, 2001). In this study, infiltration is presented by a hydrologic parameter: minimum infiltration rate (SCS, 1985). According to the NRCS-national engineering handbook (1985), the minimum infiltration rate is defined as "the rate at which water enters the soil at the surface and obtained for a bare soil after prolonged wetting". Once a soil map is prepared in the GIS-database, an assigned Hydrologic Soil Group (HSG) on each grid cell limits the degree of infiltration. Column 3 of Table 3-3 shows the mean of the range of the minimum infiltration rate at a given HSG. Since this study utilizes a 24-hour storm depth, the depths of infiltration during a given storm event are determined by multiplying 24 hours by the minimum infiltration rate. The minimum depths of infiltration during 24 hours are 9-, 5.4, 2.4-, and 0.6-inch for the HSG A, B, C and D, respectively. In order to determine the final depth of infiltration for each HSG, this study made two assumptions. The first assumption is that the process of infiltration is completed within individual cells before the runoff routing occurs. In other words, each grid cell does not recognize cumulative flow from upstream-grid cells during the infiltration-process. Therefore, infiltration should not occur beyond the rainfall of 3.2-inch. Since the potential depth of infiltration for HSG A during 24 hours exceeds the rainfall, this study constrains an upper limit so that the final depth of infiltration for HSG A is 3.2 inches. The second assumption is that the final depth of infiltration for HSG C, and D decreases in proportion to their relative quantities of the infiltration potential during 24 hours. Since the ratio of the potential depth of infiltration for HSG A to B to C to D is 9: 5.4: 2.4: 0.6, the relative infiltration-depths are 51.7% for A, 31% for B, 13.8% for C and 3.5% for D.

Considering 3.2-inch is the upper-limit for the HSG A, the second assumption in this study constrains other HSG proportionally so that upper-limits on the final depth of infiltration are 1.92-, 0.85-, 0.21-inch for HSG B, C, and D, respectively. In this study, such values are referred to as an "infiltration index", rather than infiltration. This is because these values do not describe real infiltration, but reflect relative tendencies of infiltration depending on HSG. For instance, placing a constraint on the upper-limit of infiltration is irrational in reality causing the overestimation of runoff when the water delivery rate exceeds the upper-limit.

Besides soil properties, another factor greatly affects infiltration capacity: impervious area. Infiltration decreases, thus, the runoff volume increases if IMP increases as expressed in Equation 3-2 with the term of $\alpha_{DS} F_{DS}$. This is true under the condition that the IMP mentioned in this study is directly-connected IMP. Once the runoff volume at each downstream grid cell is calculated using Equation 3-2, it accumulates toward the basin outlet. At the outlet, accumulated runoff is to be normalized by the total number of grid cells within each basin so that the comparison among basins will not be affected by the size of basins. Mathematically, Equation 3-2 at a given downstream grid cell becomes Equation 3-3 at the outlet of a basin. Figure 3-6 illustrates a schematic of the process using Equation 3-2.

$$Q_{outlet} = \frac{O_{DS,outlet}}{A} \tag{3-3}$$

where $Q_{outlet}$ = direct runoff in inches
$O_{DS, outlet}$ = accumulated direct runoff at the outlet in grid cell-inches
$A$ = basin area in number of grid cells

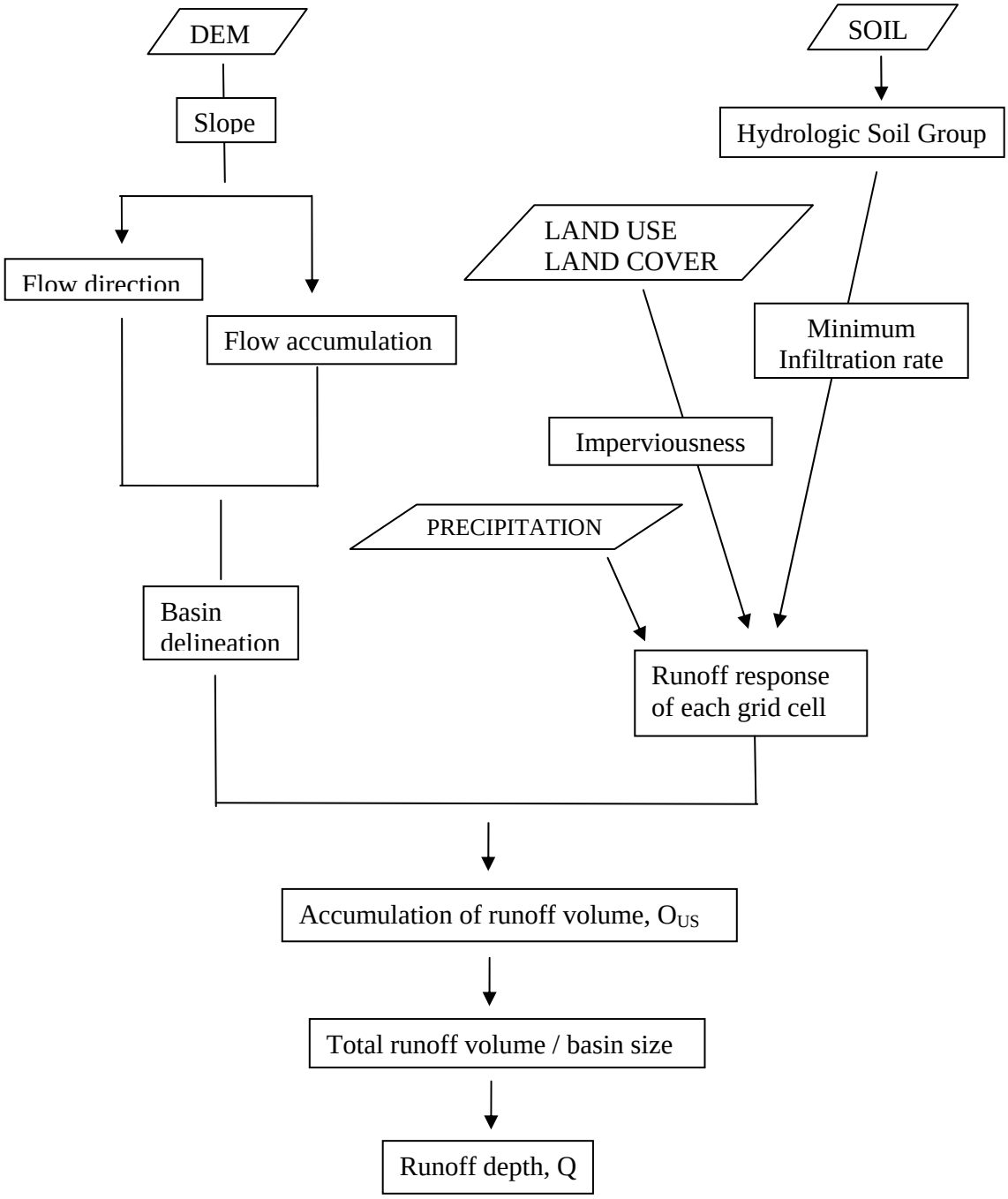


Figure 3-6. Flow chart of modeling a GIS-based IMP-descriptor using the water balance approach. This IMP-descriptor will produce indices of IMP through hydrological model developed based on the water balance approach.

### 3.5.2.2 Soil Conservation Service – curve number (SCS – CN) approach

Rather than taking into account only HSG into the infiltration process, this approach considers one more physical characteristic of the land surface: land use. In order to compute excess runoff volume for a given storm event using land use and infiltration as parameters, the Soil Conservation Service – curve number (SCS – CN) method is used in this study. The SCS-CN method is based on the water balance equation and two hypotheses: the first one states that the ratio of the amount of actual infiltration to the amount of the potential maximum retention equals the ratio of direct runoff to rainfall minus initial abstraction (Mishra and Singh, 1999). The second one states that the amount of initial abstraction is some fraction of the potential maximum retention. These are mathematically expressed in Equation 3-4, 3-5, and 3-6 respectively.

$$P = I_a + F + Q \tag{3-4}$$

$$\frac{Q}{P - I_a} = \frac{F}{S} \tag{3-5}$$

$$I_a = \lambda S \tag{3-6}$$

where $P$ = total precipitation in inches
$I_a$ = initial abstraction in inches
$F$ = cumulative infiltration retention or infiltration in inches
$Q$ = the direct runoff in inches
$S$ = the potential maximum retention in inches
$\lambda$ = empirical coefficient, commonly the value of 0.2 is assigned

If Equation 3-5 is combined with Equation 3-4, Equation 3-4 becomes Equation 3-7

$$Q = \frac{(P - 0.2S)^2}{P + 0.8S} \qquad \text{for } \lambda = 0.2 \tag{3-7}$$

The parameter S is a transformation of CN through the relationship (SCS, 1985),

$$S = (1000/CN) - 10 \quad (3\text{-}8)$$

As a model with one parameter, CN, Equation 3-7 offers some advantages for the purpose of this study. It is rather a simple model to calculate direct runoff volume for a given storm event, reflecting the effect of characteristics of basins such as soil type, land use/treatment, and antecedent moisture condition. Furthermore, the curve number for urban land uses reflects the effect of IMP on runoff volume (McCuen, 1998).

Although SCS already developed CN values for urban land uses based on assumed IMP for each urban land use, curve numbers can be computed with any value of IMP using Equation 3-9:

$$CN_{adj} = CN_p (1 - f) + CN_{imp} f \quad (3\text{-}9)$$

where $CN_{adj}$= the curve number adjusted by IMP
$CN_p$= the curve number for the pervious portion.
Values for open space with good condition: 39, 61, 74, and 80 for soil group A, B, C, and D, respectively
$CN_{imp}$= the curve number for the impervious area, which is 98
$f$ = the IMP fraction,
= 0.01 * (IMP extracted from land cover or land use layer)

In case this concept applies to the individual grid cells within a basin, runoff from the upstream grid cell as well as rainfall are both sources of an inflow to a given downstream grid cell (Moglen, 2000) resulting in Equation 3-10:

$$R_d = \left[ \frac{[(P_d + \Sigma R_u) - 0.2S_d]^2}{(P_d + \Sigma R_u) + 0.8S_d} \right] \qquad \text{for} \quad (P_d + \Sigma R_u) > 0.2S_d \qquad (3\text{-}10)$$

where $R_d$ = runoff leaving the downstream grid cell in grid cell-inches
$\Sigma R_u$ = the summation of the runoff from all immediately upstream grid cells in grid cell inches
$P_d$ = rainfall at a downstream grid cell, 3.2 grid cell inches is used in this study which corresponds to 2-year, 24-hour duration in Maryland
$S_d$ = the storage of the downstream grid cell in inches
= $(1000/CN_{adj,\,d}) - 10$

According to Moglen (2000), the term $\Sigma R_u$ is the summation of runoff from all immediate-upstream grid cells under the assumption that rainfall falling to the upstream grid cells holds until the flow in upstream grid cell is spatially routed to the outlet. Equation 3-10 is to be employed in this study except that the calculation of $R_d$ considers rainfall falling on upstream grid cells also to be a part of runoff volume toward the downstream grid cell. Further, this study assumes that infiltration is limited to the maximum inflow if infiltration exceeds rainfall so that the runoff volume at the downstream grid cell becomes at least zero, not negative. Figure 3-7 provides a schematic of this process.

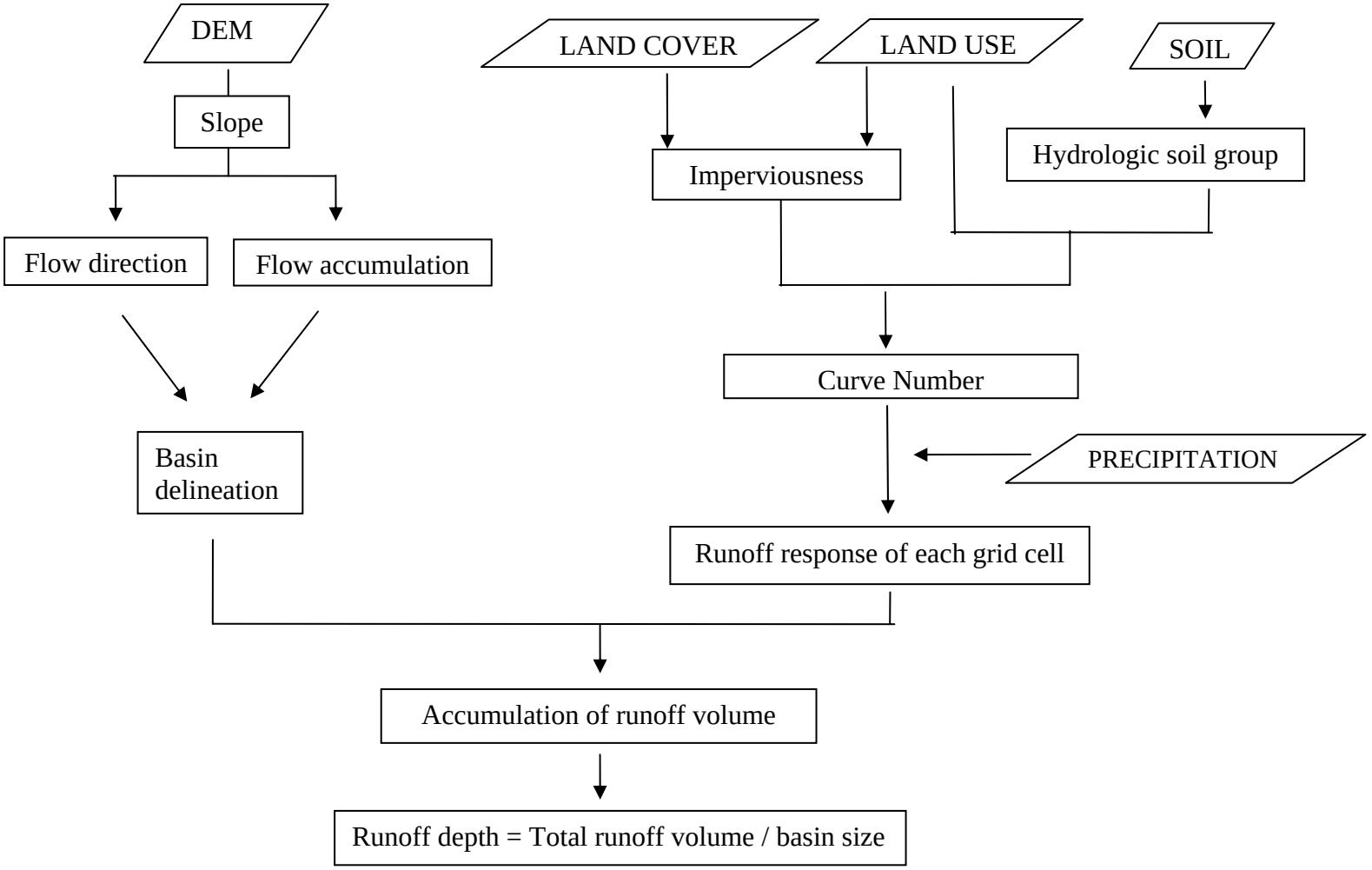


Figure 3-7. Flow chart of modeling a GIS-based IMP-descriptor using the SCS-CN approach. This IMP-descriptor will produce indices of IMP through hydrological models developed based on the SCS-CN method.

For the adjusted CN with IMP at a given grid cell, Equation 3-9 becomes Equation 3-11:

$$CN_{adj,d} = CN_{p,d}(1 - f_d) + CN_{imp} f_d \quad (3\text{-}11)$$

where $CN_{adj,d}$ = the curve number adjusted by IMP at a downstream grid cell

$CN_{p,d}$ = the curve number for the pervious portion at a downstream grid Cell values for open space with good condition: 39, 61, 74, and 80 for soil group A, B, C, and D, respectively

$CN_{imp}$ = the curve number for the impervious area at a downstream grid cell, which is 98

$f_d$ = the fraction of IMP at a downstream grid cell
= 0.01 * (IMP extracted from land cover or land use layer)

At the outlet, as seen in Equation 3-12, accumulated runoff is to be normalized by the total number of grid cells within each basin so that the comparison among basins is not affected by the size of basins. As described in the water balance approach, the quantity of $Q_{outlet}$ is to be compared among study basins.

$$Q_{outlet} = \frac{R_{d,outlet}}{A} \quad (3\text{-}12)$$

where $Q_{outlet}$ = direct runoff in inches

$R_{d,outlet}$ = accumulated direct runoff at the outlet in grid cell-inches

$A$ = basin area in number of grid cells

### 3.5.2.3 Modified approach for weighting

Neither, the water balance approach nor the SCS-CN approach, as seen in the previous section, reflects the effect of the proximity of the outlet to the location of the IMP. To take into account the distance relationship for the descriptors mentioned above, one more factor is considered: flow length. In this study, flow length is used to inversely

weight the IMP estimates at each grid cell. Mathematically speaking, the general formula to determine the weight in the inverse distance weight (IDW) method is the following:

$$\lambda_i = \frac{1}{d_{io}^{p}} \tag{3-13}$$

where $\lambda_i$ weight assigned to a given grid cell, $i$
$d_{i0}$ = flow length from the outlet to a given grid cell
$p$ = power parameter, 2 is used in this study

Equation 3-13 is combined with Equation 3-2 for the weighted water balance approach and with Equation 3-11 for the weighted SCS-CN approach.

$$O_{DS} = (P_{DS} + O_{US}) - E_{DS} - (F_{DS} - \lambda_{DS}\ \alpha_{DS} F_{DS}) \tag{3-14}$$

$$CN_{adj,\,d} = CN_p\,(1 - \lambda_d f_d) + CN_{imp}\,\lambda_d f_d \tag{3-15}$$

### 3.6 Indicators of the hydrological response

As mentioned in Section 3.5, the second and third objectives are to examine characteristics of IMP and its impacts on hydrological response. Indicators of observed hydrological response are needed in order to compare observed responses with indices of IMP generated by IMP-descriptors. For this study, the hydrological response to IMP is observed from two perspectives: the impact on water quantity and on water quality. As illustrated in Figure 3-8, flow variability (or flashiness) is employed as an indicator of water quantity change and thermal variability (stream temperature variation) is used as an indicator of water quality change. In order to examine flow variability, indices such as $R_{Q10\text{-}90}$, $R_{L1}$, $I_{R\text{-}B}$, and CV are calculated, whereas daily mean temperature difference,

DD, and $D_{SURGE}$ are calculated for the evaluation of thermal variability. These are defined below.

### 3.6.1 Indicators of flow variability

***R-B index*** **($I_{R\text{-}B}$)** Richards-Baker Flashiness Index developed by Baker et al. (2004) measures variability in flow between flood and baseflow. Baker and others derived this index by dividing the sum of the absolute value of daily change in *Q* by total *Q* for the corresponding time period as shown in Equation 3-16,

$$\frac{\sum_{i=1}^{n} |Q_i - Q_{i-1}|}{\sum_{i=1}^{n} Q_i} \tag{3-16}$$

where $Q_i$ =mean daily flow in cfs for a given day, *i*
*n* = number of days of recorded data at a given gauging station

***Coefficient of variation*** **(CV)** measures relative variability by dividing standard deviation of the daily mean flows by mean of daily mean flow.

$$CV = \frac{\sqrt{\frac{\sum_{i=1}^{n} Q_i^2 - \frac{\left(\sum_{i=1}^{n} Q_i\right)^2}{n}}{n}}}{\frac{\sum_{i=1}^{n} Q_i}{n}} \tag{3-17}$$

where $Q_i$ =mean daily flow in cfs for a given day, *i*
*n* = number of recorded days at a given gauging station

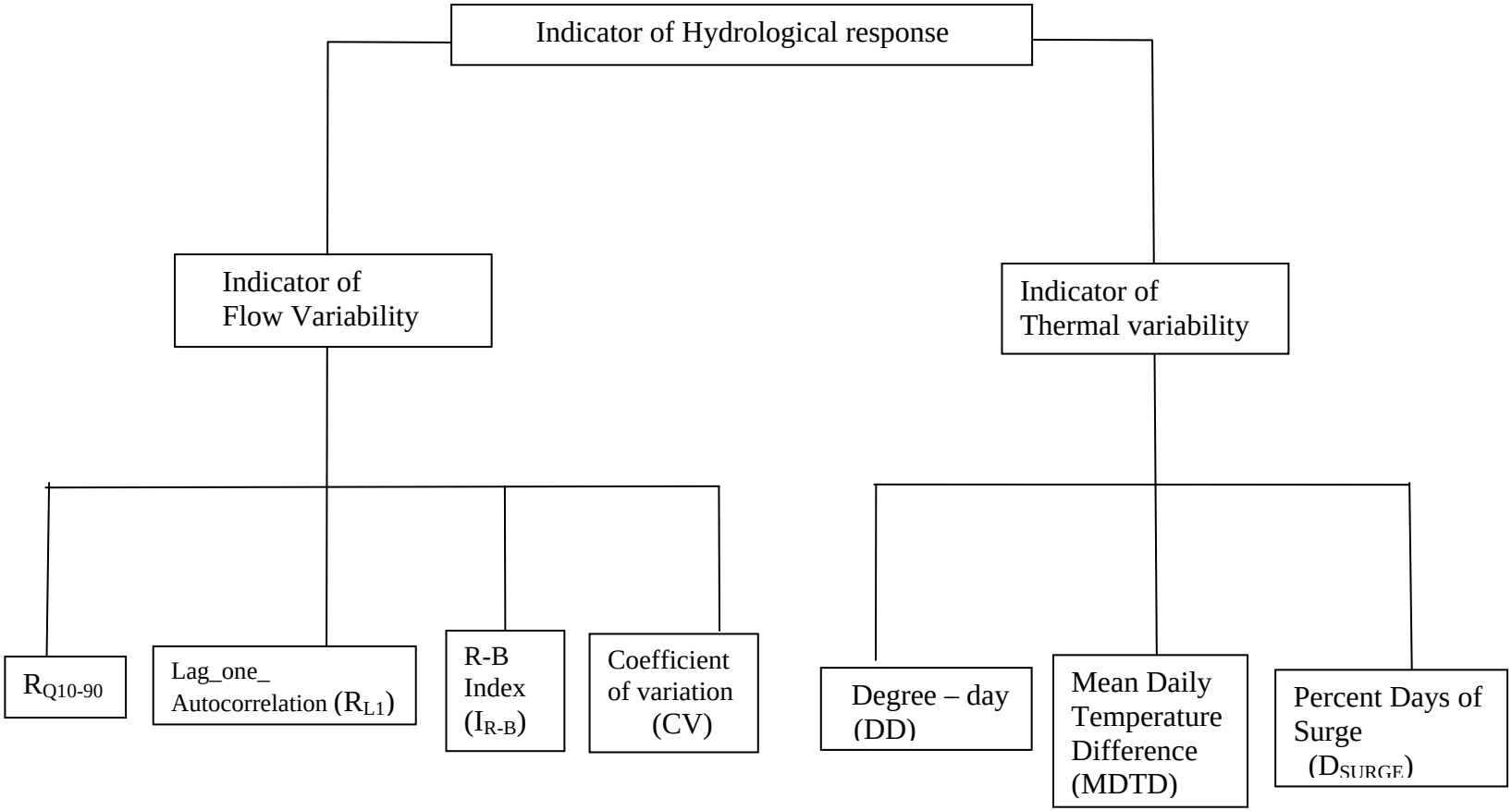


Figure 3-8. Indicators of hydrological response in the flow regime and thermal regime. Indices such as $R_{Q10-90}$, $R_{L1}$, $I_{R-B}$, or CV indicate flow variability, while indices such as MDTD, DD, or $D_{SURGE}$ indicates stream temperature change (thermal variability). $R_{Q10-90}$: Ratio of the discharge which is equaled or exceeded10% of the time to the discharge which is equaled or exceeded 90% of the time; $R_{L1}$: Lag-one autocorrelation; $I_{R-B}$: R-B index which measures relative mean daily flow change; CV: coefficient of variation. DD: Degree-day; $D_{SURGE}$: Percent days with surge; MDTD: Mean daily temperature difference.

***Lag- one autocorrelation*** **($R_{L1}$)** measures the degree of correlation between values separated by one time interval, meaning adjacent values (McCuen, 2003).

$$R_{L1} = \frac{\Sigma_{i=1}^{n-1} Q_i Q_{i+1} - \frac{1}{(n-1)}\left(\Sigma_{i=1}^{n-1} Q_i\right)\left(\Sigma_{i=2}^{n} Q_i\right)}{\left[\Sigma_{i=1}^{n-1} Q_i^2 - \frac{1}{(n-1)}\left(\Sigma_{i=1}^{n-1} Q_i\right)^2\right]^{0.5}\left[\Sigma_{i=2}^{n} Q_i^2 - \frac{1}{(n-1)}\left(\Sigma_{i=2}^{n} Q_i\right)^2\right]^{0.5}} \qquad (3\text{-}18)$$

where $Q_i$ = mean daily flow in cfs for a given day, $i$
$n$ = number of recorded days at a given gauging station

$\boldsymbol{R_{Q10\text{-}90}}$ is the ratio of the discharge which is equaled or exceeded 10% of the time to the discharge which is equaled or exceeded 90% of the time (Baker et al., 2004). The higher the value of $\boldsymbol{R_{Q10\text{-}90}}$, the greater the flow variability.

$$\boldsymbol{R_{Q10\text{-}90}} = \frac{Q_{10}}{Q_{90}} \qquad (3\text{-}19)$$

### 3.6.2 Indicators of thermal variability

***Percent days with surge*** **($D_{SURGE}$)** measures days of summer surges in percent and indicates the effect of temperature transferred from the runoff heated while passing through the radiant-absorbing impervious area.

$$\left(\frac{\sum S}{N}\right) * 100 \qquad (3 - 20)$$

where $S$ is the number of 2-degree temperature surges
$N$ is the number of summer days at a given basin

Nelson, who recorded the stream temperature data used in this study, also quantified a temperature surge: the temperature-jump more than 2 degrees in Celsius within a single 30-minute interval (Nelson, submitted). For instance, Figure 3-9 depicts a temperature surge caused by an afternoon thunderstorm event. According to Nelson, who recorded the stream temperature for a separate project, the temperature shows a typical diurnal curve for the second day (June 29) in Figure 3-9. However, the diurnal curve was interrupted on June 28th when the discharge increased by a storm runoff.

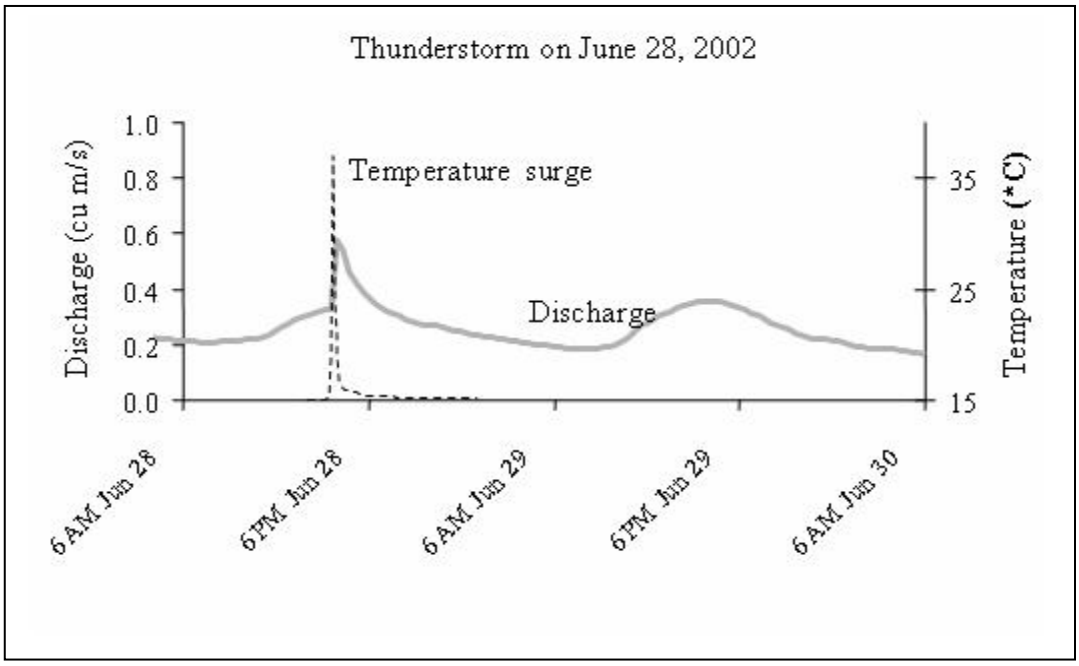


Figure 3-9. An example for a temperature surge by heated runoff during a summer storm (adapted from Nelson, submitted).

***Degree-day*** **(DD)** measures the deviation from the standard/or threshold value at a given day. Due to the lack of availability of temperature datasets, the calculation of the cumulative surge temperatures over a season is beyond the scope of this study.

Therefore, the index is utilized to measure a mean surge magnitude only during summer surges as expressed in Equation 3-21.

$$\frac{\sum_{i=1}^{n}(T_{i,SURGE} - T_{i,PRE-SURGE})}{n} \qquad (3-21)$$

where $T_{i,\ SURGE}$ is a maximum temperature of a surge in Celsius on a given day, *i*
$T_{i,\ PRE\text{-}SURGE}$ is the temperature before and after a surge on a given day, *i*
*n* is the number of summer surges occur in a given basin

***Mean daily temperature difference*** **(MDTD)** measures an average daily temperature range in a given basin.

$$\frac{\sum_{i=1}^{N}(T_{i,MAX} - T_{i,MIN})}{N} \qquad (3-22)$$

where $T_{i,\ MAX}$ is a maximum temperature in Celsius on a given day, *i*
$T_{i,\ MIN}$ is a minimum temperature in Celsius on a given day, *i*
*N* is the number of summer days in a given basin

### 3.7 Assessment of Relationships between IMP-descriptors and Indicators of hydrological response

***Regression analysis:*** will be utilized to quantify the relationship between IMP-descriptors and indicators of hydrological response. Power model structures will be calibrated by a numerical optimization method. In this study, a program called NUMOPT developed by McCuen (1993) is employed. Linear model structures will be

calibrated by a statistical optimization method which uses the principle of least squares analytically.

***Reliability of regression equations:*** will be assessed by goodness-of-fit measures which indicate the prediction accuracy. For linear regression equations, the coefficients of determination, $R^2$ will be evaluated as expressed in Equation 3-23.

$$R^2 = \frac{\left(\Sigma xy - \frac{\Sigma x \Sigma y}{n}\right)}{\left(\Sigma x^2 - \frac{(\Sigma x)^2}{n}\right)\left(\Sigma y^2 - \frac{(\Sigma y)^2}{n}\right)} \quad (3\text{-}23)$$

where $x$ = predictor, indices of IMP in this study
$y$ = criterion variable, indicators of hydrological response in this study
$n$ = number of observations:
35 for the flow regime analysis
13 for the thermal regime analysis at the basin scale
8 for the thermal regime analysis at the sub-basin scale

The relative standard error, Se/Sy will be assessed for power models.

$$Se/Sy = \frac{\left[\frac{1}{n-p-1}\sum_{i=1}^{n}(y_i - \hat{y}_i)^2\right]^{0.5}}{\left[\frac{1}{n-1}\sum_{i=1}^{n}(y_i - \bar{y}_i)\right]^{0.5}} \quad (3\text{-}24)$$

where $n$ = number of observations
$p$ = number of predictor variables
$y_i$ = the $i^{th}$ observed criterion
$\hat{y}_i$ = the $i^{th}$ predicted criterion
$\bar{y}$ = Mean value of observed criterion

### 3.8 Summary

This chapter described data collection, study sites and an experiment designed for comparing IMP-LU and IMP-LC. The relationships between these two quantities, IMP-LU and IMP-LC will be investigated to accomplish the first objective described in Chapter 1.

Various models as IMP-descriptors using IMP-LU or IMP-LC as parameters were developed, while indicators of hydrological response, flow variability and thermal variability, were selected and defined. Indicators of hydrological response are regressed on indices of IMP, which allows indices of IMP to be predictors of flow variability and thermal variability. Goodness-of-fit measures of regression equations are assessed to address the second and third objectives described in Chapter 1. The results will be discussed in Chapter 4.

# CHAPTER FOUR

# THE SENSITIVITY OF THE HYDROLOGICAL RESPONSE TO IMPERVIOUSNESS

## 4.1 Overview

In order to examine characteristics and impacts of IMP on hydrological response, three objectives were specified in Chapter 1. The first objective was to develop equations to translate between IMP-LU and IMP-LC. The second was to identify a better predictor of hydrological response, either IMP-LU or IMP-LC. The third was to determine whether lumped or spatially distributed IMP is the better at predicting hydrological response.

The first section in this chapter will explore the main concern in using IMP as a predictor of hydrological response: IMP is sensitive to measuring methods and data sources. The relationship between IMP datasets based on different data sources, one from land use (IMP-LU) and another from land cover (IMP-LC) will be examined. This will lead to the development of conversion equations between these two different datasets. After indicators of hydrological response are regressed on indices of IMP, indices of IMP as predictors of hydrological response will be assessed. Hydrological models of IMP-descriptors will also be evaluated. Hydrologic indices indicating flow variability and thermal variability will be compared in light of detecting hydrological response. All analyses and evaluations will be carried out and compared under two circumstances: using IMP extracted from land use (IMP-LU) and from land cover (IMP-LC).

## 4.2 Comparison of imperviousness estimates

### 4.2.1 Effect of aggregating imperviousness

The experiment is designed such that the study site is divided into numerous grid sampling cells as seen in Figure 3-4. To assess the effect of aggregating IMP at different scales, the grid sampling cell is aggregated and resampled from 0.25km to 10km. At a given grid sampling cell size, an aggregate IMP for each grid sampling cell is calculated by averaging all IMP values from 30 meter grid cells which are mapping units of IMP datasets, IMP-LU or IMP-LC. It is also informative to compare aggregate IMP based on two different IMP datasets: one extracted using land use (IMP-LU) and the other using land cover (IMP-LC).

The range of aggregate IMP from individual grid sampling cells over the study site are affected by aggregating scales from 0.25km to 10km as seen in Table 4-1. According to the procedures described in Sections 3.4.1.1 and 3.4.1.2, the range of IMP-LU is from 0 % to 85 % at 30-meter pixel resolution, whereas the scale of IMP-LC is from 0% to 100% at a 30-meter resolution. As the grid sampling cell size becomes larger, the area that is aggregated to produce an averaged value of IMP increases. Hence, information at a 30-meter mapping unit level becomes lost. For example, the highest value of aggregate IMP at a 10km of grid sampling cell size was only 52.1% which does not reflect the highest value of aggregate IMP using IMP-LU at 30-meter resolution. The same tendency appears using IMP-LC as seen in Table 4-1. Once the size reaches 1km x 1km, however, resampling from 1km to smaller size does rarely affect the range of aggregate IMP, either based on IMP-LU or IMP-LC.

Table 4-1. Effect of aggregating scales on the range of aggregate IMP from all individual grid sampling cells over the study area illustrated in Figure 3-4.

| Grid sampling cell size, km | The range of aggregate IMP | |
|---|---|---|
| | Based on IMP-LU | Based on IMP-LC |
| 10 x 10 | 0.0 ~ 52.1 | 0.0 ~ 48.3 |
| 5 x 5 | 0.0 ~ 60.0 | 0.0 ~ 70.9 |
| 2.5 x 2.5 | 0.0 ~ 77.5 | 0.0 ~ 81.1 |
| 1.0 x 1.0 | 0.0 ~ 85.0 | 0.0 ~ 95.0 |
| 0.8 x 0.8 | 0.0 ~ 85.0 | 0.0 ~ 95.0 |
| 0.25 x 0.25 | 0.0 ~ 85.0 | 0.0 ~ 99.0 |

To examine the relationship between IMP-LU and IMP-LC, these two quantities are plotted at various grid sampling cell sizes. For instance, Figures 4-1 (a) - (c) depict the relationships at 10 km x10 km, 1 km x1 km, and 0.25 km x 0.25 km, respectively. As the size becomes smaller, the degree of data-scatter increases as seen in Figure 4-1. In order to explain the scatter statistically, regression analysis is employed. This study assumes that a power model structure shown in Equation 4-1 is appropriate to represent the data illustrated in Figure 4-1.

$$\text{IMP-LU} = a^{*}\ \text{IMP-LC}^{\,b} \qquad (4\text{-}1)$$

where a, b = regression coefficients
IMP-LU = criterion variable in percent
IMP-LC = predictor variable in percent

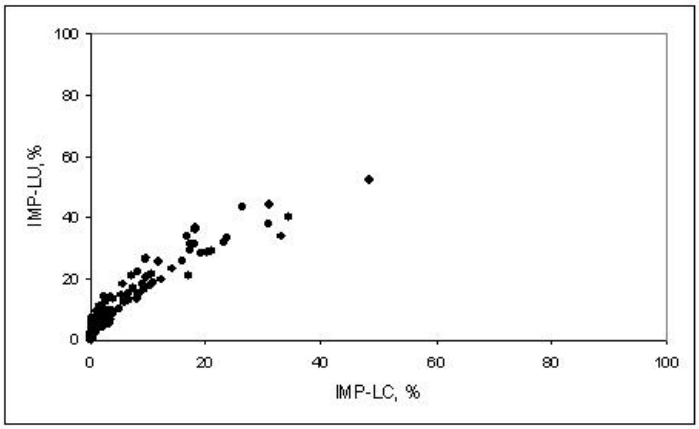


(a)

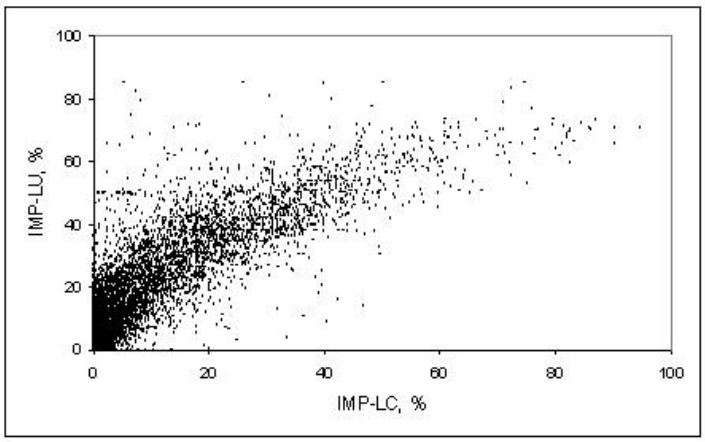


(b)

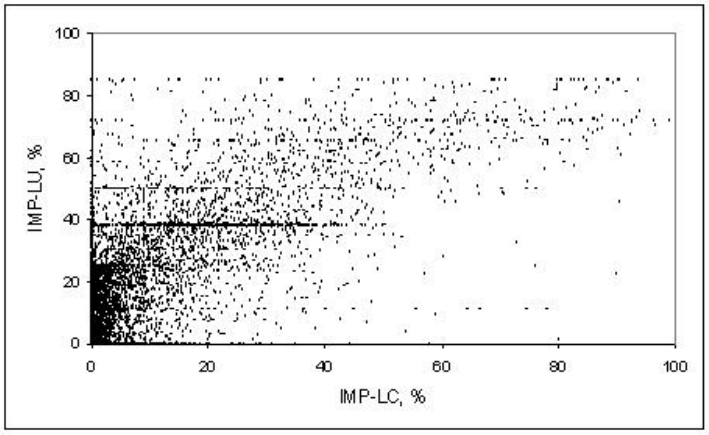


(c)

Figure 4-1. Aggregate IMP based on IMP-LU versus aggregate IMP based on IMP-LC at a different grid sampling cell size:
(a) 10x10 $km^2$ (b) 1x1 $km^2$ (c) 0.25x0.25 $km^2$.

Equation 4-1 is calibrated using the numerical optimization method that optimizes a model for the lowest relative standard error, Se/Sy, and the smallest relative bias, $\bar{e}/\bar{y}$ (McCuen, 1993). The purpose of utilizing the numerical optimization method is to calibrate a power model structure without transforming a criterion variable into the log domain. Table 4-2 summarizes the goodness-of-fit statistics for the six calibrated models. Both standard deviation, Sy, and standard error of the estimate, Se, increase such that Se/Sy increases as the grid sampling cell size becomes smaller. Prior to quantifying the relationship between IMP-LU and IMP-LC, a grid sampling cell size should be selected such that the minimum variance of IMP-LU should appear at a given value of IMP-LC (or vice versa) at the selected resolution.

Table 4-2. Summary of the goodness-of-fit statistics for the calibrated regression models using Equation 4-1 at different grid sampling cell sizes.

| Grid sampling cell size, km | Se (%) | Sy (%) | Se/Sy | a | b |
|---|---|---|---|---|---|
| 10 x 10 | 1.8632 | 7.4272 | 0.2509 | 0.0937 | 1.5539 |
| 5 x 5 | 2.7575 | 8.5227 | 0.3236 | 0.0781 | 1.5883 |
| 2.5 x 2.5 | 3.3378 | 8.9487 | 0.3730 | 0.0797 | 1.5664 |
| 1.0 x 1.0 | 4.4925 | 9.8675 | 0.4552 | 0.0953 | 1.4875 |
| 0.8 x 0.8 | 4.8000 | 10.1494 | 0.4729 | 0.0750 | 1.5430 |
| 0.25 x 0.25 | 6.9153 | 11.6571 | 0.5932 | 0.0513 | 1.5946 |

Considering the loss of information at the mapping unit level by aggregating IMP as seen in Table 4-1 and goodness-of-fit measures as shown in Table 4-2, the model at the cell size of $1km^2$ is suitable to quantify the relationship between IMP-LU and IMP-LC. According to Table 4-1, aggregate IMP at a grid sampling cell size greater than 1km does not reflect 30-meter –mapping-unit-based spatial heterogeneity within a given grid

sampling cell. On the other hand, visual interpretation of Figure 4-1and the goodness-of-fit statistics in Table 4-2 imply that the effect of data-scatter increases as aggregating scale becomes finer. Therefore, the grid sampling cell size of 1km achieves a desirable balance between the degree of data-scatter and the loss of information of spatial heterogeneities at 30-meter resolution.

### 4.2.2 Differences between IMP-LU and IMP-LC

In order to illustrate the difference in aggregate IMP depending on data sources of IMP, this study utilizes two different IMP datasets, IMP-LU and IMP-LC. IMP-LU was prepared using coefficients by land use categories, while IMP-LC refers to the impervious cover based on satellite-derived land cover. Figure 4-1(b) illustrates the difference between aggregate IMP based on IMP-LU and aggregate IMP based on IMP-LC at a grid sampling cell size of 1km. IMP-LU tends to produce larger estimates than IMP-LC for 0% to 55% of IMP which corresponds to several land cover categories including “developed and low-intensity” and “developed and open space” as shown in Table 3-9. The categories include large-lot single family housing units, parks, golf courses, and single family housing units based on the definition of land cover categories (Homer et al., 2003). These correspond to 2-ac residential, ½-ac residential, ¼-ac residential, and open urban land according to the land use categories developed by NRCS (formerly SCS).

A possible explanation for the tendency of IMP-LU to produce larger estimates than IMP-LC for “developed and low-intensity” categories is as follows. IMP-LC is estimated using land cover derived from remotely sensed data, satellite imagery.

Considering the fact that ¼-acre equals approximately 1000 $m^2$ which is approximately the size of a single pixel on satellite imagery with 30-meter resolution, it is natural to conclude that satellite imagery cannot identify impervious features smaller than this. The scale of IMP variation is smaller than the measurement scale, causing the tendency to underestimate IMP. For instance, any roads narrower than 30-meter in width which occur in ½-ac residential, or ¼-ac residential areas may not be identified by the satellite imagery with a 30-meter spatial resolution. As a result, virtually no IMP is assigned to these features. Even roads that are wider than 30-meter can not be properly sensed by satellite imagery unless the acquisition of the remotely sensed data occurs during leaf-off season. In other words, the canopy of trees blocks a view of the ground. On the contrary, IMP-LU is estimated using land use. The same features, any roads narrower than 30-meter, are assigned to 25% or 38% of IMP if the surrounding area belongs to the land use category of ½-ac residential and ¼-ac residential, respectively. Therefore, IMP-LU shows larger IMP estimates than IMP-LC.

The difference between the two depictions of IMP is that a certain feature cannot be recognized as impervious cover depending on its size and reflectance based on land surface features only, at least with current spatial and spectral resolutions. By using land use information, however, a certain feature is considered as a part of urban infrastructure and a contributor to IMP accordingly. The size or reflectance of IMP would not affect these assigned values as long as it belongs to a given land use category. As a consequence, IMP-LC tends to produce smaller estimates of IMP compared to IMP-LU over areas of lower intensity development.

For “developed and open space” categories, the assigned IMP from IMP-LC varies from zero to 20%, while IMP-LU assigns a uniform value of 12%. Although assigned values do not imply a tendency to underestimate, Figure 4-1 (b) indicates the trend exists. It depicts relative underestimation of IMP-LC for 0% to 55% where the “open urban land” category falls in. In addition to the spatial resolution issue mentioned above, the underestimation phenomenon can be explained by the part of the algorithm in producing IMP-LC dataset: filtering. Figure 4-2 shows a lack in the number of pixels with IMP between 4 and 10% relative to the rest of the distribution of IMP. As explained by one of the algorithm developers (Chengquen Huang, personal communication), the filtering process was set up so that a pixel would be filtered as described below if an isolated pixel is identified which belongs to a different land cover category from its surrounding neighbors and shows a value of less than 10% IMP.

For example, in an initial procedure, the algorithm searches for pixels surrounded by forest pixels with less than 10% IMP. The IMP of such pixels is replaced with zero since the likelihood of locating IMP in the middle of forest is considered irrational. As a result, IMP-LC shows no IMP for such a pixel, whereas IMP-LU might suggest the site as a park. As such, an IMP value of 12% would be assigned for the pixel. With remotely sensed data, it is a daunting task to distinguish a pixel representing paved ground in a park from a pixel representing bare soil in forest, based on the reflectance signatures of spectral bands at current resolutions. This pixel may have an IMP of 12%, based on the land use category of open urban land or this pixel may not have any IMP according to the land cover category of forest. The filtering process may help prevent errors of commission, but it may also cause errors of omission. This is an example of the

difference between IMP-LU and IMP-LC. A quantitative relationship between these two representations of the landscape will be discussed in the following section.

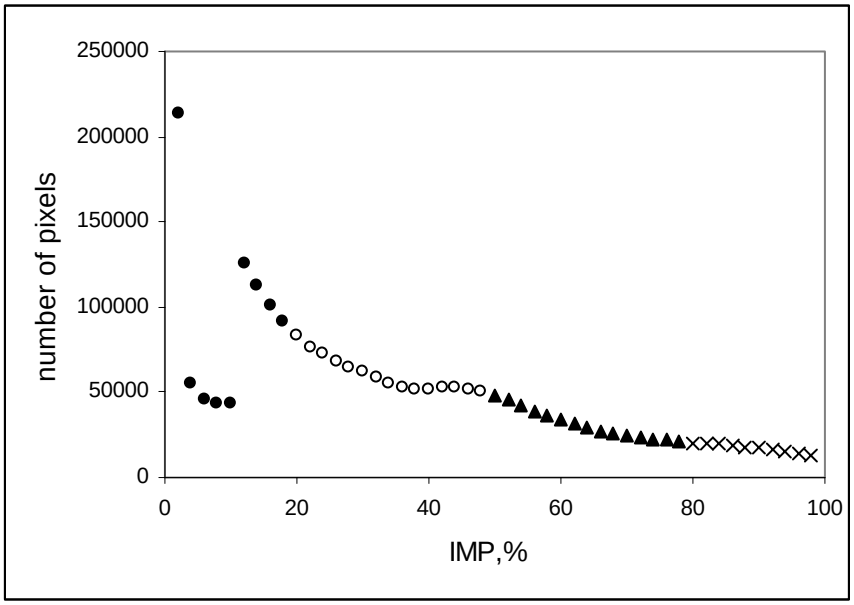


Figure 4-2. Distribution of IMP based on IMP-LC. A pixel refers to a mapping unit of IMP-LC. The unit equals to a spatial resolution of 30m x 30m. The number of pixels decreases gradually, as pixels show high IMP for urban land cover categories except the class of "developed and open space (●) ".
Developed and open space (●), Developed and low intensity (○), Developed and medium intensity (▲), Developed and high intensity (x)

### 4.2.3 Relationship between IMP-LU and IMP-LC

In order to determine the relationship between IMP-LU and IMP-LC, power model structures as expressed in Equation 4-1 and Equation 4-2 were calibrated. The regression model in Equation 4-1 is a useful tool when IMP-LC is available and IMP-LU needs to be estimated. The regression model in Equation 4-2 is for predicting IMP-LC from IMP-LU.

$$\text{IMP-LC} = c^{*}\ \text{IMP-LU}^{d} \quad (4\text{-}2)$$

where c, d = regression coefficients
IMP-LC = criterion variable in percent
IMP-LU = predictor variable in percent

To avoid the sensitivity to initial estimates of the regression coefficients on the calibration process, the numerical optimization method is repeated several times so that the calibrated outcome resulting from the first round becomes an initial estimate for the next round. Iteration continues until the input and output remains the same or the goodness-of-fit statistics are unchanged. The desirable criteria to evaluate the reliability of non-linear models are to minimize errors and to have no bias (McCuen, 2003). The coefficients in Equations 4-1 and 4-2 are calibrated, resulting in Equation 4-3 and Equation 4-4. They are calibrated based on data with IMP greater than 2%, on the assumption that an area with less than 2% of IMP is rural. According to goodness-of-fit statistics shown in Table 4-3, the relative standard error, Se/Sy is about 0.5 for both models. The regression analysis improves the reliability of prediction by one-half. Equations 4-3 and 4-4 are useful for translating between estimates of IMP-LU and IMP-LC.

$$\text{IMP-LU} = 6.63\ (\text{IMP-LC})^{0.55} \quad (4\text{-}3)$$

$$\text{IMP-LC} = 0.08\ (\text{IMP-LU})^{1.54} \quad (4\text{-}4)$$

Table 4-3. Goodness-of-fit statistics for Equation 4-3 and 4-4 at a grid sampling cell size of 1x1 $km^2$

| Regression Model | Goodness-Of-Fit Statistics | | | |
|---|---|---|---|---|
| | Bias, % | Se, % | Sy, % | Se/Sy |
| Equation 4-3 | 0.10 | 9.46 | 16.96 | 0.55 |
| Equation 4-4 | 0.11 | 6.37 | 12.88 | 0.49 |

This study has so far indicated that IMP-LU and IMP-LC are different in that IMP-LC produces lower estimates of IMP relative to IMP-LU for 0% to 55% of IMP. IMP-LC is an impervious cover based on satellite-measured reflectance. IMP-LU is an impervious cover based on coefficients, assigned values of IMP by land use categories. One way of determining coefficients for individual land use categories is to utilize values which were used in the SCS-CN method employed by the NRCS as seen in Table 3-8. It is referred to as SCS-coefficient. In the SCS-CN method, each coefficient for a given land use category is an estimate based on ancillary data, not from direct measurements. The next section discusses a direct measurement method to obtain precise values of IMP as a coefficient at a given land use category. Direct measurement method will then be compared with IMP-LU and IMP-LC.

### 4.2.4 Effect of measuring methods

The purpose of the study conducted by Capiella and Brown (2001) was to assign precise coefficients to individual land use categories. Their study areas were limited to suburban landscapes to report only recent suburban development. Coefficients for individual land use categories were determined either by actual inspection of fine-scale aerial photos or by field survey. Table 4-4 summarizes IMP for various land use categories and their corresponding land cover categories, using different measurement methods: assumed IMP fractions (SCS-coefficients) by land use categories (IMP-LU), directly measured coefficients by land use categories (IMP-C&B), and IMP from satellite-derived land cover (IMP-LC). It indicates that using the direct measured

coefficients, IMP-C&B assigns the lowest IMP among three different measurement methods for all land use categories examined.

Table 4-4. Imperviousness by land use and land cover classes. IMP-LU refers to imperviousness using SCS-coefficients, and IMP-C&B refers to imperviousness using planimetric coefficient, and IMP-LC refers to imperviousness using satellite-derived land cover

| Land cover category by USGS | Land use category by NRCS | IMP | | |
|---|---|---|---|---|
| | | IMP-LU | IMP-C&B | IMP-LC |
| Open Urban | | 12 | 10 | <20 |
| Low Density Residential | Residential (1/2 ac) | 25 | 21.2 | 20-49 |
| Medium Density Residential | Residential (1/4 ac) | 38 | 27.8 | 50-79 |
| High Density Residential | Less than 1/8 ac | 65 | 44.4 | 80-100 |
| Institutional | -- | 50 | 34.4 | -- |
| Commercial | Commercial | 85 | 72.2 | 80-100 |
| Industrial | Industrial | 72 | 53.4 | 80-100 |

At the grid sampling cell size of 1km which was used in the previous section, an aggregate IMP was calculated on individual grid sampling cells over the same study area as shown in Figure 3-4. The calculation is based on two different IMP datasets, IMP-LC and IMP-C&B. Figure 4-4 shows IMP-C&B as a function of IMP-LC. The numerical optimization method is utilized to calibrate the following power model,

$$\text{IMP-C\&B} = 5.21\ (\text{IMP-LC})^{0.53} \qquad (4\text{-}5)$$

Table 4-5. Goodness-of-fit statistics for Equation 4-5 at a grid sampling cell size of 1x1 $km^2$

| Regression Model | Bias, % | Se, % | Sy, % | Se/Sy |
|---|---|---|---|---|
| Equation 4-5 | -0.35 | 4.64 | 10.60 | 0.44 |

As seen in Table 4-5, the relative standard error, Se/Sy is less than 0.5, indicating that the reliability of prediction is improved by regression analysis. Compared to IMP-LU, in general, IMP-C&B produces lower aggregate IMP over individual grid sampling cells as depicted in Figure 4-3.

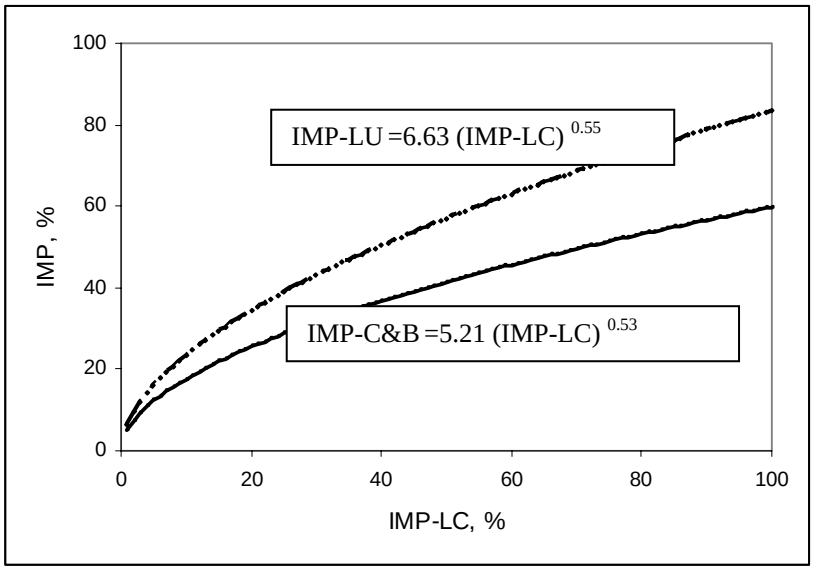


Figure 4-3. IMP-LU (---) and IMP-C&B (—) as a function of IMP-LC at a grid sampling cell size of 1$km^2$.

### 4.2.5 Summary

Thus far, aggregate IMP has been assessed using different data sources of IMP: land use and land cover. This assessment led to identify the relationship between two different IMP datasets and develop regression equations to convert IMP from one data source which is readily available for a geographic area to the other. This study also

revealed that the IMP dataset based on assumed SCS-coefficients by land use categories tends to produce higher IMP than that based on directly measured coefficients. Next section will present models developed in this study to describe IMP in various ways using such different IMP datasets.

### 4.3 IMP-descriptors

Figure 3-5 illustrated IMP-descriptors designed to generate indices of IMP. As summarized in Table 4-6, the first two descriptors are aggregate IMP: basin-averaged values of IMP extracted using IMP-LU and IMP-LC. They represent lumped models without hydrological processes involved. The other IMP-descriptors are use IMP as a parameter in a hydrological process. They represent spatially distributed hydrological models. Indices will be computed through these IMP-descriptors using two IMP datasets, IMP-LU and IMP-LC, over study sites selected for the flow regime analysis and the thermal regime analysis.

Because study areas chosen for the flow regime analysis are different from those for the thermal regime analysis as described in Chapter 3, indices of IMP are reported separately. IMP-descriptors using IMP-LU generated indices of IMP over individual study basins for the flow regime analysis are summarized in Table 4-7. Table 4-8 summarizes indices of IMP generated by IMP-descriptors using IMP-LU over study basins for the thermal regime analysis. Tables 4-9 and 4-10 summarize indices of IMP using IMP-LC over study basins for flow regime and thermal regime analysis, respectively.

Table 4-6. IMP-descriptors based on various approaches as seen in Figure 3-5. They include aggregate IMP. Hydrological models are also developed to describe IMP through hydrological process.

| Approach | | | | Name of IMP-descriptor used in this study |
|---|---|---|---|---|
| Lumped | Land use | | | Avg-IMP-LU |
| | Land cover | | | Avg-IMP-LC |
| Spatially Distributed | Water-balance | Non-weight on proximity | Land use | WB-LU |
| | | | Land cover | WB-LC |
| | | Inverse square distance | Land use | WB-ID-LU |
| | | | Land cover | WB-ID-LC |
| | SCS-CN | Non-weight on proximity | Land use | SCS-CN-LU |
| | | | Land cover | SCS-CN –LC |
| | | Inverse square distance | Land use | SCS-CN -ID-LU |
| | | | Land cover | SCS-CN-ID-LC |

Table 4-7. Indices of IMP generated by various IMP-descriptors (a)-(e) over study basins selected for the flow regime analysis.
Avg-Imp-LU is aggregate IMP at a given basin. WB-LU or SCS-CN-LU are hydrological models using IMP-LU. Indices reflecting spatial proximity of IMP to outlets use "-ID-" in their symbols.

| Basin | Basin ID | (a)Avg Imp-LU | (b)WB-LU | (c)WB-ID-LU | (d)SCS-CN-LU | (e)SCS-CN-ID-LU |
|---|---|---|---|---|---|---|
| | | IMP, % | Q, inch | Q, inch | Q, inch | Q, inch |
| 1 | 1581700 | 9.24 | 1.7262 | 1.5800 | 1.1001 | 0.9571 |
| 2 | 1583100 | 3.59 | 1.4849 | 1.4267 | 1.0803 | 1.0228 |
| 3 | 1583500 | 2.90 | 1.4954 | 1.4484 | 1.0730 | 1.0302 |
| 4 | 1583600 | 22.71 | 1.8559 | 1.4925 | 1.0992 | 0.6979 |
| 5 | 1584050 | 5.57 | 1.5842 | 1.4882 | 1.1389 | 1.0503 |
| 6 | 1584500 | 5.28 | 1.5797 | 1.4928 | 1.0400 | 0.9617 |
| 7 | 1585090 | 42.44 | 2.3818 | 1.8188 | 1.4793 | 0.7519 |
| 8 | 1585095 | 40.97 | 2.5991 | 2.2452 | 1.6001 | 0.9694 |
| 9 | 1585100 | 39.20 | 2.3647 | 1.8759 | 1.4918 | 0.8330 |
| 10 | 1585200 | 41.27 | 2.2762 | 1.6564 | 1.3713 | 0.6513 |
| 11 | 1585225 | 41.18 | 2.1403 | 1.6316 | 1.2332 | 0.6573 |
| 12 | 1585230 | 44.05 | 2.4916 | 1.9648 | 1.5557 | 0.8296 |
| 13 | 1585500 | 6.91 | 1.2687 | 1.1178 | 0.9135 | 0.8171 |
| 14 | 1586000 | 9.56 | 1.4146 | 1.2350 | 1.0483 | 0.8886 |
| 15 | 1586210 | 11.69 | 1.3524 | 1.1215 | 0.9275 | 0.7541 |
| 16 | 1586610 | 4.90 | 0.9939 | 0.8810 | 0.7927 | 0.7331 |
| 17 | 1589100 | 44.88 | 2.4902 | 2.0246 | 1.6042 | 0.8551 |
| 18 | 1589180 | 37.36 | 1.8804 | 1.2322 | 1.0707 | 0.4249 |
| 19 | 1589197 | 35.39 | 2.0434 | 1.4447 | 1.1956 | 0.5768 |
| 20 | 1589300 | 30.98 | 2.1414 | 1.6793 | 1.2515 | 0.7076 |
| 21 | 1589330 | 46.02 | 2.7818 | 2.4555 | 1.8257 | 1.1069 |
| 22 | 1589352 | 38.84 | 2.3576 | 1.8810 | 1.4669 | 0.8037 |
| 23 | 1589440 | 15.49 | 1.7596 | 1.5014 | 0.9475 | 0.7028 |
| 24 | 1589500 | 39.90 | 1.7423 | 0.9204 | 1.1464 | 0.4406 |
| 25 | 1589795 | 15.10 | 1.8740 | 1.6512 | 1.1273 | 0.8581 |
| 26 | 1591000 | 2.17 | 1.5965 | 1.5648 | 1.0848 | 1.0553 |
| 27 | 1591400 | 4.62 | 1.4395 | 1.3571 | 1.0581 | 0.9866 |
| 28 | 1591700 | 10.19 | 1.8136 | 1.6578 | 1.0842 | 0.9249 |
| 29 | 1593500 | 27.31 | 2.0072 | 1.5763 | 1.1968 | 0.7201 |
| 30 | 1594000 | 18.01 | 1.7951 | 1.5075 | 1.0906 | 0.7852 |
| 31 | 1594526 | 21.48 | 1.9526 | 1.6433 | 1.1181 | 0.7563 |
| 32 | 1643500 | 4.65 | 2.1358 | 2.0688 | 1.2337 | 1.1667 |
| 33 | 1644600 | 22.07 | 2.2801 | 1.9705 | 1.3237 | 0.9521 |
| 34 | 1649500 | 36.88 | 2.3467 | 1.8609 | 1.3998 | 0.7861 |
| 35 | 1650500 | 22.02 | 1.9942 | 1.6324 | 1.0312 | 0.6662 |

Table 4-8. Indices of IMP generated by various IMP-descriptors (a)-(e) over study basins selected for the thermal regime analysis.

| Basin | Basin ID | (a) Avg-Imp-LU | (b)WB-LU | (c)WB-ID-LU | (d)SCS-CN-LU | (e)SCS-CN-ID-LU |
|---|---|---|---|---|---|---|
| | | IMP, % | Q, inch | Q, inch | Q, inch | Q, inch |
| 1 | HR18 | 3.44 | 1.8735 | 1.8020 | 1.1680 | 1.1027 |
| 2 | HR19 | 29.15 | 2.0916 | 1.4338 | 1.1119 | 0.4989 |
| 3 | NWB5 | 10.22 | 1.9579 | 1.8359 | 1.0831 | 0.9467 |
| 4 | NWB13 | 25.11 | 2.1961 | 1.7371 | 1.1521 | 0.6762 |
| 5 | NWB18 | 34.83 | 2.2370 | 1.6322 | 1.2948 | 0.6235 |
| 6 | PB1 | 18.42 | 1.9658 | 1.6358 | 0.9960 | 0.6834 |
| 7 | PB2 | 16.39 | 1.9805 | 1.6850 | 1.0522 | 0.7610 |
| 8 | PB3 | 18.22 | 1.9952 | 1.6709 | 1.0238 | 0.7082 |
| 9 | PB7 | 20.22 | 2.0844 | 1.7346 | 1.0661 | 0.7067 |
| 10 | PB8 | 30.19 | 2.1747 | 1.6080 | 1.2101 | 0.6218 |
| 11 | PB9 | 21.68 | 2.1067 | 1.7237 | 1.0879 | 0.6912 |
| 12 | PB13 | 32.11 | 2.1315 | 1.5553 | 1.1864 | 0.5896 |
| 13 | PB20 | 57.62 | 2.6623 | 1.9704 | 1.8639 | 0.8169 |

Table 4-9. Indices of IMP generated by various IMP-descriptors (f)-(j) over study basins selected for the flow regime analysis.
Avg-Imp-LC is aggregate IMP at a given basin. WB-LC or SCS-CN-LC uses hydrological models using IMP-LC. Indices reflecting spatial proximity of IMP to outlets use "-ID-" in their symbols.

| Basin | Basin ID | (f)Avg Imp-LC | (g)WB-LC | (h)WB-ID-LC | (i)SCS-CN-LC | (j)SCS-CN-ID-LC |
|---|---|---|---|---|---|---|
| | | IMP, % | Q, inch | Q, inch | Q, inch | Q, inch |
| 1 | 1581700 | 2.44 | 1.6157 | 1.5800 | 0.8957 | 0.8603 |
| 2 | 1583100 | 0.86 | 1.4401 | 1.4267 | 0.9168 | 0.9030 |
| 3 | 1583500 | 0.38 | 1.4539 | 1.4484 | 0.9001 | 0.8947 |
| 4 | 1583600 | 12.56 | 1.6825 | 1.4925 | 0.9484 | 0.7238 |
| 5 | 1584050 | 0.73 | 1.5016 | 1.4882 | 0.9201 | 0.9065 |
| 6 | 1584500 | 0.49 | 1.5000 | 1.4928 | 0.9123 | 0.9060 |
| 7 | 1585090 | 30.49 | 2.1950 | 1.8188 | 1.2879 | 0.8022 |
| 8 | 1585095 | 27.04 | 2.4697 | 2.2452 | 1.3913 | 0.9965 |
| 9 | 1585100 | 27.17 | 2.2070 | 1.8759 | 1.3428 | 0.9143 |
| 10 | 1585200 | 24.17 | 2.0122 | 1.6564 | 1.0815 | 0.6690 |
| 11 | 1585225 | 39.91 | 2.0909 | 1.6316 | 1.2522 | 0.6815 |
| 12 | 1585230 | 33.46 | 2.3593 | 1.9648 | 1.3796 | 0.8364 |
| 13 | 1585500 | 0.57 | 1.1292 | 1.1178 | 0.8171 | 0.8107 |
| 14 | 1586000 | 2.03 | 1.2725 | 1.2350 | 0.8879 | 0.8541 |
| 15 | 1586210 | 1.45 | 1.1473 | 1.1215 | 0.7659 | 0.7468 |
| 16 | 1586610 | 0.18 | 0.8847 | 0.8810 | 0.7754 | 0.7736 |
| 17 | 1589100 | 35.99 | 2.3911 | 2.0246 | 1.4674 | 0.8864 |
| 18 | 1589180 | 17.43 | 1.5109 | 1.2322 | 0.7603 | 0.4832 |
| 19 | 1589197 | 15.06 | 1.6895 | 1.4447 | 0.8331 | 0.5914 |
| 20 | 1589300 | 16.60 | 1.9106 | 1.6793 | 1.0369 | 0.7627 |
| 21 | 1589330 | 30.84 | 2.6671 | 2.4555 | 1.5781 | 1.1233 |
| 22 | 1589352 | 24.92 | 2.1607 | 1.8810 | 1.2418 | 0.8379 |
| 23 | 1589440 | 3.62 | 1.5553 | 1.5014 | 0.8169 | 0.7616 |
| 24 | 1589500 | 18.42 | 1.2506 | 0.9204 | 0.8235 | 0.5707 |
| 25 | 1589795 | 4.98 | 1.7294 | 1.6512 | 1.1562 | 1.0765 |
| 26 | 1591000 | 0.38 | 1.5683 | 1.5648 | 0.9185 | 0.9134 |
| 27 | 1591400 | 0.27 | 1.3622 | 1.3571 | 0.9145 | 0.9103 |
| 28 | 1591700 | 2.78 | 1.6992 | 1.6578 | 1.0162 | 0.9743 |
| 29 | 1593500 | 10.13 | 1.7288 | 1.5763 | 0.9142 | 0.7536 |
| 30 | 1594000 | 5.56 | 1.5907 | 1.5075 | 0.9516 | 0.8648 |
| 31 | 1594526 | 12.98 | 1.8232 | 1.6433 | 0.9656 | 0.7549 |
| 32 | 1643500 | 0.99 | 2.0791 | 2.0688 | 1.1556 | 1.1431 |
| 33 | 1644600 | 9.72 | 2.1051 | 1.9705 | 1.2044 | 1.0517 |
| 34 | 1649500 | 18.77 | 2.0978 | 1.8609 | 1.1065 | 0.8047 |
| 35 | 1650500 | 7.75 | 1.7561 | 1.6324 | 0.8903 | 0.7696 |

Table 4-10. Indices of IMP generated by various IMP-descriptors (f)-(j) over study basins selected for the thermal regime analysis.

| Basin | Basin ID | (f)Avg-Imp-LC | (g)WB-LC | (h)WB-ID-LC | (i)SCS-CN-LC | (j)SCS-CN-ID-LC |
|---|---|---|---|---|---|---|
| | | IMP, % | Q, inch | Q, inch | Q, inch | Q, inch |
| 1 | HR18 | 1.56 | 1.8239 | 1.8020 | 1.1015 | 1.0830 |
| 2 | HR19 | 11.73 | 1.6434 | 1.4338 | 0.7499 | 0.5807 |
| 3 | NWB5 | 2.60 | 1.8793 | 1.8359 | 1.0039 | 0.9558 |
| 4 | NWB13 | 10.49 | 1.8845 | 1.7371 | 0.7956 | 0.6567 |
| 5 | NWB18 | 18.75 | 1.9371 | 1.6322 | 1.0417 | 0.7277 |
| 6 | PB1 | 5.92 | 1.7295 | 1.6358 | 0.8364 | 0.7548 |
| 7 | PB2 | 4.88 | 1.7671 | 1.6850 | 0.9229 | 0.8475 |
| 8 | PB3 | 5.76 | 1.7627 | 1.6708 | 0.8832 | 0.8008 |
| 9 | PB7 | 8.61 | 1.8541 | 1.7346 | 0.9408 | 0.8285 |
| 10 | PB8 | 16.29 | 1.8663 | 1.6080 | 0.8631 | 0.5981 |
| 11 | PB9 | 9.78 | 1.8695 | 1.7237 | 0.8887 | 0.7456 |
| 12 | PB13 | 17.24 | 1.8286 | 1.5553 | 0.9004 | 0.6080 |
| 13 | PB20 | 45.82 | 2.4681 | 1.9704 | 1.6118 | 0.8178 |

### 4.3.1 The effect of IMP-LU and IMP-LC on IMP-descriptors

As mentioned earlier in this study, IMP is sensitive to measuring methods and data sources. Knowing that IMP is one of the crucial driving forces of hydrological response, it is important to understand how differently quantified values of IMP affect models describing IMP in various ways. This section will examine indices of IMP generated by various IMP-descriptors using IMP-LU and IMP-LC. Before relating such indices of IMP to indicators of hydrological response, it is instructive to investigate how indices of IMP compare to one another.

#### 4.3.1.1 Lumped IMP-descriptors

Two IMP-descriptors, Avg-Imp-LU and Avg-Imp-LC, are lumped models in seen in Table 4-6. Aggregate IMP, basin-averaged values using IMP-LU and IMP-LC over individual study basins for the flow regime analysis are summarized in Tables 4-7 (a) and 4-9 (f), respectively. Tables 4-8 (a) and 4-10 (f) summarize Avg-Imp-LU and Avg-Imp-LC over basins selected for the thermal regime analysis. They show that aggregate IMP calculated using IMP-LU and IMP-LC are different from each other. IMP-LC tends to produce smaller estimates of IMP compared to IMP-LU. As seen in Figures 4-4 and 4-5, all study basins selected either for the flow regime analysis or for the thermal regime analysis show the similar trend which is consistent with the earlier observation in Section 4.1.

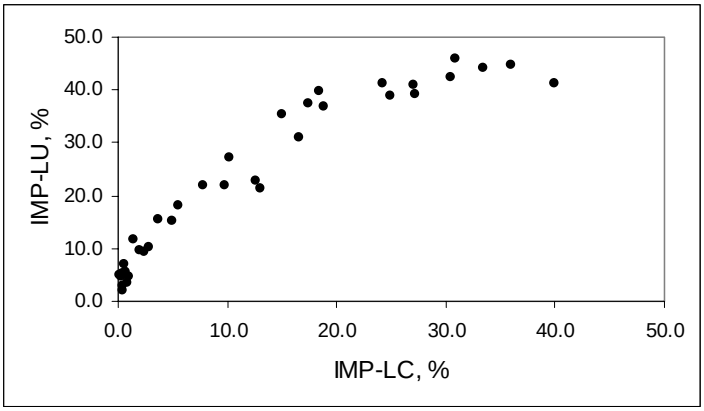


Figure 4-4 Aggregate IMP based on IMP-LU versus aggregate IMP based on IMP-LC over study basins selected for the flow regime analysis. There are 35 study basins. Two observed values of IMP, one from IMP-LU and the other from IMP-LC at a given basin are plotted.

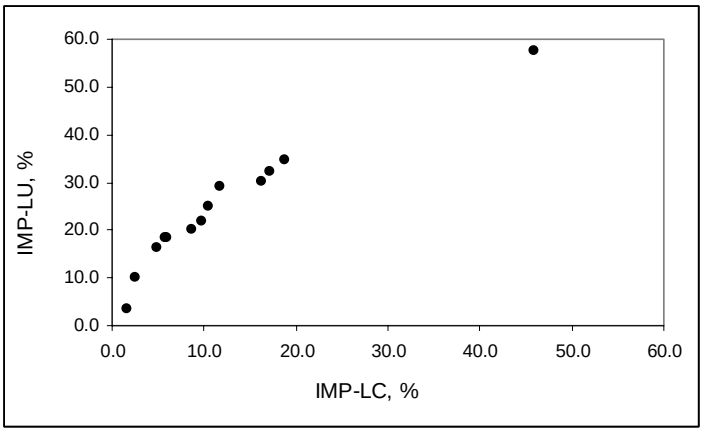


Figure 4-5. Aggregate IMP based on IMP-LU versus aggregate IMP based on IMP-LC over study basins selected for the thermal regime analysis. There are 13 study basins. One value is almost overlapped with another as if there are only 12 basins. Two observed values of IMP, one from IMP-LU and the other from IMP-LC at a given basin are plotted.

#### 4.3.1.2 Spatially distributed IMP-descriptors

As summarized in Table 4-6, IMP-descriptors representing spatially distributed models are WB-LU, WB-ID-LU, SCS-CN-LU, and SCS-CN-ID-LU if hydrological models employ IMP-LU. WB-LC, WB-ID-LC, SCS-CN-LC, and SCS-CN-ID-LC are IMP-descriptors representing hydrological models using IMP-LC. Indices from these models are computed by routing flow from pixel to pixel with pixel-based measurements of IMP. The units of indices resulting from these IMP-descriptors are runoff, Q, in inches. This section will assess the effect of data sources of IMP, land use and land cover, on these IMP-descriptors.

Over basins selected for the flow regime analysis, Figures 4-6 (a) and (b) illustrate the difference depending on IMP-LU or IMP-LC. Both the WB-based IMP-descriptor and the SCS-CN-based IMP-descriptor consistently support the idea that using a high IMP results in a high index value. IMP-descriptors using IMP-LU show greater indices

than those using IMP-LC: WB-LU > WB-LC; SCS-CN-LU > SCS-CN-LC.

Furthermore, the SCS-CN-based IMP-descriptor reacts more sensitively to the data source of IMP compared to the WB-based IMP-descriptor as seen in Table 4-11. The mean value of the data in the column of "WB-LU" in Table 4-7 is 1.9249, while the mean of the data in the column of "WB-LC" in Table 4-9 is 1.7612. Using IMP-LC, WB-based IMP-descriptors produces smaller indices by 8.5% compared to indices resulting from using IMP-LU. On the other hand, SCS-CN-based IMP-descriptors shows 14% of reduction, according to the calculation in Equation 4-6b.

$$\left(\frac{1.9249-1.7612}{1.9249}\right) * 100 = 8.5\ \%\ \text{for the WB} \qquad (4\text{-}6a)$$

$$\left(\frac{1.2109-1.0393}{1.2109}\right) * 100 = 14\ \%\ \text{for the SCS-CN} \qquad (4\text{-}6b)$$

Table 4-11. Mean values resulting from IMP-descriptors. Indices utilizing IMP-LU, either based on WB or SCS-CN approach, are greater than those using IMP-LC.

| Approach | Data source of IMP | IMP-descriptor | Mean, inch |
|---|---|---|---|
| WB-based | Land use | WB-LU | 1.9249 |
| | Land cover | WB-LC | 1.7612 |
| SCS-CN-based | Land use | SCS-CN-LU | 1.2109 |
| | Land cover | SCS-CN-LC | 1.0393 |

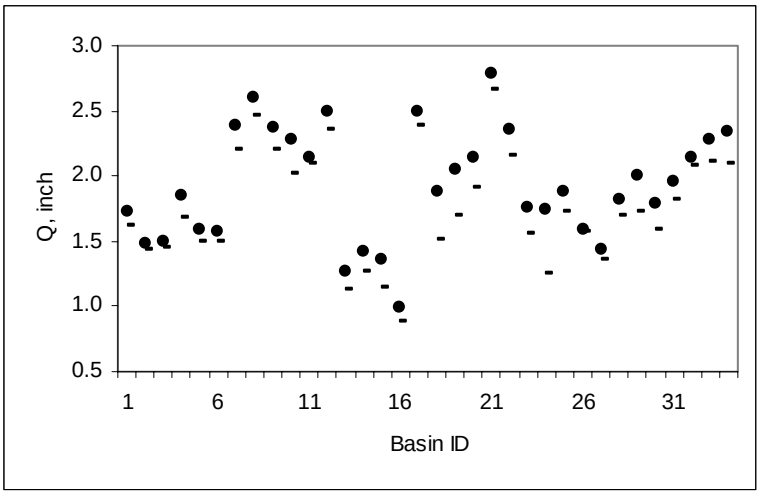


(a)

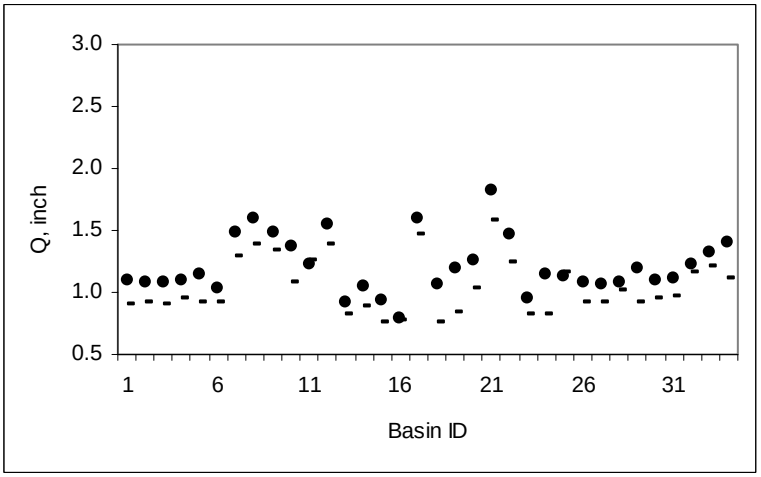


(b)

Figure 4-6. Comparison of indices of IMP using IMP-LU and IMP-LC over study basins selected for the flow regime analysis.
(a) WB-LU (●) versus WB-LC (–)
(b) SCS-CN-LU (●) versus SCS-CN-LC (–)

Once the inverse distance weight (IDW) method is integrated into the WB-based IMP-descriptor to give a spatial weight to the proximity of IMP to the outlet in a basin, WB-ID-LU and WB-ID-LC do not differ as seen in Figure 4-7. Data sources of IMP, land use or land cover, do not affect the performance of IMP-descriptors. Figure 4-8

illustrates that a similar trend occurs with the SCS-CN-based IMP-descriptor. The comparison of Figure 4-8 with Figure 4-6 (b) indicates that indices also show less variation with a weighting mechanism.

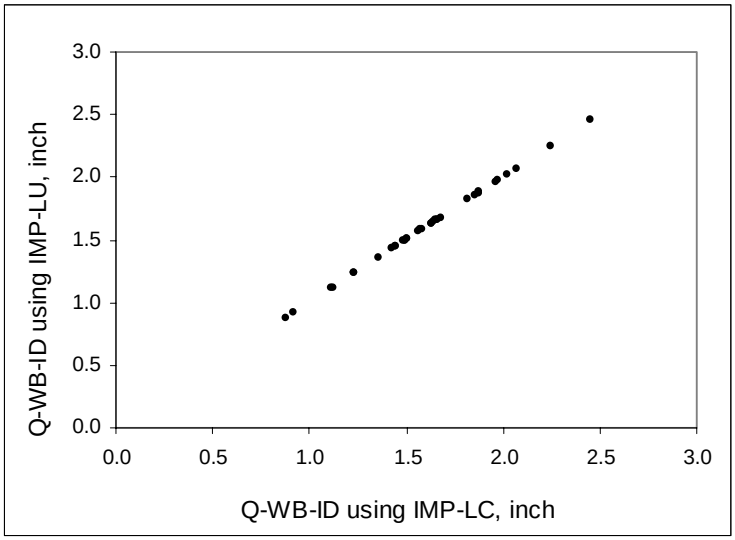


Figure 4-7. WB-ID-LU versus WB-ID-LC over study basins selected for the flow regime analysis. IMP-descriptors reflecting the proximity of IMP to outlets of basins do not show difference in using land use or land cover as data sources of IMP.

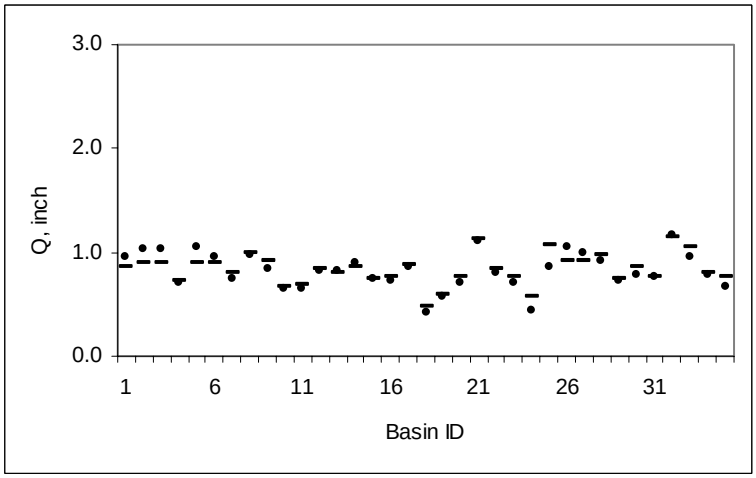


Figure 4-8. SCS-CN-ID-LU (●) versus SCS-CN-ID-LC (━ ) over study basins selected for the flow regime analysis.

Thermal regime analysis shows the similar trend to the flow regime analysis. Figure 4-9 (a) shows the difference between the WB-LU and the WB-LC over basins selected for the thermal regime analysis. Figure 4-9 (b) illustrates the SCS-CN-based IMP-descriptor using IMP-LU and IMP-LC. In both cases, IMP-descriptors using IMP-LU result in greater indices than those using IMP-LC.

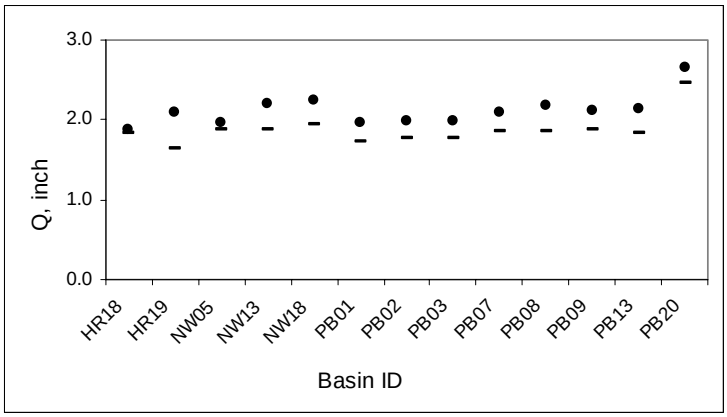


(a)

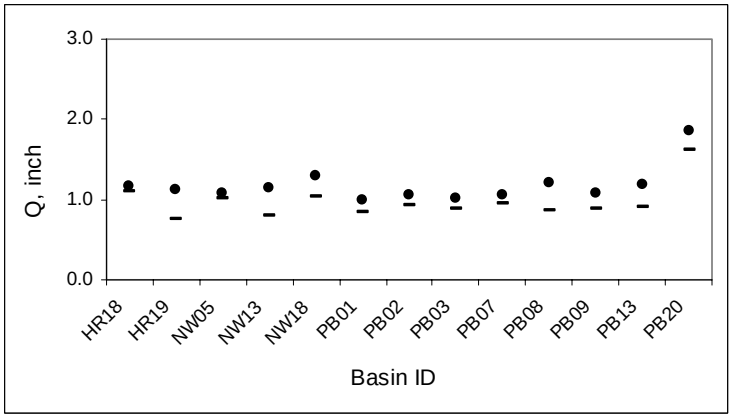


(b)

Figure 4-9. Comparison of indices of IMP using IMP-LU and IMP-LC over study basins selected for the thermal regime analysis.
(a) WB-LU (●) versus WB-LC (━)
(b) SCS-CN-LU (●) versus SCS-CN-LC (━)

As depicted in Figure 4-9, basins such as HR19, NWB13, and PB13 show relatively much smaller indices using IMP-LC than counterparts using IMP-LU: WB-LU > WB-LC; SCS-CN-LU > SCS-CN-LC. A possible explanation is that more than 80% of land uses within such individual basins belong to the "medium density residential" and "low density residential" as seen in Table 4-12. Considering IMP-LC tends to produce smaller IMP than IMP-LU over these particular land use categories as observed in Section 4.2, it is not surprising that IMP-descriptors using IMP-LC result in smaller indices than those using IMP-LU relative to other basins.

Table 4-12. Pattern of land use within individual basins selected for the thermal regime analysis. Only the "residential" class is presented.

| Basin | Residential, Medium density and low density , % | Residential, High density, % |
|---|---|---|
| HR18 | 9.06 | 0.00 |
| **HR19** | **88.99** | 3.06 |
| NWB5 | 16.34 | 0.00 |
| **NWB13** | **81.48** | 0.00 |
| NWB18 | 44.19 | 23.92 |
| PB1 | 59.83 | 0.00 |
| PB2 | 53.63 | 0.00 |
| PB3 | 59.40 | 0.00 |
| PB7 | 57.04 | 2.26 |
| PB8 | 77.61 | 2.45 |
| PB9 | 59.92 | 2.36 |
| **PB13** | **81.33** | 3.80 |
| PB20 | 5.25 | 55.31 |

With the consideration of the inverse distance weight (IDW) method to give a weight to the proximity of IMP to the outlet in a basin, IMP-descriptors show no difference between using IMP-LU or IMP-LC. This is the same trend that was appeared in the flow regime analysis as seen in Figures 4-7 and 4-8.

Both the WB and the SCS-CN-based IMP-descriptors measured over all study basins selected both for flow regime and thermal regime analysis consistently show that using IMP-LU results in higher indices than using IMP-LC. Knowing that data sources of IMP, land use or land cover, affect IMP-descriptors, it is of interest to examine its impact on the prediction of hydrological response. Prior to determining the relationship between indices of IMP and hydrological response, indicators of hydrological response need to be computed over individual study basins.

### 4.4 Indicators of hydrological response

This section will compute indicators of hydrological response which were selected and defined in Chapter 3. Indicators of flow variability such as $R_{Q10\text{-}90}$, $I_{R\text{-}B}$, CV, and $R_{L1}$ are calculated base on measured mean daily stream flow from the water year 1997 to 2003 and summarized in Table 4-13. Indicators of the hydrological response in the thermal regime such as DD, $D_{SURGE}$ , and MDTD are calculated based on measured stream temperature and summarized in Table 4-14.

Table 4-13. Indices indicating flow variability at individual basins selected for the flow regime analysis. $R_{Q10\text{-}90}$: Ratio of the discharge which is equaled or exceeded 10% of the time to the discharge which is equaled or exceeded 90% of the time; $R_{L1}$: Lag-one autocorrelation; $I_{R\text{-}B}$: R-B index which measures relative mean daily flow change; CV: coefficient of variation.

| Basin | Basin ID | Area (sq. miles) | $R_{Q10-90}$ | $R_{L1}$ | $I_{R-B}$ | CV |
|---|---|---|---|---|---|---|
| 1 | 1581700 | 34.80 | 7.4000 | 0.3258 | 0.4220 | 1.5098 |
| 2 | 1583100 | 12.30 | 4.8980 | 0.4684 | 0.3047 | 1.0412 |
| 3 | 1583500 | 59.80 | 6.1667 | 0.5952 | 0.2721 | 1.0028 |
| 4 | 1583600 | 20.90 | 6.0714 | 0.3136 | 0.5221 | 1.3223 |
| 5 | 1584050 | 9.40 | 6.9565 | 0.3224 | 0.4044 | 1.5062 |
| 6 | 1584500 | 36.10 | 5.2308 | 0.3517 | 0.3511 | 1.3762 |
| 7 | 1585090 | 2.73 | 29.7297 | 0.1684 | 1.1935 | 3.1172 |
| 8 | 1585095 | 1.34 | 55.5556 | 0.2117 | 1.1786 | 2.8790 |
| 9 | 1585100 | 7.61 | 25.0000 | 0.2041 | 1.0920 | 2.8248 |
| 10 | 1585200 | 2.13 | 22.0690 | 0.1563 | 1.0453 | 2.1584 |
| 11 | 1585225 | 0.21 | 23.0000 | 0.1330 | 1.1689 | 2.6551 |
| 12 | 1585230 | 3.52 | 20.9524 | 0.1287 | 1.2930 | 3.1282 |
| 13 | 1585500 | 3.29 | 21.6000 | 0.3820 | 0.6363 | 1.9207 |
| 14 | 1586000 | 56.60 | 7.8000 | 0.5058 | 0.4012 | 1.2485 |
| 15 | 1586210 | 14.00 | 7.2500 | 0.6259 | 0.2950 | 1.0558 |
| 16 | 1586610 | 28.00 | 8.3333 | 0.5445 | 0.3250 | 1.3154 |
| 17 | 1589100 | 2.47 | 15.1064 | 0.1789 | 1.0835 | 2.7175 |
| 18 | 1589180 | 0.23 | 46.0000 | 0.1675 | 0.9644 | 2.7165 |
| 19 | 1589197 | 4.23 | 5.4615 | 0.1561 | 0.7295 | 2.0149 |
| 20 | 1589300 | 32.50 | 7.3636 | 0.2613 | 0.6772 | 1.7465 |
| 21 | 1589330 | 5.52 | 32.7273 | 0.1454 | 1.2317 | 2.8967 |
| 22 | 1589352 | 65.90 | 7.9524 | 0.2284 | 0.7616 | 1.9827 |
| 23 | 1589440 | 25.20 | 6.4935 | 0.2817 | 0.5047 | 1.6225 |
| 24 | 1589500 | 4.97 | 3.5833 | 0.3992 | 0.3342 | 1.0884 |
| 25 | 1589795 | 1.00 | 4.1429 | 0.1245 | 0.7576 | 4.1393 |
| 26 | 1591000 | 34.80 | 11.0606 | 0.5023 | 0.3909 | 1.5063 |
| 27 | 1591400 | 22.90 | 7.0909 | 0.3309 | 0.4472 | 1.6652 |
| 28 | 1591700 | 27.00 | 11.4583 | 0.4352 | 0.4823 | 1.7082 |
| 29 | 1593500 | 38.00 | 10.8000 | 0.3764 | 0.6478 | 1.8226 |
| 30 | 1594000 | 98.40 | 9.4762 | 0.3684 | 0.5476 | 1.6806 |
| 31 | 1594526 | 89.70 | 27.0886 | 0.5736 | 0.6042 | 1.9796 |
| 32 | 1643500 | 62.80 | 13.8542 | 0.3847 | 0.4676 | 2.0603 |
| 33 | 1644600 | 50.70 | 5.6087 | 0.3862 | 0.5079 | 1.4485 |
| 34 | 1649500 | 72.80 | 15.5000 | 0.3047 | 0.7907 | 2.3104 |
| 35 | 1650500 | 21.10 | 18.2609 | 0.2815 | 0.7699 | 2.2386 |

Table 4-14. Indices indicating thermal variability at individual basins selected for the thermal regime analysis. DD: Degree-day; $D_{SURGE}$: Percent days with surge; MDTD: Mean daily temperature difference.

| Basin | Basin ID | DD | $D_{SURGE}$ | MDTD |
|---|---|---|---|---|
| | | $C^{\circ}$ | % day | $C^{\circ}$ |
| 1 | HR18 | 6.71 | 1.0 | 4.02 |
| 2 | HR19 | 5.61 | 3.5 | 3.91 |
| 3 | NWB5 | 7.26 | 1.0 | 2.90 |
| 4 | NWB13 | 6.04 | 1.0 | 2.86 |
| 5 | NWB18 | 3.27 | 5.1 | 1.91 |
| 6 | PB1 | 0.00 | 0.0 | 1.98 |
| 7 | PB2 | 0.00 | 0.0 | 1.67 |
| 8 | PB3 | 0.00 | 0.0 | 2.06 |
| 9 | PB7 | 0.00 | 0.0 | 2.28 |
| 10 | PB8 | 2.90 | 1.7 | 2.86 |
| 11 | PB9 | 2.90 | 1.7 | 2.37 |
| 12 | PB13 | 3.80 | 10.0 | 2.05 |
| 13 | PB20 | 4.32 | 10.1 | 3.36 |

### 4.5 Regression between IMP-descriptors and indicators of hydrological response

Regression analyses are conducted to identify relationships between predictors (IMP-descriptors in this study) and criterions (hydrological response-indicators in this study). This allows for predicting the next occurrence of hydrological response through a functional relationship. The reliability of regression equations will be determined by goodness-of-fit measures. It indicates if an IMP-descriptor is effective as a predictor of hydrological response in a given regression equation.

Within the scope of this study, four types of regression models will be evaluated as summarized in Table 4-15. Each type of regression will be presented in individual figures from 4-10 to 4-13. For instance, Figure 4-10 illustrates that four indicators such as $R_{Q10\text{-}90}$, $R_{L1}$, $I_{R\text{-}B}$, and CV are regressed on five IMP-descriptors using IMP-LU, (a) through (e). This generates twenty regression models using IMP-LU for the flow regime analysis. Using IMP-LC, the same number of regression models will be generated for the

flow regime as depicted in Figure 4-12. For the thermal regime analysis, Figures 4-11 generates 15 models, regressing three indicators of thermal variability on five IMP-indicators using IMP-LU. For the thermal regime analysis, regressions will be performed at two different spatial scales: basin scale and sub-basin scale. As a result, there will be thirty regression models, fifteen at the basin scale and another fifteen at the sub-basin scale. For the same reason, there will be thirty regression models using IMP-LC in the thermal regime. Table 4-15 summarizes number of regression models generated from each set of two quantities.

Table 4-15. Summary of regression models examined in this study. Indicative Indices of hydrological response, flow variability and thermal variability, are regressed on IMP-descriptors using IMP-LU and IMP-LC. Due to lack of data availability, no regression models exist at a sub-basin scale for the flow regime analysis.

| Regression | | Figure | Number of regression models | |
|---|---|---|---|---|
| Indicators of: | IMP-descriptors using: | | Basin scale | Sub-basin scale |
| Flow variability | IMP-LU | 4-10 | 20 | -- |
| Thermal variability | IMP-LU | 4-11 | 15 | 15 |
| Flow variability | IMP-LC | 4-12 | 20 | -- |
| Thermal variability | IMP-LC | 4-13 | 15 | 15 |

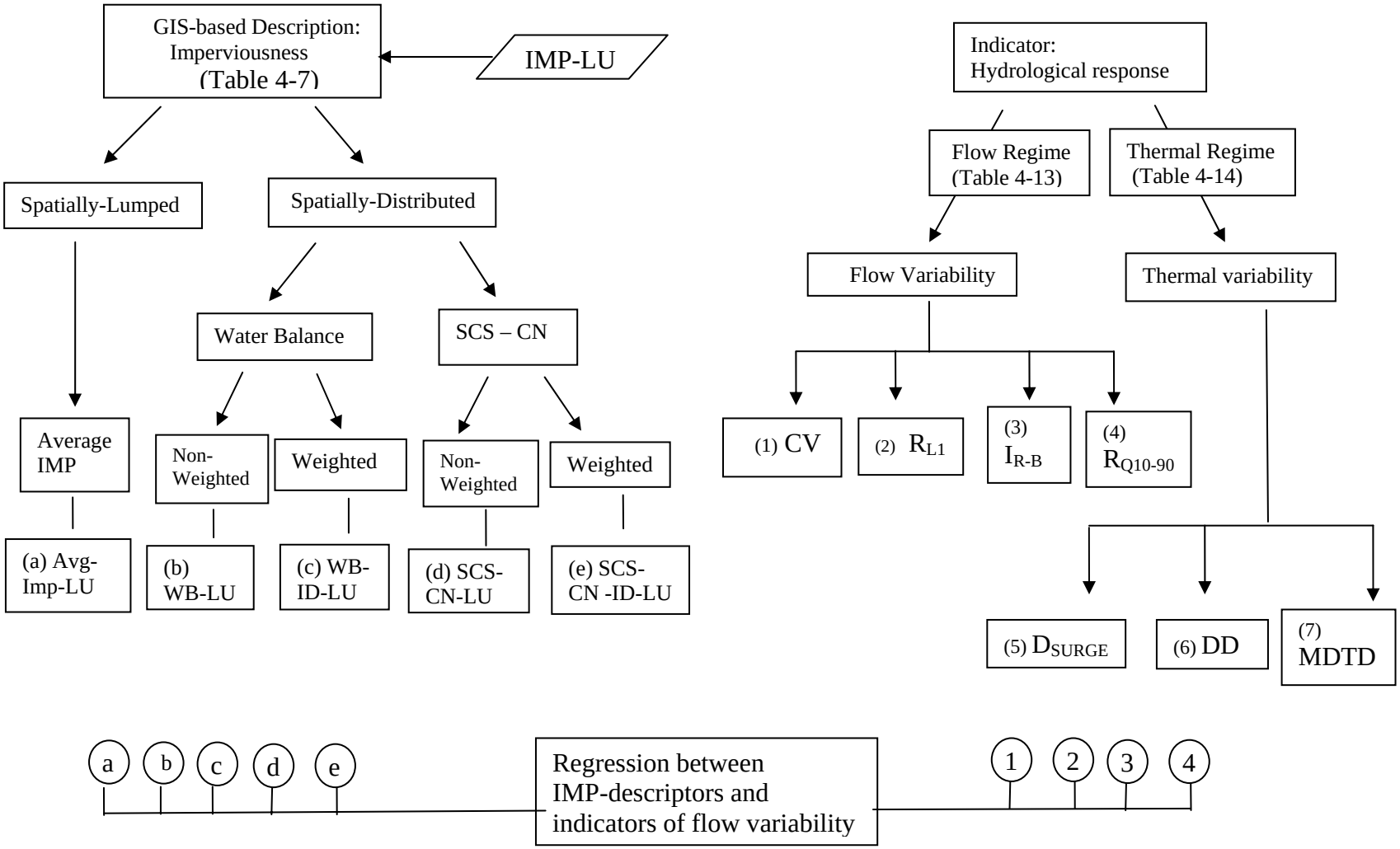


Figure 4-10. Indicators of hydrological response in the flow regime such as $R_{Q10-90}$, RL1, $I_{R-B}$, and CV are regressed on IMP-descriptors using IMP-LU. It results in 20 regression equations.

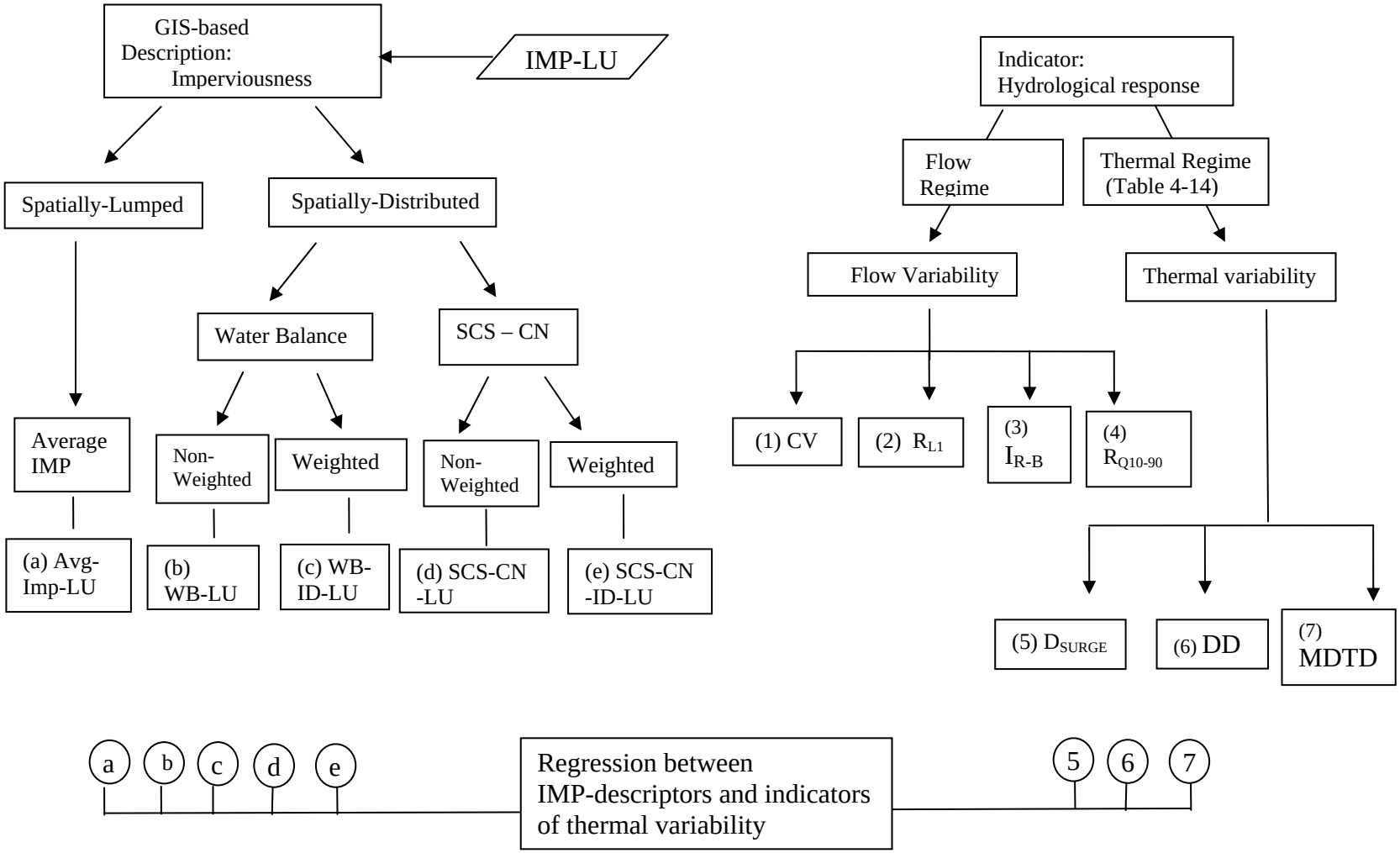


Figure 4-11. Indicators of hydrological response in the thermal regime such as DD, $D_{SURGE}$, and MDTD are regressed on IMP-descriptors using IMP-LU. It results in 15 regression equations at the basin scale and 15 at the sub-basin scale.

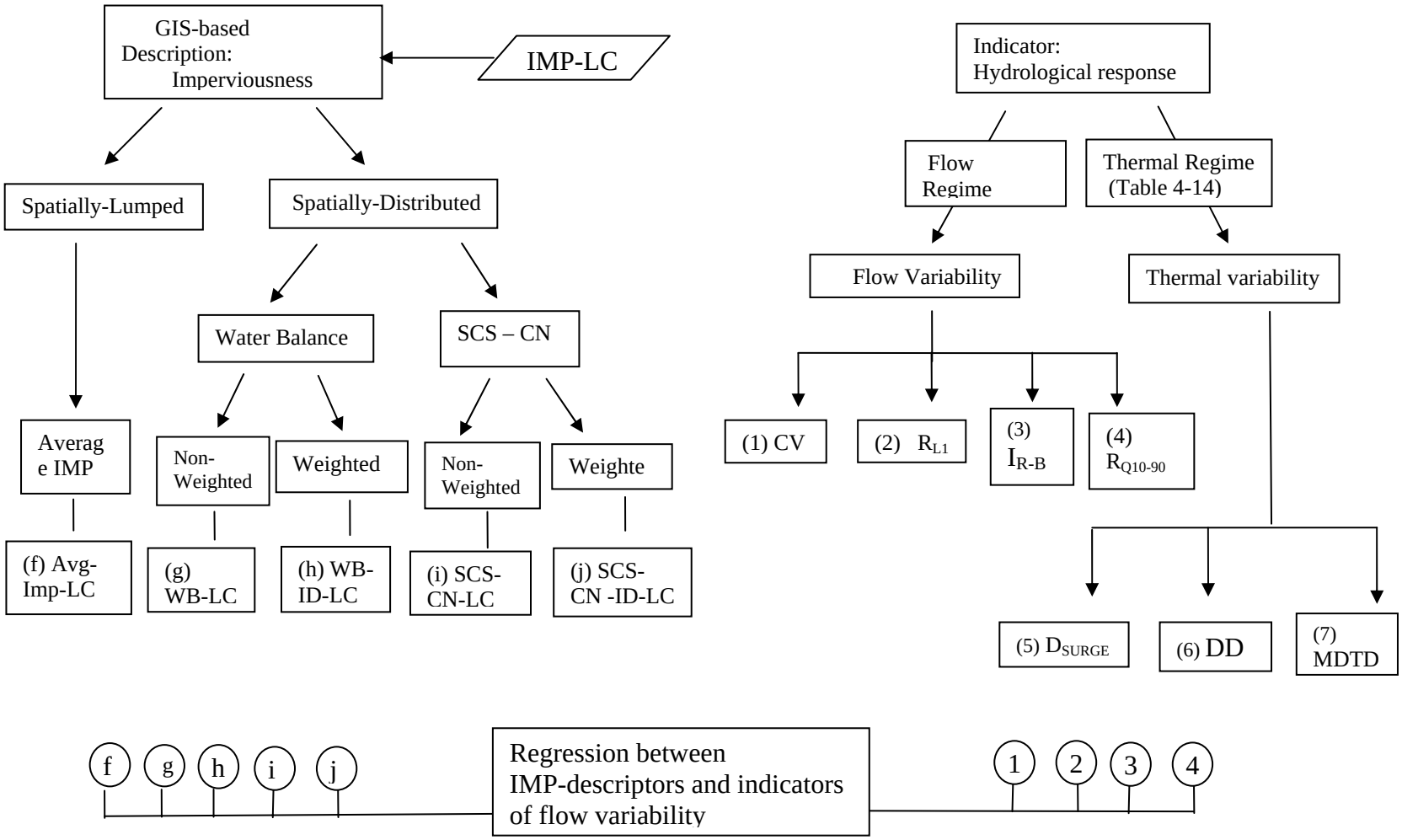


Figure 4-12. Indicators of hydrological response in the flow regime such as $R_{Q10-90}$, RL1, $I_{R-B}$, and CV are regressed on IMP-descriptors using IMP-LC. It results in 20 regression equations.

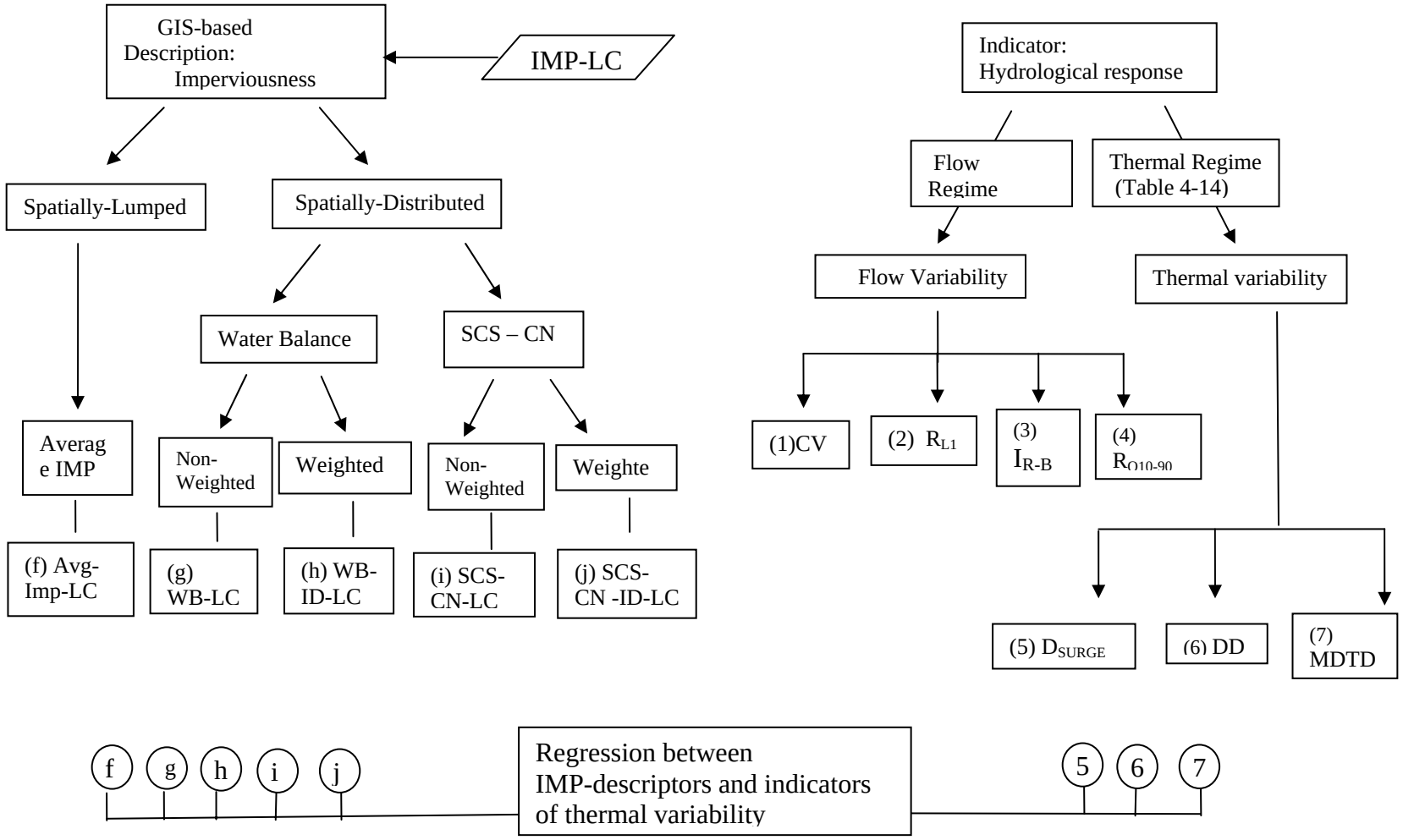


Figure 4-13. Indicators of hydrological response in the thermal regime such as DD, $D_{SURGE}$, and MDTD are regressed on IMP-descriptors using IMP-LC. It results in 15 regression equations at the basin scale and 15 at the sub-basin scale.

In order to select a model structure for regressions described in Figures 4-10 and 4-12 for the flow regime analysis, two quantities are plotted as illustrated in Figure 4-14 for a visual interpretation. Two quantities refer to one of IMP-predictors as a predictor and one of hydrological-response indicator as a criterion. The size of a basin is also related to flow variability as depicted in Figure 4-15 (a) and (b). For this reason, basin scale is included as a predictor in the regression equation. Therefore, the indicator of flow variability is mathematically expressed as a function of the size of a basin and imperviousness as seen in Equation 4-7:

$$Y = f(X_1, X_2) \tag{4-7}$$

where Y = indicators of flow variability as unitless indices
$X_1$= the size of a basin in square miles
$X_2$= IMP-descriptors in terms of either averaged value of imperviousness in percent or runoff depth in inches

A power model structure is the best fit based on the plot in Figure 4-14. Equation 4-8 is calibrated using a numerical optimization mentioned in Section 4.2.1:

$$Y = C_1 X_1^{C2} X_2^{C3} \tag{4-8}$$

where $C_1$, $C_2$, $C_3$ = unknown coefficients to be calibrated
Y, $X_1$, $X_2$= variables as defined in Equation 4-7

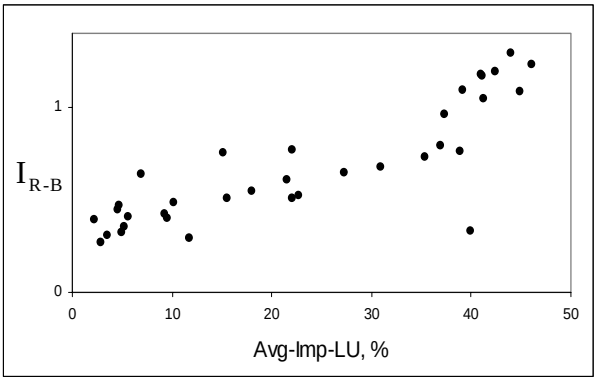

Figure 4-14. An example of the scatter plot between an IMP-descriptor (Avg-Imp-LU in this case) and an indicator of flow variability ($I_{R-B}$ in this case) over basins selected for the flow regime analysis. A power model structure is the best fit in this plot.

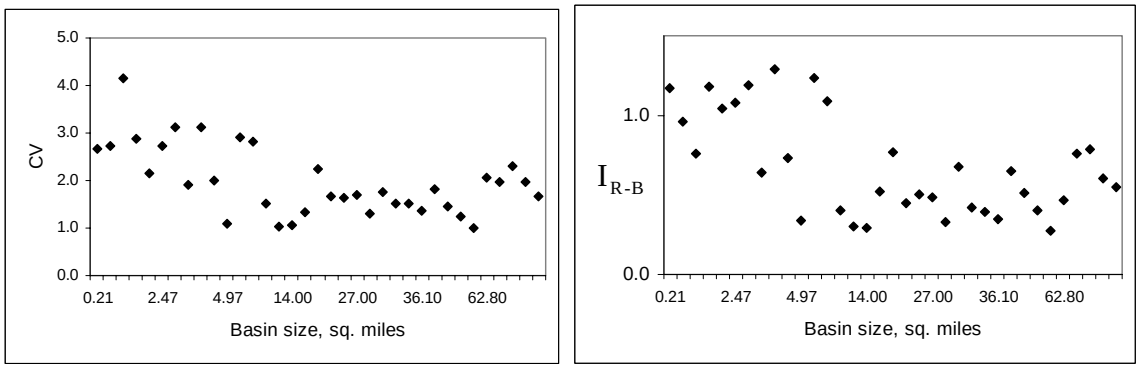


(a) (b)

Figure 4-15. Indicators of flow variability as a function of basin size. The size of a basin is related to indicators of flow variability such as (a) coefficient of variation, CV and (b) the mean value of daily flow change, $I_{R-B.}$

In contrast to the flow variability analysis, any relationship between basin sizes and indicators of thermal variability is not apparent in Figure 4-17 (a) and (b). Therefore, basin scale will not be included as a predictor in the thermal regime regression equations. Based on the visual interpretation of Figure 4-16, a linear model will be calibrated.

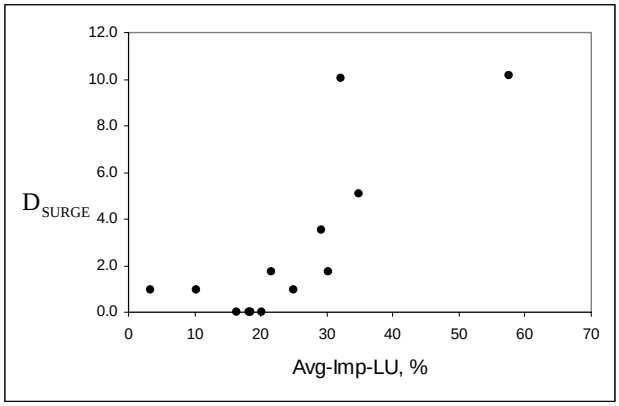


Figure 4-16. An example of the scatter plot between an IMP-descriptor (Avg-Imp-LU in this case) and an indicator of thermal variability ($D_{SURGE}$ in this case) over basins selected for the thermal regime analysis. A Linear model structure is the best fit in this plot.

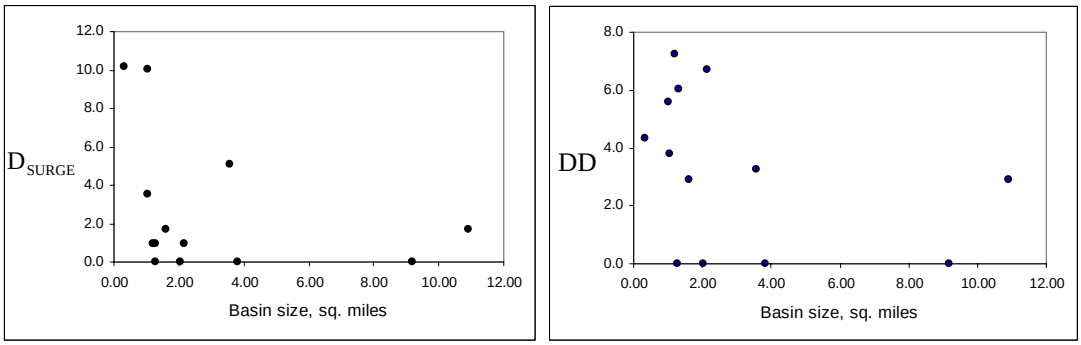


(a) (b)

Figure 4-17. Indicators of thermal variability as a function of basin size. The size of a basin is rarely related to indicators of thermal variability such as (a) $D_{SURGE}$ and (b) DD.

Once indicators of hydrological response are regressed on IMP-descriptors, goodness-of-fit (GOF) measures such as relative standard errors or coefficients of determination are assessed and summarized in Table 4-17. Such GOF measures will be used to determine the effectiveness of IMP-descriptors as predictors of hydrological response, either flow variability or thermal variability. Table 4-17 is divided into largely four parts as seen in Table 4-16. For instance, the relative standard error for the

regression model between CV and WB-LU at the basin scale is 0.6477 presented at the cell in the third row and the third column.

Table 4-16. Locations of goodness-of-fit statistics for individual regression equations between IMP-descriptors and indicators of hydrological response in Table 4-17. Hydrological response include the flow variability and thermal variability. IMP-descriptors can be divided largely into two categories base on the data source of IMP: land use and land cover.

| Regress | on | Goodness-of-fit statistics in Table 4-17 | |
|---|---|---|---|
| | | Row | Column |
| Indicators of Flow variability | IMP-LU | 1-10 | 1- 4 |
| Indicators of Thermal variability | IMP-LU | 1-10 | 5 - 7 |
| Indicators of Flow variability | IMP-LC | 11 - 20 | 1- 4 |
| Indicators of Thermal variability | IMP-LC | 11 - 20 | 5 - 7 |

Table 4-17. Goodness-of-fit (GOF) statistics for regression equations between IMP-descriptors and indicators of hydrological response. For power models, relative standard errors are reported, while $R^2$ is reported for linear models. Relative standard errors for linear models are reported in Table 4-24. These GOF measures are indices indicating the effectiveness of IMP-descriptors as predictors of flow variability or thermal variability. Due to the lack of data availability, the flow regime analysis was not performed at the sub-basin scale. The analysis at the sub-basin scale is performed only within the Paint Branch basin (PB). An example of interpretation: $R^2$ for the regression model between $D_{SURGE}$ and WB-LU at the sub-basin scale is 0.5597 at the box intersecting row 4 and column 7.

| Goodness-of-fit Statistics | | | | Indicator of flow variability | | | | Indicator of thermal variability | | |
|---|---|---|---|---|---|---|---|---|---|---|
| | | | | (1) | (2) | (3) | (4) | (5) | (6) | (7) |
| IMP | IMP-descriptor | row | scale | $R_{L1}$ | $R_{Q10-90}$ | CV | $I_{R-B}$ | MDTD | DD | $D_{SURGE}$ |
| IMP-LU | (a) Avg-Imp_LU | (1) | Basin | 1.0610 | 0.7902 | 0.7349 | 0.5199 | 0.0011 | 0.0000 | 0.6247 |
| | | (2) | PB sub-basin | - | - | - | - | 0.7258 | 0.6453 | 0.7132 |
| | (b) WB-LU | (3) | Basin | 0.6730 | 0.7266 | 0.6477 | 0.3799 | 0.0165 | 0.0123 | 0.5221 |
| | | (4) | PB sub-basin | - | - | - | - | 0.8005 | 0.5598 | 0.5597 |
| | (c) WB-ID-LU | (5) | Basin | 0.7727 | 0.7696 | 0.6879 | 0.5871 | 0.0291 | 0.0392 | 0.0038 |
| | | (6) | PB sub-basin | - | - | - | - | 0.4246 | 0.0712 | 0.0972 |
| | (d) SCS-CN-LU | (7) | Basin | 0.5491 | 0.7361 | 0.6477 | 0.4322 | 0.1101 | 0.0778 | 0.5654 |
| | | (8) | PB sub-basin | - | - | - | - | 0.7137 | 0.5088 | 0.5785 |
| | (e) SCS-CN-ID-LU | (9) | Basin | 0.9310 | 0.8862 | 0.8387 | 0.8639 | 0.1181 | 0.1175 | 0.0456 |
| | | (10) | PB sub-basin | - | - | - | - | 0.0701 | 0.0736 | 0.0000 |
| IMP-LC | (f) Avg-Imp_LC | (11) | Basin | 1.0610 | 0.7988 | 0.7233 | 0.4932 | 0.0232 | 0.0085 | 0.6609 |
| | | (12) | PB sub-basin | - | - | - | - | 0.7358 | 0.5918 | 0.6601 |
| | (g) WB-LC | (13) | Basin | 0.7141 | 0.7646 | 0.6611 | 0.4409 | 0.0313 | 0.0363 | 0.3712 |
| | | (14) | PB sub-basin | - | - | - | - | 0.7287 | 0.4276 | 0.4673 |
| | (h) WB-ID-LC | (15) | Basin | 0.7727 | 0.7696 | 0.6879 | 0.5871 | 0.0291 | 0.0392 | 0.0038 |
| | | (16) | PB sub-basin | - | - | - | - | 0.7287 | 0.4276 | 0.4673 |
| | (i) SCS-CN-LC | (17) | Basin | 0.5703 | 0.8149 | 0.6041 | 0.4974 | 0.0666 | 0.0333 | 0.3139 |
| | | (18) | PB sub-basin | - | - | - | - | 0.5487 | 0.2754 | 0.4228 |
| | (j) SCS-CN-ID-LC | (19) | Basin | 0.8826 | 0.8880 | 0.7098 | 0.8249 | 0.0328 | 0.0169 | 0.0997 |
| | | (20) | PB sub-basin | - | - | - | - | 0.0221 | 0.2903 | 0.1107 |

### 4.6 Sensitivity of hydrological response to IMP-LU and IMP-LC

The effect of using IMP-LU and IMP-LC on the prediction of hydrological response will be evaluated by conducting regression analyses employing two quantities: an IMP-descriptor and an indicator of hydrological response. If the reliability of a regression equation is high, the IMP utilized in that equation will be considered as a good predictor of hydrological response. This study employs Se/Sy and $R^2$ as indices indicating the level of accurate prediction for regressed power models and for regressed linear models, respectively. The evaluation of these indices at the basin scale is conducted in the flow regime and the thermal regime. Due to the lack of data availability, only the thermal regime analysis is performed at the sub-basin level. Further, thermal regime analyses include hypothesis-testing on correlation coefficients for linear regression models. Table 4-25 in Section 4.10 at the end of this chapter summarize the results explained below.

#### 4.6.1 Effectiveness of IMP-LU and IMP-LC on the prediction of the flow variability

Goodness-of-fit measures for regression equations between IMP-descriptors using IMP-LU and indicators of flow variability are summarized in columns 1 through 4 and rows 1 through 10 in Table 4-17. For regression models using IMP-LC, this study examines columns 1 through 4 and rows 11 through 20 in Table 4-17. The index for each IMP-LU regression equation will be compared with its IMP-LC counterpart. Both indices use the same regression model structure and indicator of flow variability, but with different IMP datasets, IMP-LU or IMP-LC. For instance, the index in column 1 and row 1 will be compared to the one in column 1 and row 11.

For the flow regime, there are twenty indices from IMP-LU regression equations to be compared with their IMP-LC counterparts. Nine out of the twenty cases show that IMP-descriptors using IMP-LU have a higher level of accurate prediction with indicators of flow variability. They are better at predicting hydrological response than IMP-descriptors using IMP-LC. Five cases are not affected by data sources of IMP and six cases show that using IMP-LC is better. Provided that a regression equation with Se/Sy > 0.8 indicates a poor relationship between two quantities, the comparison was re-performed with indices of Se/Sy < 0.8. Only three cases show that IMP-LC is a better predictor than IMP-LU. However, eight indices indicate that IMP-LU is better at predicting flow variability. These analyses are summarized in Table 4-18. The table suggests that IMP-LU is a better predictor of hydrological response than IMP-LC in the flow regime at the basin scale.

Table 4-18. Number of indices indicating the effectiveness of IMP-descriptors as predictors of flow variability.

| Flow regime | Number of index (Se/Sy) | | |
|---|---|---|---|
| | $Se/Sy_{IMP\text{-}LU} < Se/Sy_{IMP\text{-}LC}$ | $Se/Sy_{IMP\text{-}LC} < Se/Sy_{IMP\text{-}LU}$ | No difference |
| Overall | 9 | 6 | 5 |
| Se/Sy <0.8 | 8 | 3 | 4 |

### 4.6.2 Effectiveness of IMP-LU and IMP-LC on the prediction of the thermal variability

Goodness-of-fit measures for regression equations between IMP-descriptors using IMP-LU and indicators of thermal variability are summarized in columns 5 through 7 and rows 1 through 10 in Table 4-17. For regression models using IMP-LC, this study

examines columns 5 through 7 and rows 11 through 20 in Table 4-17. There will be two spatial scales in the thermal regime study, basin and sub-basin scales. Odd-numbered rows will be used for the basin scale, while even-numbered rows are for the sub-basin comparison. For each scale, there are fifteen indices from IMP-LU regression equations to be compared with their IMP-LC counterparts.

At the basin scale, six out of fifteen cases indicate IMP-LU is a better predictor than IMP-LC, while six cases indicate the opposite. Three cases are not affected by IMP-LU and IMP-LC. No distinction appears at the basin scale. At the sub-basin scale, however, nine out of fifteen cases show that IMP-descriptors using IMP-LU are better predictors of thermal variability. These analyses include a case when $R^2$ of 0.0 is compared with the value of 0.11, in which both do not show any relationship at all. Since the comparison of $R^2$ is not meaningful if the value is so low that there exists no relationship, it is of interest to assess only relationships that are significant.

In order to statistically determine the significance of relationships between IMP-descriptors and indicators of thermal variability, hypothesis testing is conducted. The hypotheses test is the following:

$H_O$: there exists no linear relationship between the two quantities

$H_A$: there is a linear relationship between the two quantities

These hypotheses are tested utilizing a *t*-statistic given by:

$$t = \frac{R}{\sqrt{\frac{\left(1 - R^2\right)}{n-2}}} \tag{4-9}$$

where $R$=Correlation coefficient
$n$=number of study basins
(13 and 8 for the basin and sub-basin scales, respectively)
$t$ =the value of random variable that has a t-distribution with (n-2) degrees of freedom

To determine statistically significant R, Equation 4-9 is rearranged resulting in Equation 4-10.

$$R_{\min} = \sqrt{\frac{t^2}{\left(t^2 + n - 2\right)}} \tag{4-10}$$

R resulting from using a selected level of significance is the lowest value of R in order to reject the null hypothesis for each defined statistical condition. For example, as summarized in Table 4-19, R should be greater than 0.6836 to have a statistically significant relation between two quantities for 11 degrees of freedom at a 1% level of significance. Therefore, the R-value in Table 4-19 is named as $R_{min.}$ Since Table 4-17 summarizes $R^2$, $R_{min}$ is converted into $R_{min}^2$ prior to examining the Table 4-17.

In order to determine if indices show statistically significant relationships between IMP-descriptors and indicators of thermal variability at a given the level of significance, each $R^2$ in Table 4-17 will be compared with $R_{min}^2$. Among fifteen indices using IMP-LU at the basin scale in Table 4-17, indices greater than $R_{min}^2$ are counted and compared with counterparts using IMP-LC at a given level of significance. The first row in Table 4-20 indicates that three among fifteen indices using IMP-LU as seen in Table 4-17 show significant linear relationships at a 1% level of significance at the basin scale. On the other hand, only one index among fifteen indices using IMP-LC shows a significant

relationship at a 1% level of significance. Therefore, it can be said that thermal variability is more sensitive to IMP-LU than IMP-LC for $\alpha$ =1% at the basin scale. While levels of significance change from 1% to 10%, the general tendency that IMP-LU is a better predictor of thermal variability than IMP-LC remains unchanged. The analysis is repeated at the sub-basin scale. Both the basin scale and sub-basin scales indicate the same trend that IMP-LU yields a better prediction of thermal variability than IMP-LC except at a 10% level of significance.

Table 4-19. t-value and the lowest value of R for rejecting the null hypothesis. Rejecting the null hypothesis indicates that a linear relationship exists. $R_{min}$ refers to a minimum value of R to show a linear relationship.

| Scale | Degrees of freedom | Level of significance $\alpha$ , (%) | Test, Two-sided | t-value | $R_{min}$ |
|---|---|---|---|---|---|
| Basin | 11 | 1 | 0.005 | 3.106 | 0.6836 |
| | | 2 | 0.01 | 2.718 | 0.6339 |
| | | 5 | 0.025 | 2.201 | 0.5530 |
| | | 10 | 0.05 | 1.796 | 0.4762 |
| Sub-basin | 6 | 1 | 0.005 | 3.707 | 0.8343 |
| | | 2 | 0.01 | 3.143 | 0.7888 |
| | | 5 | 0.025 | 2.447 | 0.7068 |
| | | 10 | 0.05 | 1.943 | 0.6215 |

Table 4-20. Number of regression equations showing a statistically significant linear relationship at a given level of significance. To have a statistically significant relationship, a regression equation needs to show higher $R^2$ than $R_{min}^2$.

| Scale | Degrees of freedom | Level of significance $\alpha$, (%) | $R_{min}^2$ | Number of $R^2 > R_{min}^2$ | |
|---|---|---|---|---|---|
| | | | | Using IMP-LU | Using IMP-LC |
| Basin | 11 | 1 | 0.4673 | 3 | 1 |
| | | 2 | 0.4018 | 3 | 1 |
| | | 5 | 0.3058 | 3 | 3 |
| | | 10 | 0.2268 | 3 | 3 |
| Sub-basin | 6 | 1 | 0.6961 | 4 | 3 |
| | | 2 | 0.6222 | 5 | 4 |
| | | 5 | 0.4996 | 9 | 6 |
| | | 10 | 0.3863 | 10 | 11 |

Overall, the flow regime analysis at the basin scale suggests that indices using IMP-LU provide a better prediction of flow variability as concluded in Section 4.6.1. The thermal analysis at the basin scale rarely differentiates the effect of using IMP-LU and IMP-LC. Further, the correlation coefficients, indices for the level of agreement for regression equations between IMP-descriptors and hydrological-response indicators, are so low that any strong conclusions cannot be derived at the basin scale. On the other hand, the thermal analysis at the sub-basin scale supports the earlier findings in the flow regime: IMP-LU turns out to be a better predictor than IMP-LC.

### 4.7 Sensitivity of hydrological response to IMP-descriptors

One recent study suggests that outcomes from a simple hydrological model considering spatial distribution and orientation of IMP are different from those resulting from using aggregate IMP (Moglen, 2000). From the hydrological perspective, it is of

interest to investigate if model structures employed as IMP-descriptors affect the prediction of hydrological response.

Model structures are designed such that IMP are integrated as parameters to examine the effect of IMP on the prediction of hydrological response. This study utilizes spatially lumped models reflecting an averaged value of IMP over a computational unit (individual basins or sub-basins in this study) and spatially distributed models requiring IMP based on individual 30-meter mapping unit of IMP-LU/IMP-LC. There are two different approaches for spatially distributed models: the WB and the SCS-CN. These model structures were described in detail in Chapter 3. In this section, the effect of model structures using IMP-LU and IMP-LC on the prediction of hydrological response will be discussed.

### 4.7.1 Spatially lumped versus spatially distributed

#### 4.7.1.1 Flow regime

In Figure 4-18 (a)-(d), Se/Sy is plotted with respect to regression equations for the flow regime analysis. Criterions are indicators of flow variability such as $R_{L1}$, $R_{Q10\text{-}90}$, CV, or $I_{R\text{-}B}$, while predictors in regression equations are IMP-descriptors such as Avg-Imp-LU, Avg-Imp-LC, WB-LU, WB-LC, or SCS-CN-LU, or SCS-CN-LC. The WB-based and the SCS-CN-based IMP-descriptors are modeled to have IMP utilized as a spatially distributed parameter, whereas the Avg-Imp approach requires only an averaged value of IMP for a given basin. Figure 4-18 corresponds to columns 1 through 4 and rows 1 through 20 in Table 4-17.

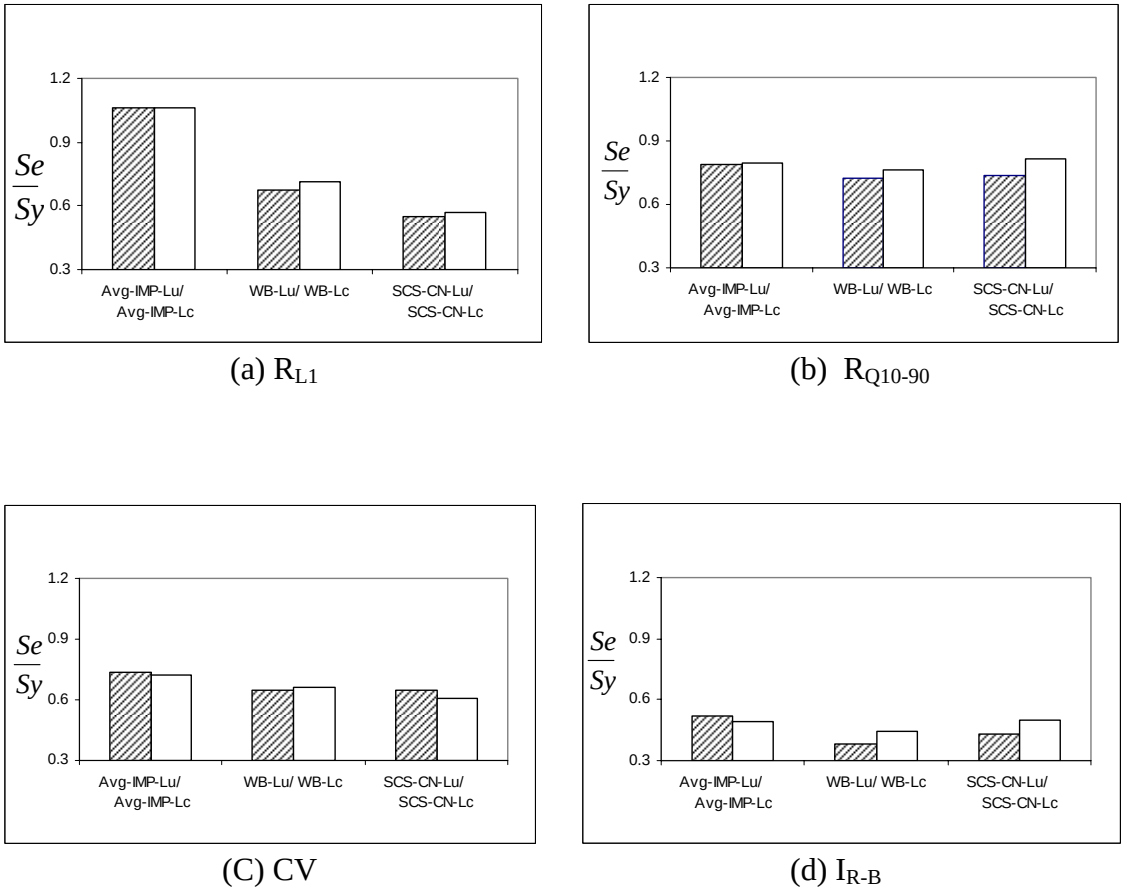


(a) $R_{L1}$ (b) $R_{Q10-90}$

(C) CV (d) $I_{R-B}$

Figure 4-18. Relative standard errors versus IMP-descriptors using IMP-LU ▨ ) and IMP-LC (□ ) over basins selected for the flow regime analysis with a given indicator of flow variability: (a) $R_{L1}$; (b) $R_{Q10-90}$; (c) CV; (d) $I_{R-B}$.

For all indicators of flow variability such as $R_{L1}$, $R_{Q10-90}$, CV, and $I_{R-B}$, spatially distributed models show a higher level of accurate prediction than lumped models do as seen Figure 4-18. Figure 4-18 depicts lower values of Se/Sy both for the WB-LU/LC and for the SCS-CN-LU/LC compared to the Avg-Imp-LU/LC. In other words, IMP-descriptors considering the spatial distribution of IMP are better predictors of flow variability than IMP-descriptors using aggregate IMP. For the data analyzed in this study

so far, it can be said that spatially distributed models are better predictors of flow variability than lumped models.

In order to investigate the effect of the use of IMP-LU versus IMP-LC on the prediction of hydrological response, a pair of adjacent bars (▨,□) within a model set is assessed in Figure 4-18 (a)-(d). For instance, the first pair of bars in Figure 4-18 (a) shows Se/Sy for spatially lumped models using IMP-LU (▨) and using IMP-LC (□). The same values of Se/Sy imply that the prediction of hydrological response is of essentially the same prediction accuracy for the use of IMP-LU versus IMP-LC if spatially lumped models of an IMP-descriptors are used. Note that the regression between the Avg-Imp-LU/LC models and $R_{L1}$ is poor with Se/Sy slightly greater than 1. On the other hand, the WB-based or the SCS-CN-based descriptors generally produce smaller Se/Sy if IMP-LU is used. Figures 4-18 (b), (c), and (d) show similar trends that the WB-based or the SCS-CN-based descriptor using IMP-LU produces a higher level of accurate prediction compared to counterparts using IMP-LC.

These results show that models considering the spatial distribution of IMP are better predictors of flow variability than models using a lumped value of IMP. Furthermore, models employing spatially distributed IMP-LU are better at predicting flow variability compared to models using spatially distributed IMP-LC. For the data examined in this study, lumped models are rarely affected by data sources of IMP.

#### 4.7.1.2 Thermal regime

For the thermal regime analysis, columns 5 through 7 and rows 1 through 20 in Table 4-17 are plotted as seen in Figure 4-19. At the basin scale, Figure 4-19 (a) and (b)

show that $R^2$ is too small to have any meaningful interpretation for the relationships between IMP-descriptors and thermal-variability indicators such as DD or MDTD. Although $D_{SURGE}$ shows relatively strong relationships with IMP-descriptors at the basin scale as shown in Figure 4-19 (c), the sub-basin scale will be mainly focused in the thermal regime analysis.

As depicted in Figure 4-19 (c) at the basin scale and (d)-(f) at the sub-basin scale, lumped models seem to predict thermal variability as well as distributed models. Avg-Imp-LU/LC shows comparable to or higher $R^2$ than WB-LU/LC or the SCS-CN-LU/LC.

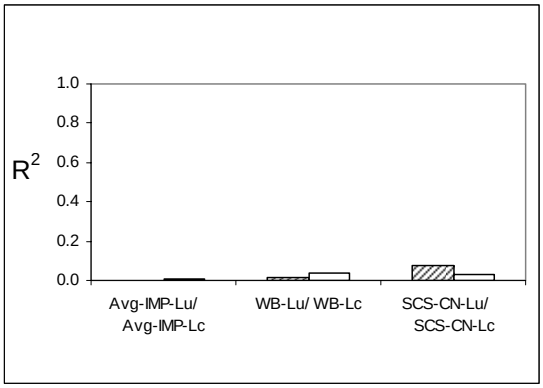


(a) DD

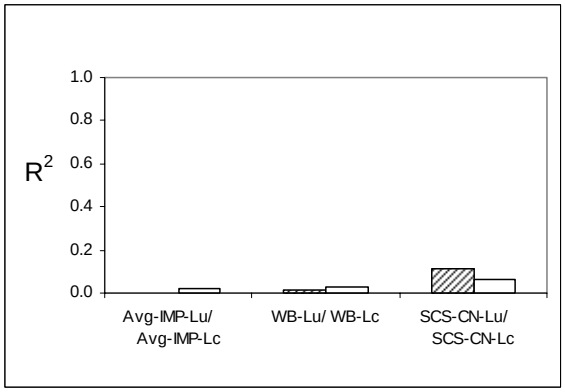


(b) MDTD

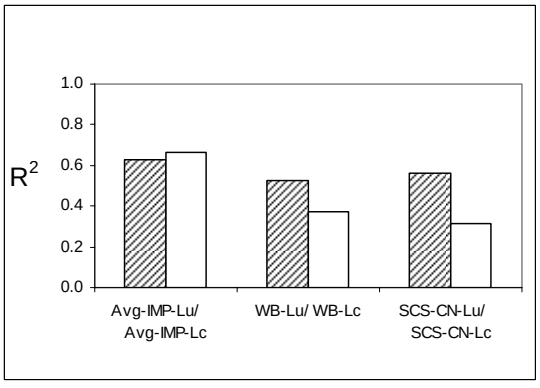


(c) $D_{SURGE}$

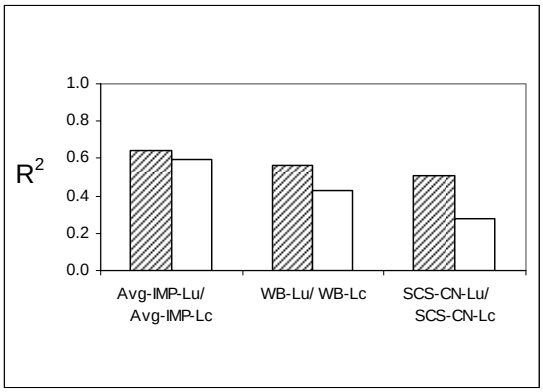


(d) DD

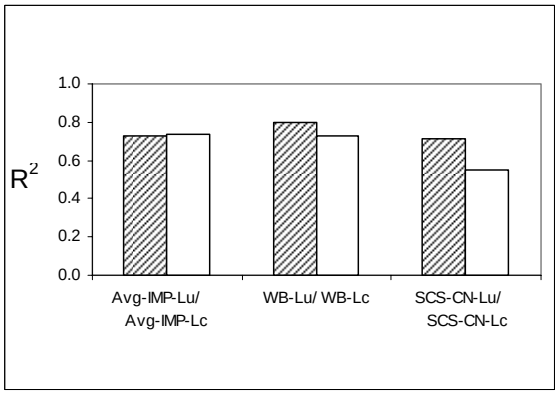


(e) MDTD

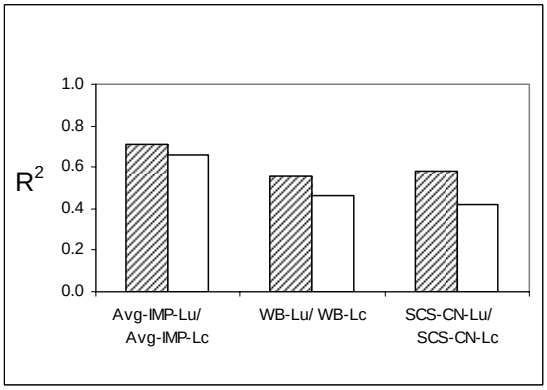


(f) $D_{SURGE}$

Figure 4-19. $R^2$ versus IMP-descriptors using IMP-LU (▨) and IMP-LC (□) over basins selected for the thermal regime analysis with a given indicator of thermal variability:
at the basin scale: (a) DD; (b) MDTD; (c) $D_{SURGE}$
at the sub-basin scale: (d) DD; (e) MDTD; (f) $D_{SURGE}$

In order to investigate the effect of the use of IMP-LU versus IMP-LC on the prediction of hydrological response, a pair of adjacent bars (▨ , □) within a model set using IMP-LU ( ▨ ) and using IMP-LC ( □) is assessed. The first pair of bars (Avg-Imp-LU and Avg-Img-LC) in Figures 4-19 (c), (d) and (f) illustrate that there exist differences in $R^2$ between using lumped values of IMP-LU and IMP-LC. This is in contrast to the flow regime analysis where the prediction of flow variability was rarely

affected by lumped value of IMP-LU or IMP-LC. The question is whether the observed difference is statistically significant or not.

In order to assess whether the difference between two correlation coefficients is statistically significant, hypothesis testing is conducted. For instance, $R^2_{\text{Avg-IMP-LC}}$ is 0.6609, while $R^2_{\text{Avg-IMP-LU}}$ is 0.6247 according to Table 4-17 as illustrated in Figure 4-19 (c). The hypotheses test is the following:

$H_O$: there exists no difference between the two correlation coefficients

$H_A$: there is a difference between the two correlation coefficients

These hypotheses are tested utilizing a $\chi^2$-statistic given by:

$$\chi^2 = \frac{(z_1 - z_2)^2 \times (n1-3) \times (n2-3)}{(n1+n2-6)} \tag{4-11}$$

where $z_i = \frac{1}{2}\ln(\frac{(1+R_i)}{(1-R_i)}$ , $i$= 1 or 2

$R_i$ = correlation coefficient, $R_1$ and $R_2$

$n1$, $n2$ = number of study basins for $R_1$ and $R_2$

$\chi^2$ =the value of $\chi^2$-distribution with 1 degree of freedom

$R_1$ and $R_2$ are 0.8130 and 0.7904 which correspond to $R^2$-values of 0.6609 and 0.6247 in Table 4-17. In this case, the number of study basins is 13. Equation 4-11 becomes Equation 4-12, resulting in a value of 0.0200 for $\chi^2$. Table 4-21 indicates that the null hypothesis should be accepted even at $\alpha$ =10%. Accepting the null hypothesis means

there is no statistical difference between two correlation coefficients, 0.6609 of $R^2_{\text{Avg-IMP-LC}}$ and 0.6247 of $R^2_{\text{Avg-IMP-LU}}$ as seen in Figure 4-19 (c)

$$\chi^2 = \frac{\left(0.5\ln\left(\frac{1+0.8130}{1-0.8130}\right) - 0.5\ln\left(\frac{1+0.7904}{1-0.7904}\right)\right)^2 \times (13-3)\times(13-3)}{(13+13-6)} = 0.02 \qquad (4\text{-}12)$$

Table 4-21. Summary of decisions for $\chi^2$ =0.02 based on $R^2_{\text{Avg-IMP-LU}}$ (=0.6247) and $R^2_{\text{Avg-IMP-LC}}$ (= 0.6609) at a given level of significance: accepting the null hypothesis implies no significant difference between 0.6247 and 0.6609. In this case, $D_{SURGE}$ is regressed on Avg-Imp-LU and Avg-Imp-LC at the basin scale as seen in Figure 4-19 (c).

| $\alpha$ , Level of significance (%) | $\chi^2$ -value | Decision |
|---|---|---|
| 1 | 6.63 | Accept $H_O$ |
| 5 | 3.84 | Accept $H_O$ |
| 10 | 2.71 | Accept $H_O$ |

Table 4-21 summarizes the result of the hypothesis testing for the two lumped IMP-descriptors using IMP-LU and IMP-LC on which $D_{SURGE}$ at the basin scale is regressed as seen in Figure 4-19 (c). The hypothesis testing was also performed for regression equations between lumped IMP-descriptors using IMP-LU/IMP-LC and DD or $D_{SURGE}$ at the sub-basin scale as illustrated in Figure 4-19 (d) and (f). The results of the hypothesis testing are summarized in Table 4-22. Accepting null hypothesis for all cases, the table indicates that the prediction of thermal variability is rarely affected by using lumped value of IMP-LU or IMP-LC. In contrast, spatially distributed models are affected in predicting thermal variability such that spatially distributed IMP-LU is a better predictor of thermal variability compared to IMP-LC. IMP-descriptors using IMP-

LU(▨) show higher $R^2$ than counterparts using IMP-LC (□) in Figure 4-19. These tendencies also appear in the flow regime analysis.

Table 4-22 (a). Summary of decisions for $\chi^2$ =0.04 based on $R^2_{\text{Avg-IMP-LU}}$ (=0.6453) and $R^2_{\text{Avg-IMP-LC}}$ (= 0.5918) at a given level of significance: accepting the null hypothesis implies no significant difference between 0.6453 and 0.5918. In this case, DD is regressed on Avg-Imp-LU and Avg-Imp-LC at the sub-basin scale as seen in Figure 4-19 (d).

| $\alpha$ , Level of significance (%) | $\chi^2$ -value | Decision |
|---|---|---|
| 1 | 6.63 | Accept $H_O$ |
| 5 | 3.84 | Accept $H_O$ |
| 10 | 2.71 | Accept $H_O$ |

Table 4-22 (b). Summary of decisions for $\chi^2$ =0.05 based on $R^2_{\text{Avg-IMP-LU}}$ (=0.7132) and $R^2_{\text{Avg-IMP-LC}}$ (= 0.6601) at a given level of significance: accepting the null hypothesis implies no significant difference between 0.7132 and 0.6601. In this case, $D_{SURGE}$ is regressed on Avg-Imp-LU and Avg-Imp-LC at the sub-basin scale as seen in Figure 4-19 (f).

| $\alpha$ , Level of significance (%) | $\chi^2$ -value | Decision |
|---|---|---|
| 1 | 6.63 | Accept $H_O$ |
| 5 | 3.84 | Accept $H_O$ |
| 10 | 2.71 | Accept $H_O$ |

### 4.7.2 Simple versus complicated

Among IMP-descriptors employed for this study, lumped IMP-descriptors such as Avg-IMP-LU/Avg-Imp-LC are the simplest models. Within the spatially distributed models, the difference between the WB and the SCS-CN, regarding parameters each model structure needs, is as follows. The WB-based descriptor requires one parameter,

infiltration which is a function of a soil type, while the SCS-CN-based descriptor needs one parameter CN which is a function of two factors: soil type and land use. In general, the WB-based descriptor is simpler than the SCS-CN-based descriptor.

#### 4.7.2.1 Flow regime

Section 4.7.1 showed that spatially distributed models were better than lumped models in predicting flow variability. Between the two spatially distributed models for the flow regime analysis, no clear trend was found. At a given criterion of $I_{R\text{-}B}$, the regression equation using WB-based IMP-descriptor shows a better agreement than using SCS-CN-based IMP-descriptor as seen in Figure 4-18 (d), whereas the SCS-CN-based IMP-descriptor produces better agreement than WB-based IMP-descriptors as illustrated in Figure 4-18 (a). Figures 4-18 (b) and (c) show no difference between the WB and the SCS-CN-based descriptors.

#### 4.7.2.2 Thermal regime

For the thermal regime, lumped models predict thermal variability as well as spatially distributed models. Within the two spatially distributed models using IMP-LU for the thermal regime analysis, no difference was observed between the WB or the SCS-CN-based descriptors based on Figure 4-19 (d), (e), and (f) This finding also appeared in the flow regime analysis, which was described just above. However, there exists difference between spatially distributed models using IMP-LC. The WB based IMP-descriptors are better predictors than SCS-CN-based IMP-descriptors.

### 4.7.3 Non-weighted versus weighted

Adding one more factor to consider with the existing model structures, the WB and the SCS-CN-based IMP-descriptors integrate a weighting scheme. The scheme is to examine whether IMP equally contributes to the hydrological behavior regardless of its location relative to the outlet of a basin. As seen in Figure 4-20 for the flow regime analysis, IMP-descriptors integrating a weighting scheme: the WB-ID or the SCS-CN-ID, produce larger relative standard errors than the WB or the SCS-CN. IMP-descriptors with a weighting scheme are poorer predictors of flow variability than their counterparts without a weighting scheme.

For the thermal regime at the basin scale as illustrated in Figure 4-21(a), the relationships between indicators of thermal variability and IMP-descriptors integrating a weighting scheme are so poor that a comparison study does not have any physical meaning. At the sub-basin scale, IMP-descriptors integrating a weighting scheme produce smaller $R^2$ than their counterparts without a weighting scheme as shown in Figure 4-21 (b). It implies that the hydrological response is not sensitive to model structures with weighted spatial variability of IMP, which is consistent both in the flow regime and in the thermal regime.

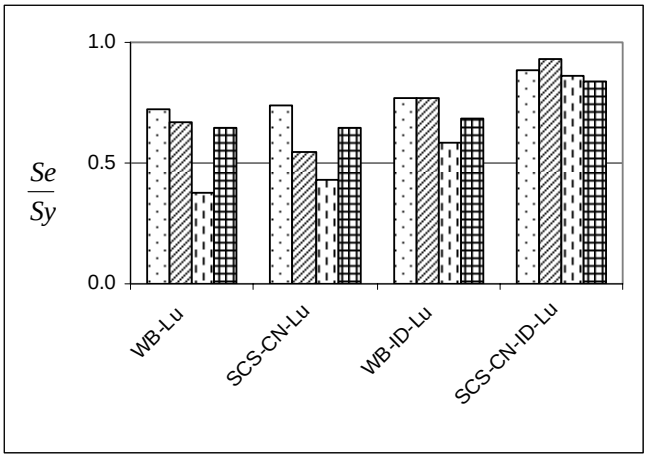


Figure 4-20. Relative standard errors for spatially distributed IMP-descriptors as predictors of flow variability:
$R_{Q10-90}$ ( ); $R_{L1}$ ( ); $I_{R-B}$ ( ); CV ( )

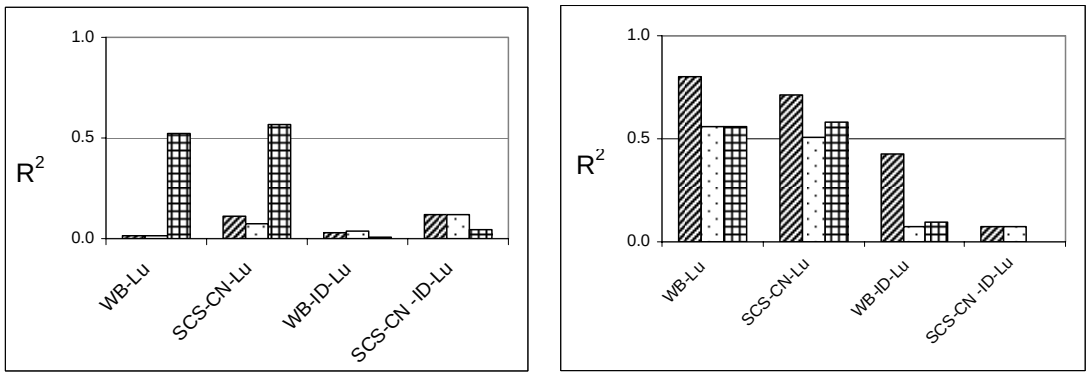


(a) at the basin scale (b) at the sub-basin scale

Figure 4-21. $R^2$ for spatially distributed IMP-descriptors as predictors of thermal variability:
MDTD ( ); DD ( ); $D_{SURGE}$ ( )

### 4.7.4 Summary

In this section, the evaluation of models used as IMP-descriptors from earlier sections will be summarized and compared from various perspectives. From the model structure viewpoint, this study reveals that spatially distributed IMP-descriptors, either the WB or the SCS-CN, are more effective than lumped IMP-descriptors in predicting

flow variability. Between the two spatially distributed ones, the WB and the SCS-CN, no difference is found. From the thermal regime analysis, this study finds that lumped IMP-descriptors are as good as spatially distributed IMP-descriptors as predictors of thermal variability. Between the two spatially distributed ones, no difference is found if IMP-LU is used.

In comparison of models using IMP extracted from different data source, land use or land cover, the SCS-CN-based IMP-descriptors are affected the most in this study. As seen in Figures 4-18 and 4-19, the level of accurate prediction for regression equations involving the SCS-CN-based IMP-descriptors experienced substantial change between using IMP-LU( ▨ ) and IMP-LC ( □ ), relative to pairs ( ▨,□) of other IMP-descriptors.

The poorest predictors in this study are any IMP-descriptors weighting the proximity of IMP to the outlet at a given basin. Particularly, SCS-CN-ID-based descriptor is the poorest predictor among IMP-descriptors in this study. The WB-ID performs better than SCS-CN-ID, although the WB-ID was not a good predictor overall. The flow regime analysis and the thermal regime analysis show their consistency in this finding. Besides, this finding remains unchanged regardless of the type of flow-variability indicators.

### 4.8 Comparison of hydrologic indices as indicators of hydrological response

This study utilized four indicators of flow variability: $R_{L1,}$ $R_{Q10-90}$, CV, $I_{R-B}$. Figure 4-22 illustrates that the sensitivity of each flow-variability indicator to IMP-descriptors is different from each other. $I_{R-B}$ is the indicator that is predicted the best by

the IMP-descriptors used in this study, showing relatively low Se/Sy compared to other indicators such as $R_{L1}$, $R_{Q10\text{-}90,}$ or CV. This result consists with Baker et al. (2004)'s study: $I_{R\text{-}B}$ is suitable for detecting flow change associated with land use changes. According to Baker et al., $I_{R\text{-}B}$ has lower interannual variability than other indicators such as coefficient of variation, CV.

For thermal variability, three indicators such as DD, $D_{SURGE,}$ and MDTD were used. Based on Figure 4-23 at the sub-basin scale, Mean daily temperature difference (MDTD) is the indicator of thermal variability that can be predicted the best by IMP-descriptors utilized in this study.

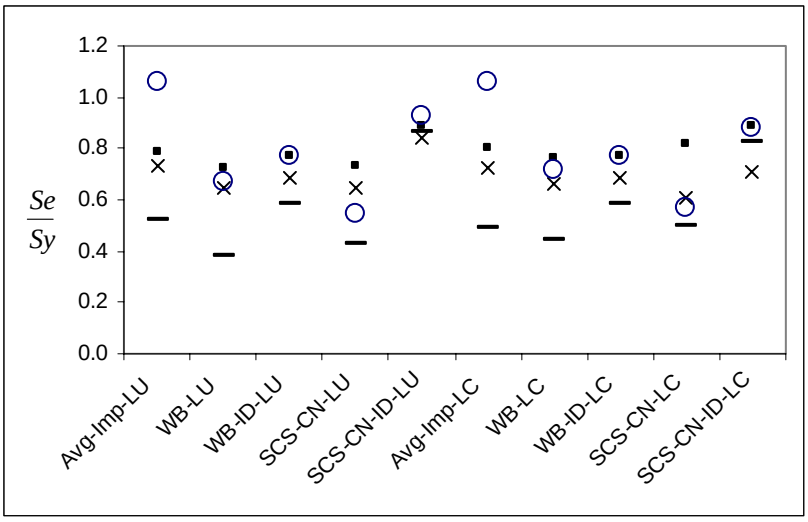


Figure 4-22. Relative standard errors for indicators of flow variability: $R_{L1}$ (○); $R_{Q10\text{-}90}$ (□); CV (x); $I_{R\text{-}B}$ (—) at a given IMP-descriptors.

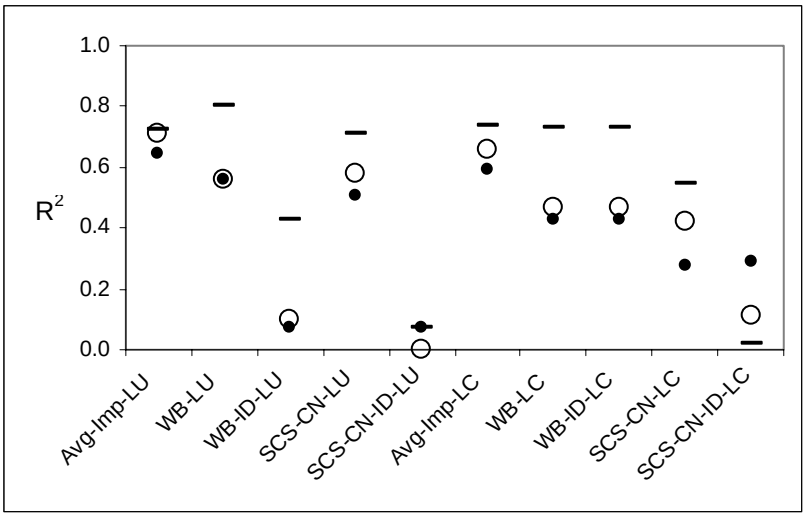


Figure 4-23. $R^2$ for indicators of thermal variability: DD (●); $D_{SURGE}$ (○); MDTD (—) at a given IMP-descriptors at the sub-basin scale.

### 4.9 Overall evaluation of hydrological response to IMP: Flow variability vs. thermal variability

In order to compare indicators of flow variability to thermal variability-indicators, the comparison should be conducted based on the same goodness-of-fit (GOF) measures. In this study, Se/Sy for all regression equations are calculated as seen in Table 4-24. Table 4-23 compares number of regression equations based on Table 4-24, satisfying certain statistical criteria. Table 4-23 indicates that regression equations predicting flow variability have higher level of accurate prediction than those predicting thermal variability: IMP-descriptors predict flow variability better than thermal variability.

Table 4-23. Regression equations (in percent) satisfying a given criteria of Se/Sy based on Table 4-24: number inside parenthesis is an actual number of regression equations that satisfy criteria.

| | Flow Regime | Thermal Regime | |
|---|---|---|---|
| Scale | Basin | Basin | Sub-basin |
| Number of regression equation | 40 | 30 | 30 |
| Se/Sy <0.8 | 75% (30) | 13% (4) | 50% (15) |
| Se/Sy <0.6 | 25%(10) | 0% (0) | 20% (6) |

Table 4-24. Relative standard errors for regression equations between an IMP-descriptor and an indicator of hydrological response in flow regime and in the thermal regime.

| Goodness-of-fit Statistics | | | | Indicator of flow variability | | | | Indicator of thermal variability | | |
|---|---|---|---|---|---|---|---|---|---|---|
| | | | | (1) | (2) | (1) | (2) | (1) | (2) | (1) |
| | | | | $R_{L1}$ | $R_{Q10-90}$ | $R_{L1}$ | $R_{Q10-90}$ | $R_{L1}$ | $R_{Q10-90}$ | $R_{L1}$ |
| IMP -LU | (a) Avg-Imp_LU | (1) | Basin | 1.0610 | 0.7902 | 0.7349 | 0.5199 | 1.0439 | 1.0445 | 0.6398 |
| | | (2) | PB sub-basin | - | - | - | - | 0.5656 | 0.6432 | 0.5784 |
| | (b) WB-LU | (3) | Basin | 0.6730 | 0.7266 | 0.6477 | 0.3799 | 1.0358 | 1.0380 | 0.7220 |
| | | (4) | PB sub-basin | - | - | - | - | 0.5825 | 0.7167 | 0.7167 |
| | (c) WB-ID-LU | (5) | Basin | 0.7727 | 0.7696 | 0.6879 | 0.5871 | 1.0292 | 1.0238 | 1.0425 |
| | | (6) | PB sub-basin | - | - | - | - | 0.8193 | 1.0410 | 1.0263 |
| | (d) SCS-CN-LU | (7) | Basin | 0.5491 | 0.7361 | 0.6477 | 0.4322 | 0.9853 | 1.0030 | 0.6885 |
| | | (8) | PB sub-basin | - | - | - | - | 0.5780 | 0.7570 | 0.7012 |
| | (e) SCS-CN-ID-LU | (9) | Basin | 0.9310 | 0.8862 | 0.8387 | 0.8639 | 0.9808 | 0.9812 | 1.0204 |
| | | (10) | PB sub-basin | - | - | - | - | 1.0416 | 1.0701 | 1.0801 |
| IMP -LC | (f) Avg-Imp_LC | (11) | Basin | 1.0610 | 0.7988 | 0.7233 | 0.4932 | 1.0323 | 1.0400 | 0.6082 |
| | | (12) | PB sub-basin | - | - | - | - | 0.5552 | 0.6901 | 0.6297 |
| | (g) WB-LC | (13) | Basin | 0.7141 | 0.7646 | 0.6611 | 0.4409 | 1.0280 | 1.0253 | 0.8282 |
| | | (14) | PB sub-basin | - | - | - | - | 0.5626 | 0.8172 | 0.7884 |
| | (h) WB-ID-LC | (15) | Basin | 0.7727 | 0.7696 | 0.6879 | 0.5871 | 1.0292 | 1.0238 | 1.0425 |
| | | (16) | PB sub-basin | - | - | - | - | 0.8193 | 1.0410 | 1.0263 |
| | (i) SCS-CN-LC | (17) | Basin | 0.5703 | 0.8149 | 0.6041 | 0.4974 | 1.0091 | 1.0269 | 0.8651 |
| | | (18) | PB sub-basin | - | - | - | - | 0.7256 | 0.9194 | 0.8206 |
| | (j) SCS-CN-ID-LC | (19) | Basin | 0.8826 | 0.8880 | 0.7098 | 0.8249 | 1.0272 | 1.0356 | 0.9910 |
| | | (20) | PB sub-basin | - | - | - | - | 1.0681 | 0.9099 | 1.0186 |

## 4.10 Summary of results

Table 4-25 summarizes the results of the comparison conducted to evaluate the sensitivity of hydrological response to IMP in the flow regime and in the thermal regime. The evaluation of the flow regime is based on the basin-scale experiments, while the evaluation of the thermal regime is based on experiments conducted at the sub-basin scale.

Table 4-25. Evaluation of the sensitivity of hydrological response to IMP

| Comparison | Flow regime | Thermal regime |
|---|---|---|
| Relations to be compared | IMP-descriptors using IMP-LU or IMP-LC and indicators of flow variability | IMP-descriptors using IMP-LU or IMP-LC and indicators of thermal variability |
| Basins vs. Sub-basins | N/A | The correlations are higher within sub-basins than across all study basins |
| IMP-LU vs. IMP-LC | 1. IMP-LU is a better predictor than IMP-LC overall. (section 4.6.1)<br><br>2. No difference if imperviousness is used as a lumped value. (section 4.7.1.1)<br><br>3. Spatially distributed IMP-LU is a better predictor than spatially distributed IMP-LC. (section 4.7.1.1) | 1. IMP-LU is a better predictor than IMP-LC overall. (section 4.6.2)<br><br>2. No difference if imperviousness is used as a lumped value. (proved with hypothesis testing in section 4.7.1.2)<br><br>3. spatially distributed IMP-LU is a better predictor than spatially distributed IMP-LC. (section 4.7.1.2) |

| | | |
|---|---|---|
| IMP-descriptors | 1. Model structures using spatially explicit IMP are better predictors of flow variability than ones using aggregate IMP. (section 4.7.1.1 and 4.7.4)<br><br>2.Between spatially distributed models, the WB and the SCS-CN do not show a difference in prediction of flow variability, either using IMP-LU or IMP-LC. (section 4.7.2.1 and 4.7.4)<br><br>3. Models without weighting schemes are better in predicting flow variability than models with weighting (section 4.7.3 and 4.7.4)<br><br>4. The SCS-CN is relatively the most sensitive to data sources of IMP among IMP-descriptors (section 4.7.4) | 1. model structures using lumped IMP predict thermal changes as well as models using a spatially explicit IMP. (section 4.7.1.2 and 4.7.4)<br><br>2-1. Using IMP-LU, there is no difference between the WB and the SCS-CN. (section 4.7.2.2 and 4.7.4)<br><br>2-2. Using IMP-LC, the WB is better than the SCS-CN (section 4.7.2.2)<br><br>3.Models without weighting schemes are better in predicting flow variability than models with weighting (section 4.7.3 and 4.7.4)<br><br>4. The SCS-CN is relatively the most sensitive to data sources of IMP among IMP-descriptors (section 4.7.4) |
| Indicators of hydrological response | $I_{R-B}$ is the most sensitive indicator of flow variability to IMP-descriptors used in this study (section 4.8) | Mean daily temperature difference (MDTD) is predicted the best by IMP-descriptors (section 4.8) |
| Hydrological response to IMP | IMP-descriptors predict flow variability better than thermal variability (section 4.9) | |

# CHAPTER FIVE

# SUMMARY, CONCLUSIONS, POLICY IMPLICATIONS, AND RECOMMENDATIONS

## 5.1 Overview

The main goal was to examine characteristics of IMP and its impacts on hydrological response. Based on this goal, three specific objectives were developed as follows: (1) to develop equations to translate between IMP estimates using land use (IMP-LU) and IMP estimates derived from land cover (IMP-LC); (2) to determine whether IMP-LU or IMP-LC is more effective at predicting the hydrological response in terms of flow variability and thermal variability, and (3) to determine whether spatially lumped IMP (aggregate) is a better predictor of hydrological response than spatially distributed IMP in terms of flow variability and thermal variability. This chapter will summarize results for the individual objectives. Based on the results, conclusions and recommendations are presented. Policy implications are also included.

## 5.2 Summary of the study

The first objective was to develop equations that translate between IMP estimates using land use and land cover. To meet this objective, the power model structure were selected for the relationship between IMP-LU and IMP-LC. A numerical optimization method was employed to calibrate the regression models, which resulted in Equation 4-3 and 4-4. These equations translate between IMP estimates using two different data sources and are useful tools in utilizing consistent data sources for hydrological models.

The second objective was to study the impact of using different data sources of IMP from a hydrological perspective. This analysis determined whether IMP-LU or IMP-LC is more effective at predicting hydrological response in terms of flow variability and thermal variability. Goodness-of-fit measures were used to assess the sensitivity of hydrological response to IMP-descriptors. The assessment revealed that IMP-LU was better in predicting flow variability and thermal variability than IMP-LC. A possible explanation for this finding is that IMP-LU reflects the modified flow network through drainage infrastructure compared to IMP-LC which describes the nature of the land surface.

The third objective was to determine whether spatially lumped or spatially distributed IMP was a better predictor of flow variability and thermal variability. The relationships between IMP-descriptors and indicators of hydrological response showed that spatially distributed IMP was a better predictor than spatially lumped (or aggregate) IMP in the flow regime analysis. The former reflects spatial heterogeneity of IMP within a given basin, while the latter represents a mean value across a given basin. Therefore, it is not surprising that spatially distributed IMP explains hydrological processes better than lumped IMP. However, the superiority of spatially distributed IMP does not hold true in all cases: the thermal regime analysis showed that the predictive power of spatially lumped IMP is comparable to or better than that of spatially distributed IMP. The reasons for this finding are unclear, but a possible explanation is that spatial heterogeneity of IMP is simply not a significant factor in predicting thermal variability.

Between spatially distributed IMP-descriptors, the WB-based IMP-descriptor generally predicted hydrological response as well as the SCS-CN-based IMP-descriptor.

The WB-based descriptor requires one parameter, an infiltration index, which is a function of soil type, whereas the SCS-CN-based descriptor needs the curve number that is a function of soil type and land use. A simple model with fewer inputs (the WB-based descriptor) was comparable to a model requiring more inputs (the SCS-CN-based descriptor) in predicting flow variability. A similar trend was found in the thermal regime.

Having summarized the characteristics of IMP and its impacts on hydrological response, a question arises: What do these results mean to hydrologists, engineers, and decision makers? The next section will address practical benefits from the findings in this study.

### 5.3 Conclusions

The conclusions in this study are drawn from the results of two experiments: flow regime analysis at a basin scale and thermal regime analysis at a sub-basin scale. The thermal regime analysis at the basin-scale as seen Figure 4-19 (a) and (b) are excluded from these conclusions because relationships between IMP-descriptors and indicators of hydrological response at the basin scale were not found.

IMP is data source-specific and relationships between hydrological response and either IMP-LU or IMP-LC may be different. It is necessary to use the same data source when modeling future predictions as was used in calibrating any hydrological models. For that reason, it becomes problematic when a data source is needed and is not available. The conversion equations between IMP-LU and IMP-LC developed in this study will

serve the role: these equations facilitate the conversion of IMP estimates from one data source to its equivalent value using the other data source.

This study revealed that generally IMP-LU is a more effective predictor of hydrological response than IMP-LC. IMP-LU is therefore, of greater value than IMP-LC from the perspective of modeling hydrological predictions. However, obtaining IMP-LC is cost- and time-efficient, compared to obtaining IMP-LU, since IMP-LC can be prepared from satellite remote sensing which facilitates rapid, direct mapping of land cover. IMP-LC is available over nearly all geographic locations at different points in time, which allows land cover changes with time to be easily studied. It is likely that IMP-LC is available, while IMP-LU is needed for hydrological modeling and not available. In this circumstance, the conversion equations between two different data sources developed in this study will play a great role.

Considering IMP as a tool for estimating hydrological response to land use/land cover change and supporting decision makers and land use planners, a simple model that can be easily understood and used by non-experts is needed. In this study, simple models were shown to work as well as complicated models. If simpler models perform analyses at a comparable level to complex models, the former has a higher practical value than the latter, especially for supporting planning level decisions. Further, compared to lumped values of IMP, calculating spatially distributed measures of IMP can be a complicated task. This study revealed that lumped IMP was comparable to spatially distributed IMP in predicting thermal variability. Using lumped IMP also means that hydrological response in the thermal regime can be predicted by aggregate IMP without the use of complex hydrological models. These findings will encourage non-experts to

quantitatively estimate the impacts of land use change on hydrological response. Such estimates would be useful to anticipate the consequences of different planning alternatives.

### 5.4 Policy implications

The essential idea of a threshold-based approach is to identify a threshold level at which negative impacts of IMP on the ecological and hydrological system occur and to limit land development to remain less than the identified threshold level. As the implementation of threshold-based policies grows, the issue of identifying a threshold value of IMP should be closely examined. However, since IMP is method- and data source-specific, it is difficult to associate a single value of IMP with a certain level of degradation.

With the finding that IMP-LC tends to produce smaller values of IMP than IMP-LU, a decision made based on IMP-LC may cause an underestimation error. A planner might incorrectly find that IMP does not surpass a policy threshold and allow the land be developed further. Such an error would result in damages to the ecosystem. To avoid this type of error, a standardized method to both measure IMP and predict future value of IMP should be established.

### 5.5 Limitations and recommendations

Throughout the study, several research items would have been useful if included. Further investigation of the following issues is recommended.

First, the sample size for the thermal regime analysis was limited when compared with that for the flow regime analysis. As a result of both temporal and spatial sample limitations, this study could not find a consistent trend or could not find an appropriate explanation for the observed phenomena in the thermal regime. For instance, the thermal analysis at a basin scale shows very little correlation between IMP-descriptors and indicators of thermal variability. One of possible explanation is that the heat is dissipated quickly and subjects to considerable sampling variation. Further studies can be extended to increase sample sizes at a basin scale as well as at a sub-basin scale. Also, it is important to make an effort to maintain temperature loggers in already existing study basins.

Second, regression equations developed in this study to translate between IMP from two different data sources should be examined from a hydrological perspective. Translated IMP from IMP using another data source, IMP-LU from IMP-LC or vice versa, may contain substantial uncertainty in predicting hydrological response. The cause of such an uncertainty reflects the nature of the relationship between IMP-LU and IMP-LC. There is a wide range of variance around the developed regression equations.

Third, there was considerable uncertainty was evident in the process of assigning a CN value based on land cover. For example, one of the land cover categories, “grass” can belong to either “institutional” or “open urban land”. Depending on the land use of institutional or open land, the curve number varies dramatically from the range of 81-93 to 49-84, respectively, for various hydrologic soil groups. This may explain why the

SCS-CN approach using IMP-LC did not show strong relationships with indicators of hydrological response. Further study may require visual interpretation of fine-resolution images or aerial photos to assign an appropriate CN value to a given land cover category.

Forth, this study consistently showed that model structures weighting the proximity of IMP to an outlet in a basin were not sensitive to the hydrological response. Maybe it is because model structures were inappropriately designed to assign weights on the spatial proximity of IMP to basin outlets. Further research can include developing models such that the impact of spatial proximity of IMP differentiates model outcomes substantially.

# APPENDIX A

This appendix recorded temperature plotted over the time period of 2002-2004. The time period of the interest for this study was only from May to September due to seasonal variation.

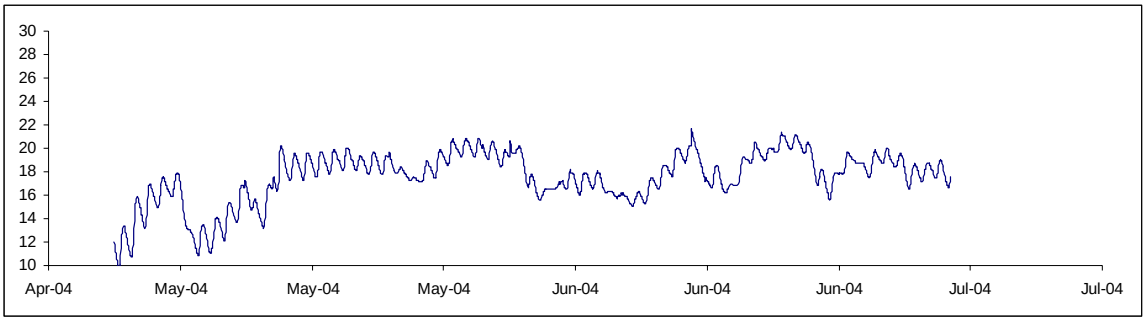


Figure A-1 PB01

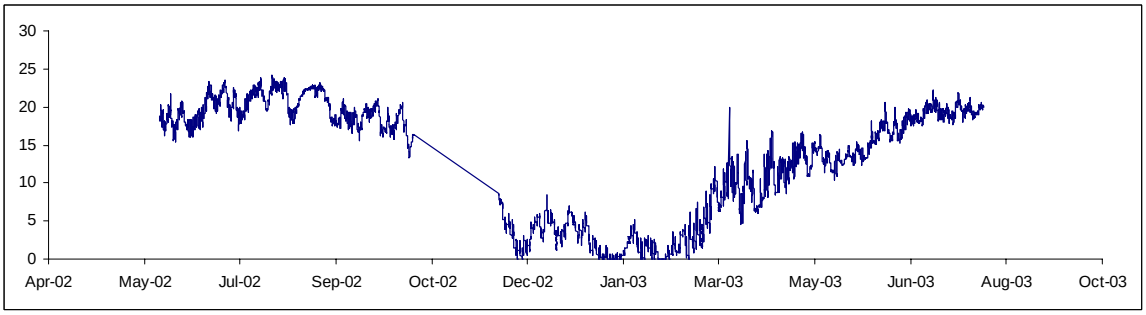


Figure A-1 PB02

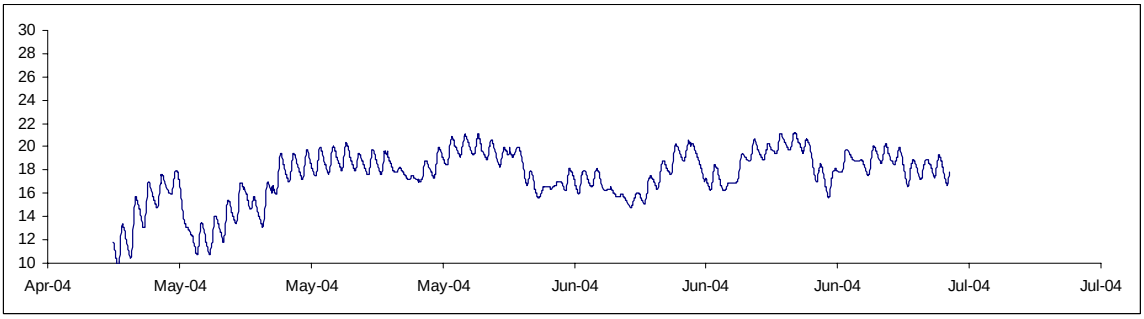


Figure A-1 PB03

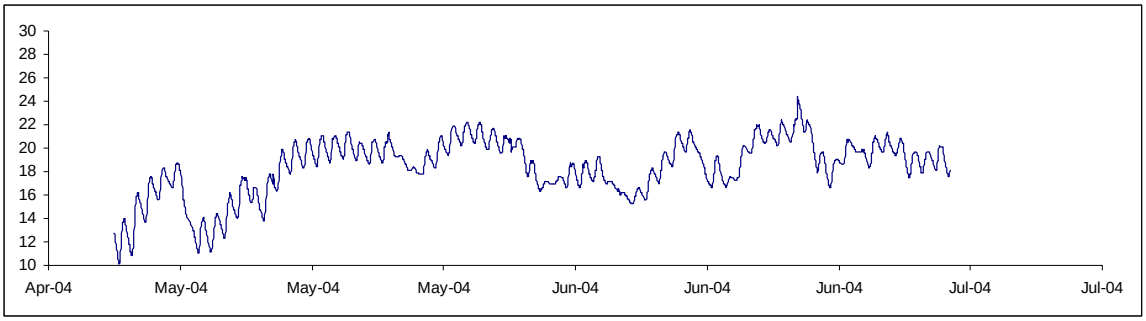


Figure A-1 PB07

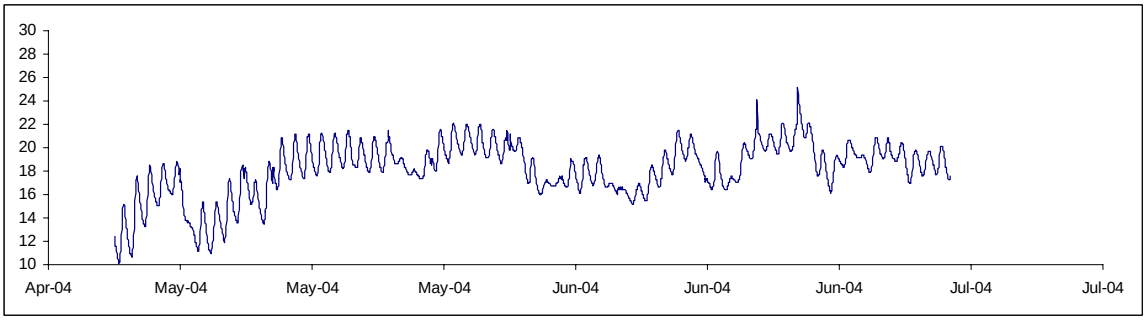


Figure A-1 PB08

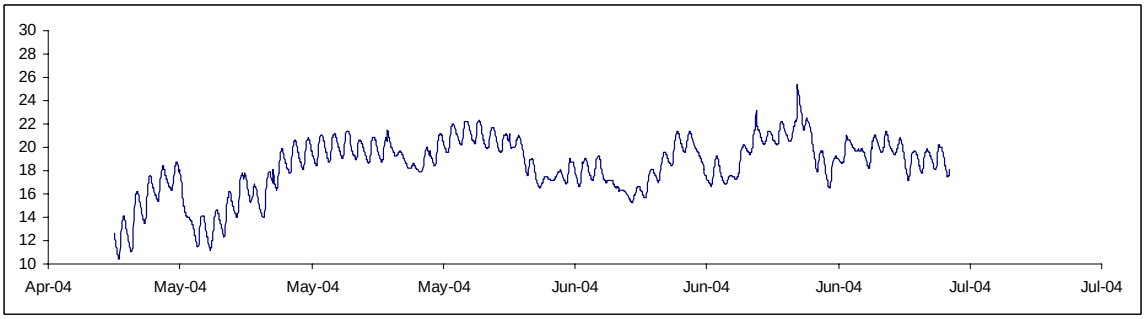


Figure A-1 PB09

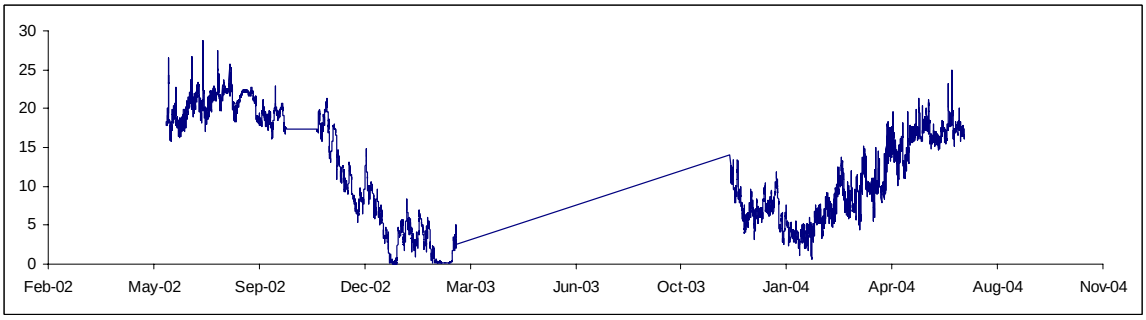


Figure A-1 PB13

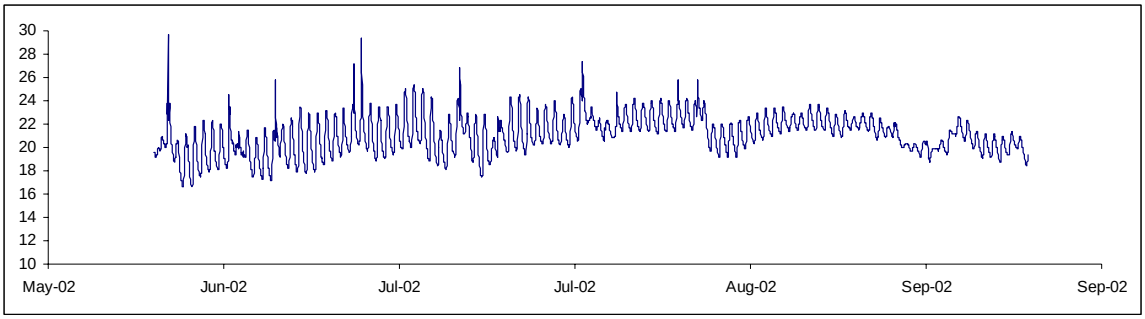


Figure A-1 PB20

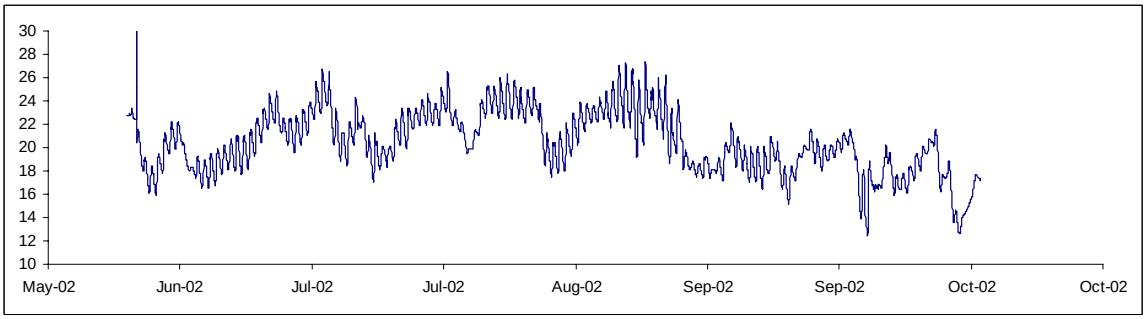


Figure A-1 NWB05

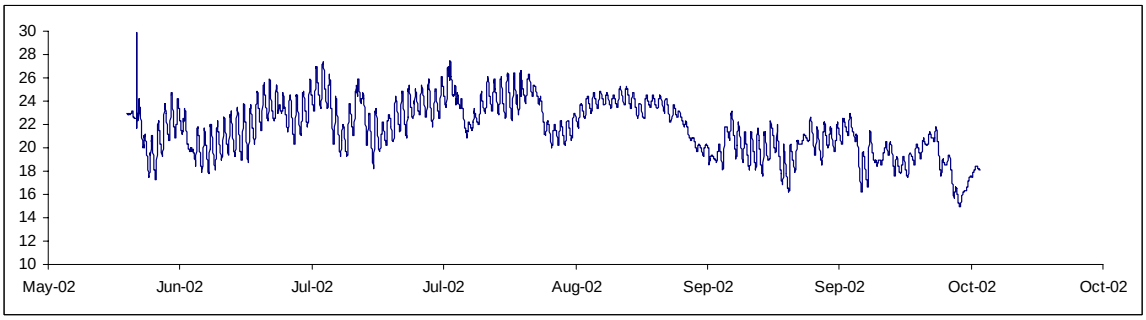


Figure A-1 NWB13

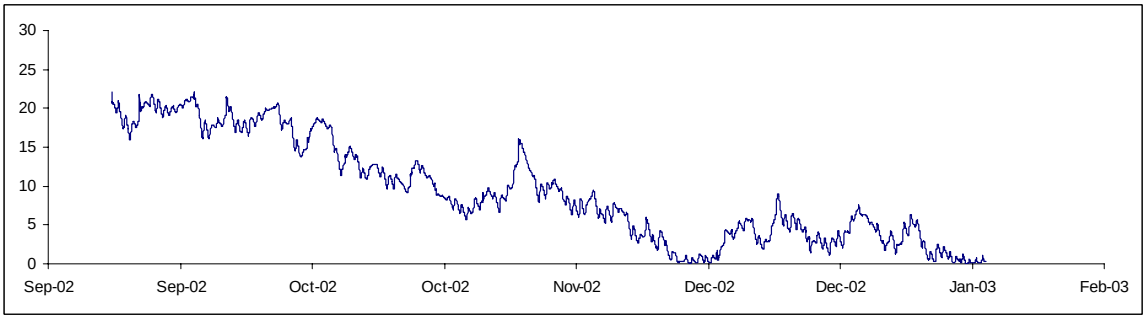


Figure A-1 NWB18

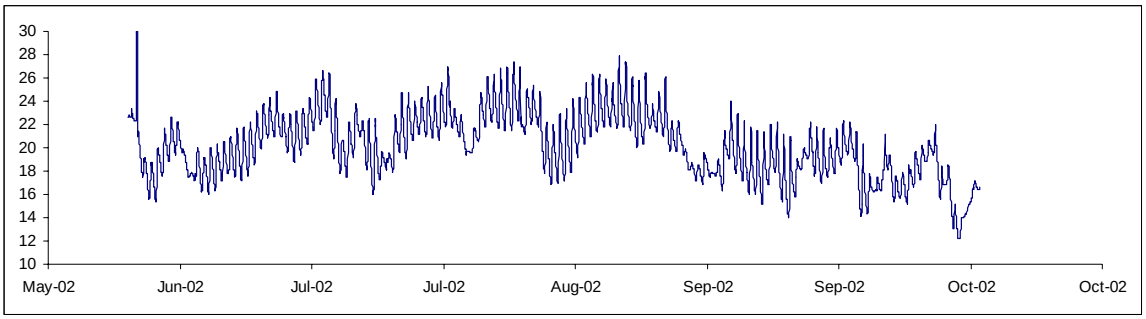


Figure A-1 HR18

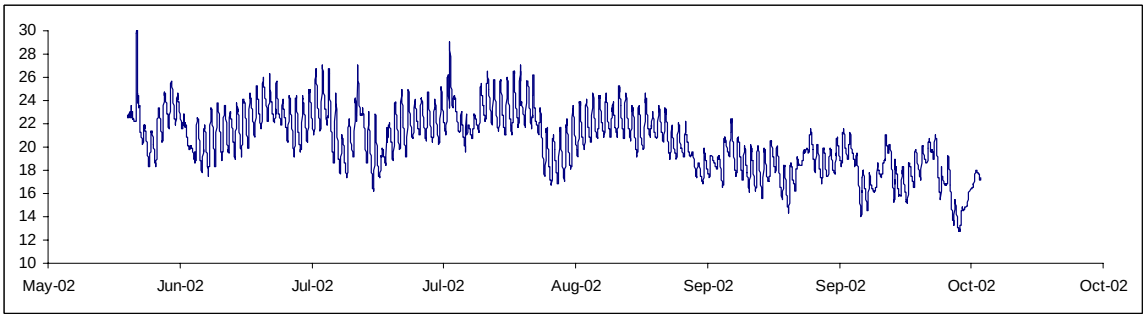


Figure A-1 HR19

# APPENDIX B

In this section, Mean daily stream flow datasets are plotted over the study period, from the water year 1997 to the water year 2003. The stream flow is recorded in units of cubic-feet per-second (cfs).

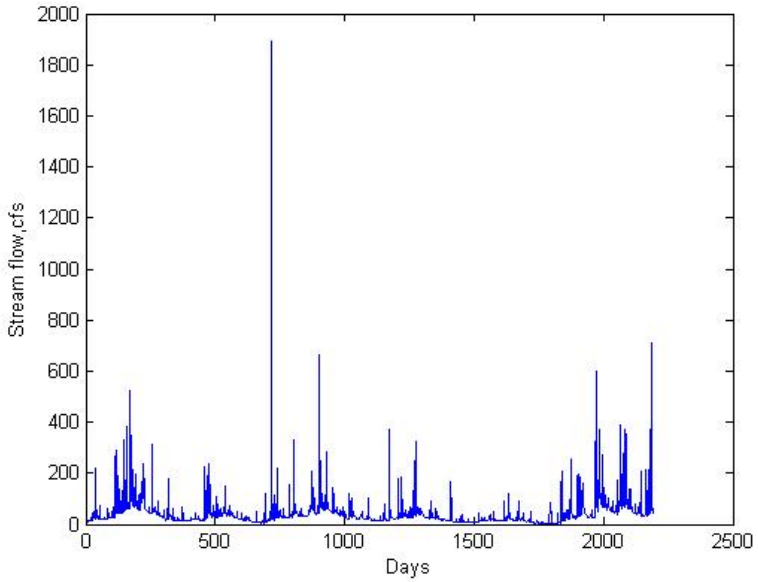


Figure B-1 Gage ID 1581700

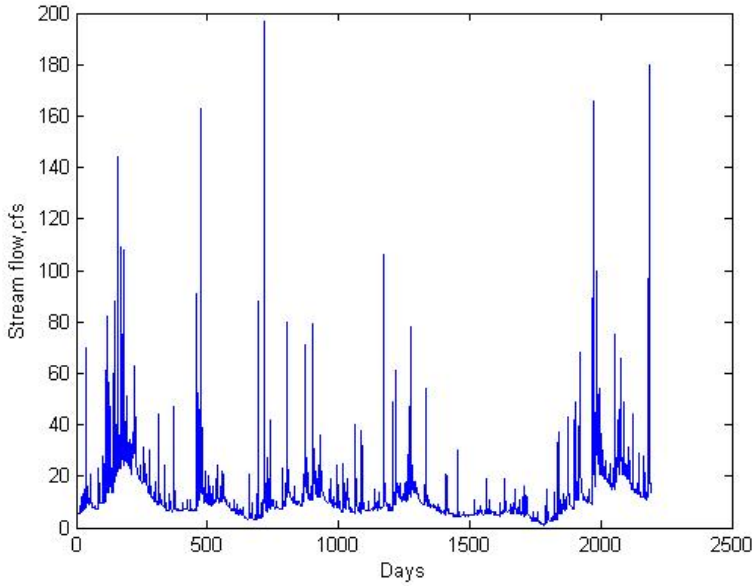


Figure B-2 Gage ID 1583100

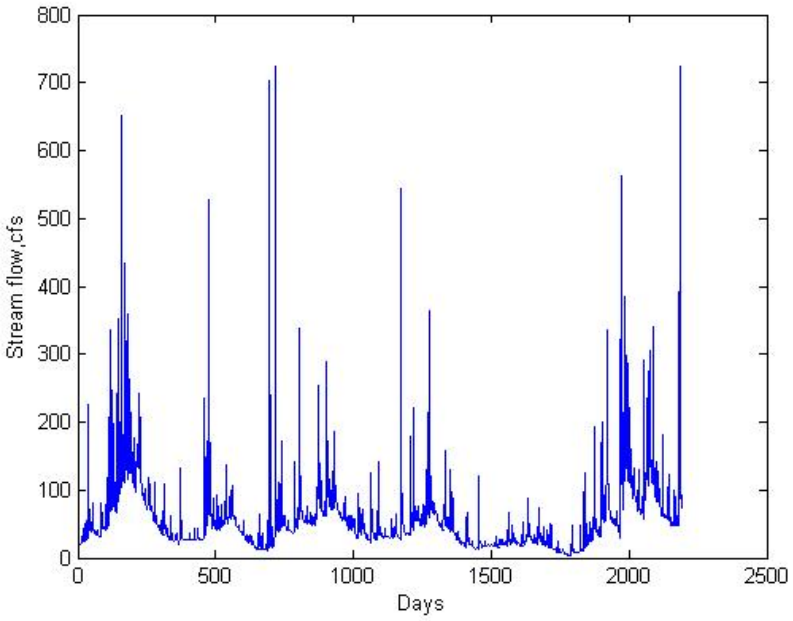


Figure B-3 Gage ID 1583500

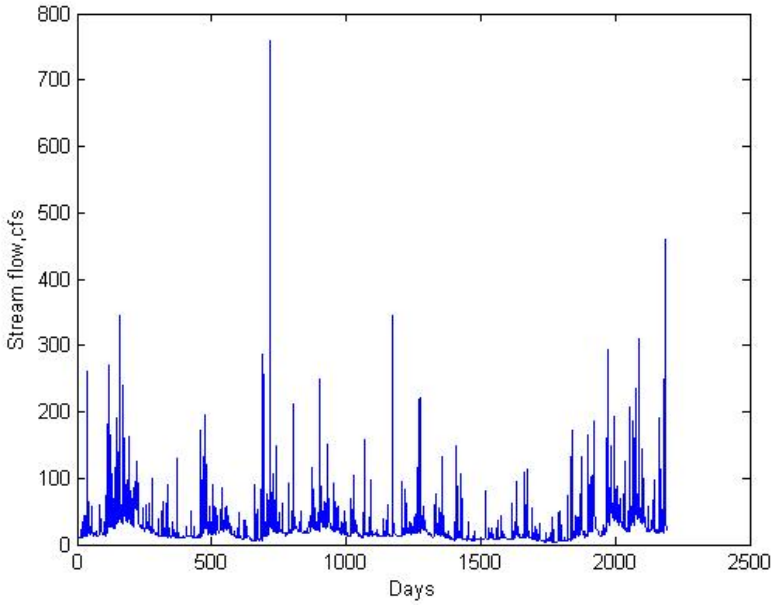


Figure B-4 Gage ID 1583600

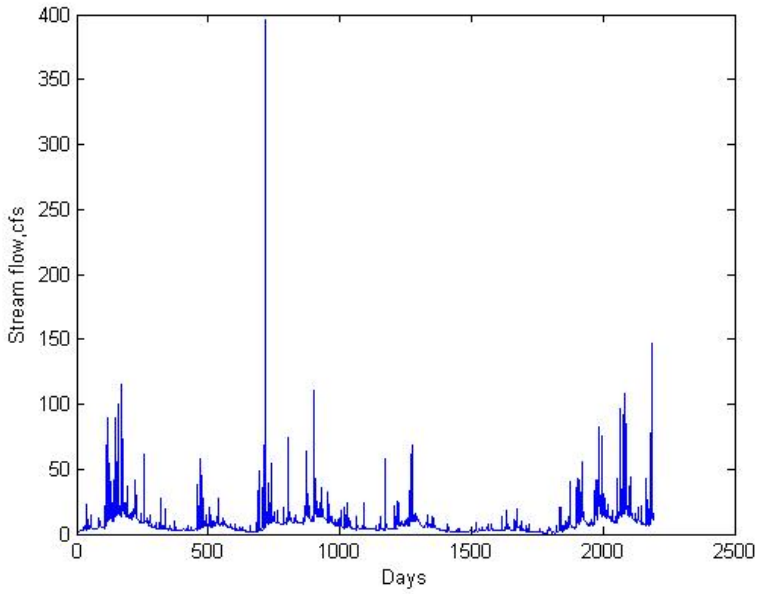


Figure B-5 Gage ID 1584050

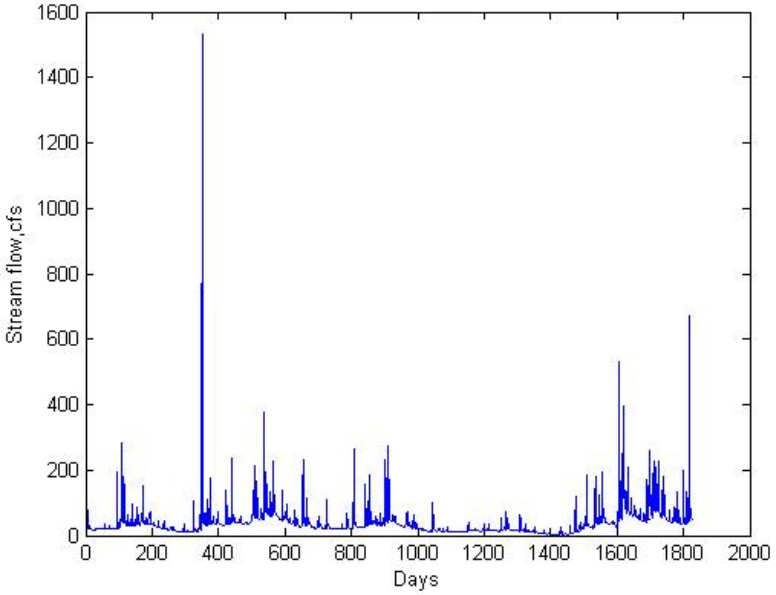


Figure B-6 Gage ID 1584500

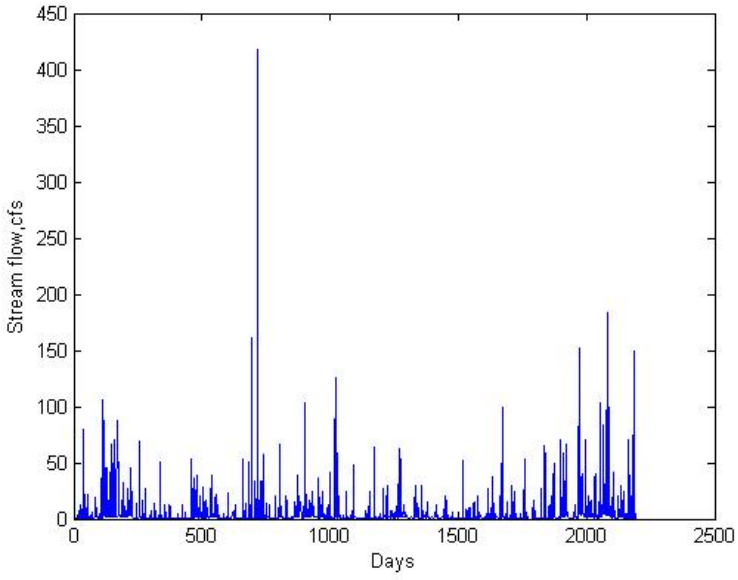


Figure B-7 Gage ID 1585090

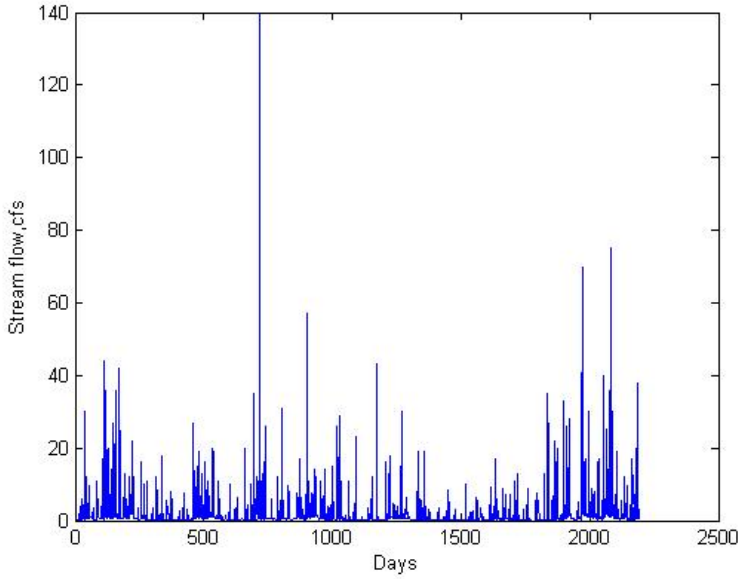


Figure B-8 Gage ID 1585095

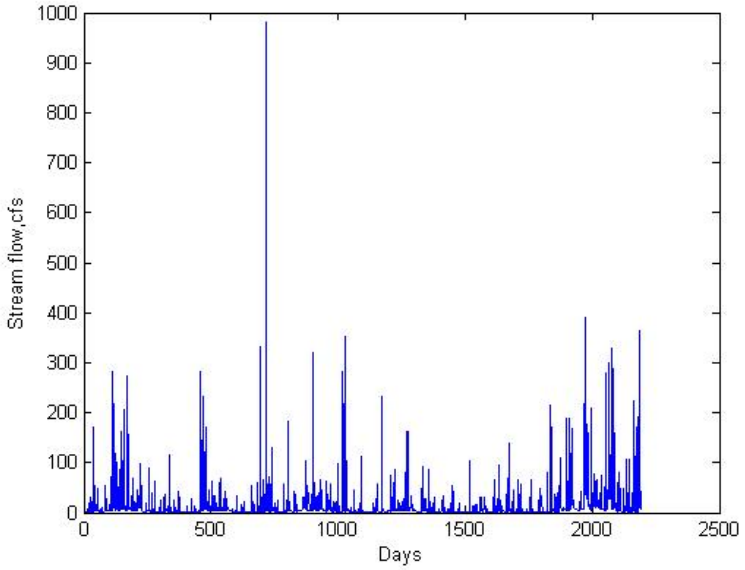


Figure B-9 Gage ID 1585100

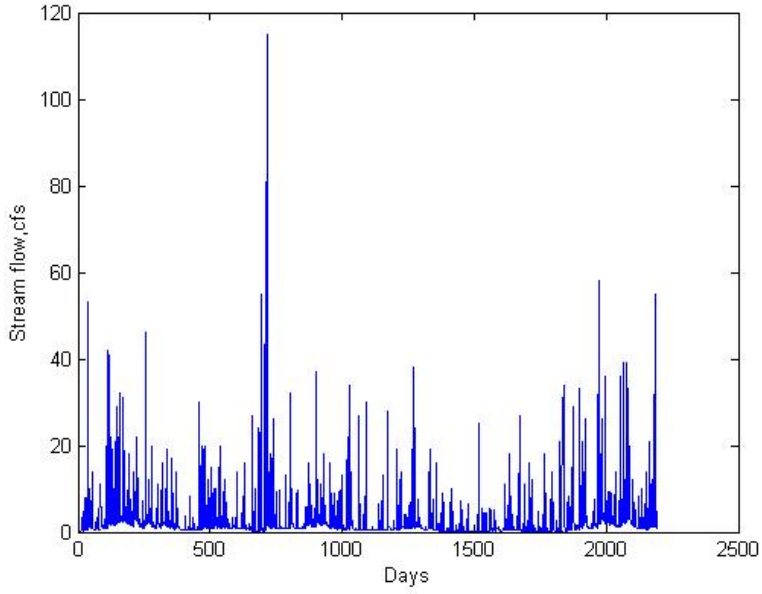


Figure B-10 Gage ID 1585200

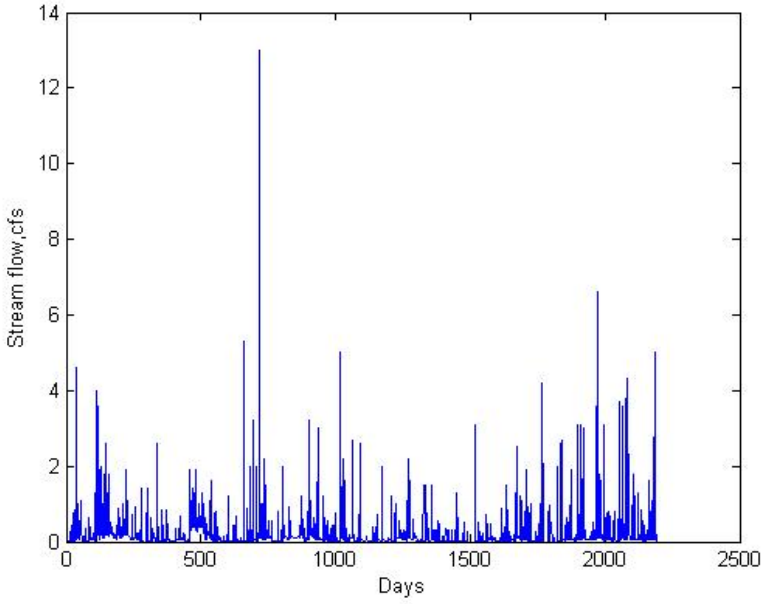


Figure B-11 Gage ID 1585225

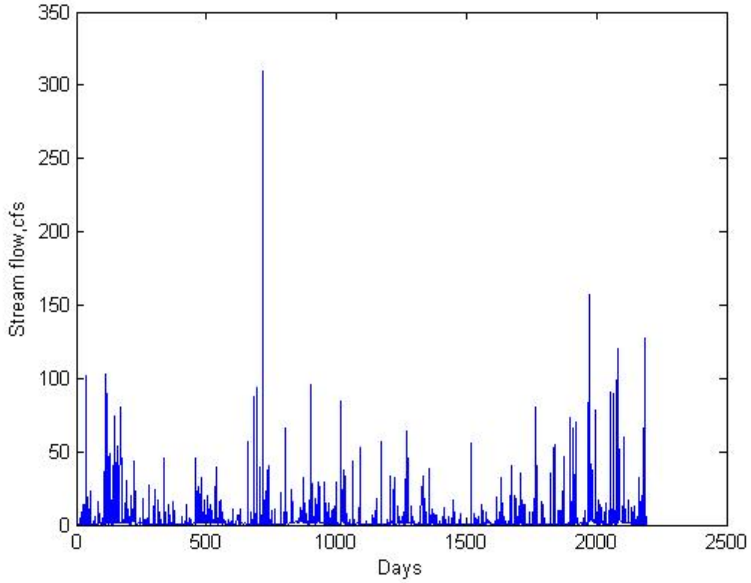


Figure B-12 Gage ID 1585230

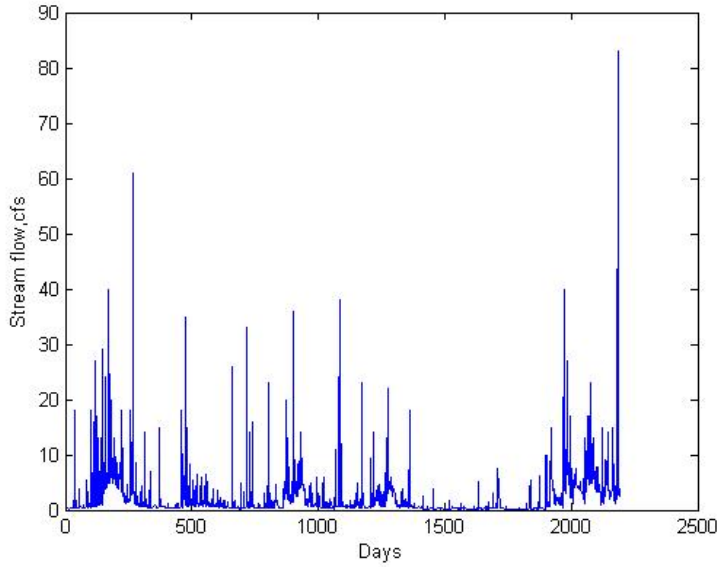


Figure B-13 Gage ID 1585500

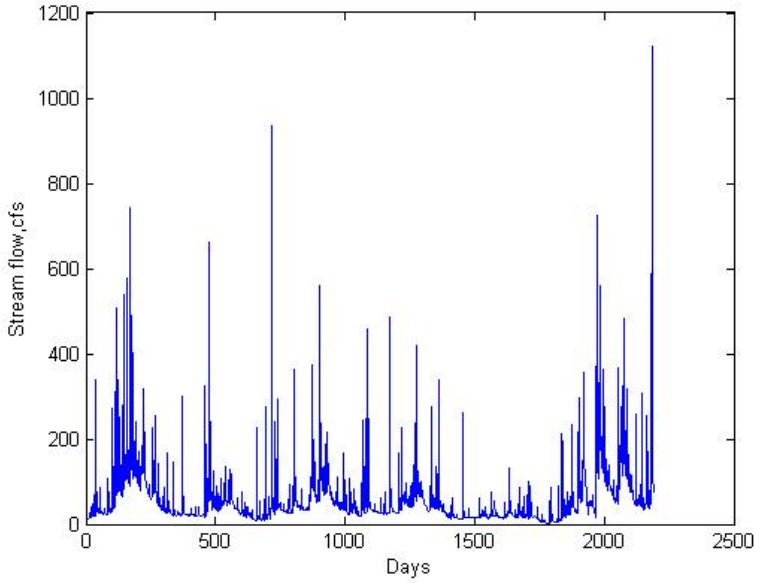


Figure B-14 Gage ID 1586000

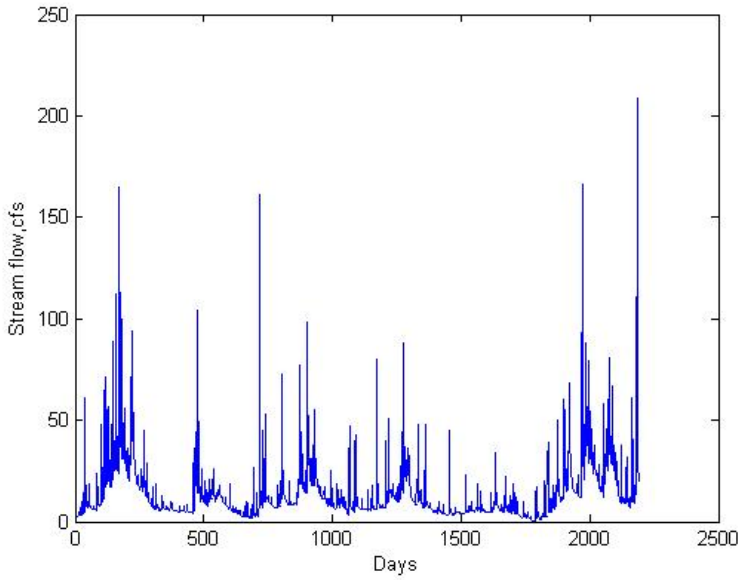


Figure B-15 Gage ID 1586210

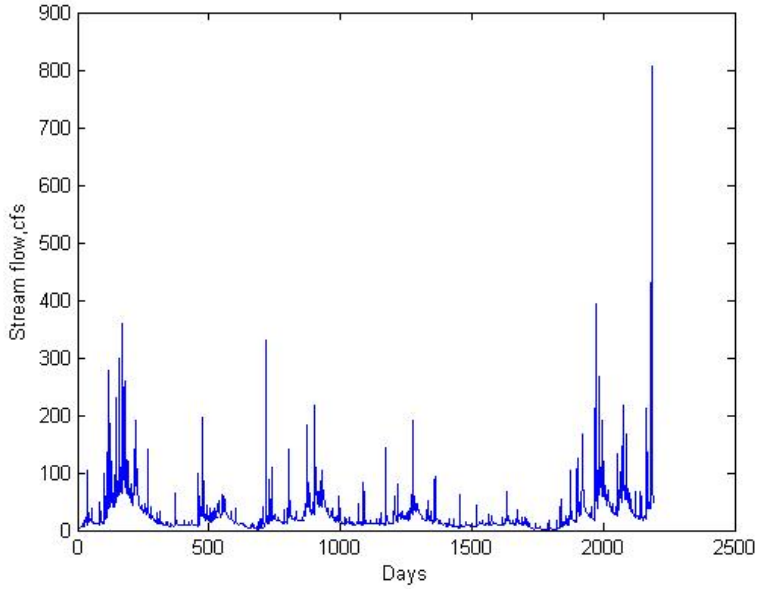


Figure B-16 Gage ID 1586610

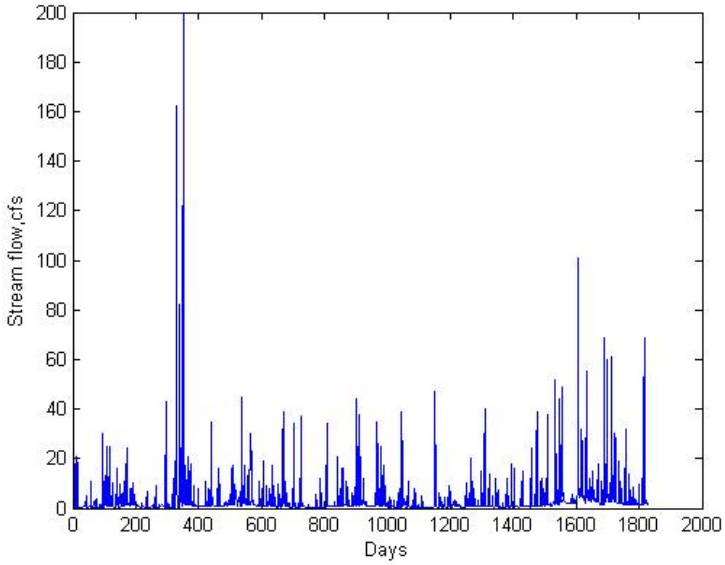


Figure B-17 Gage ID 1589100

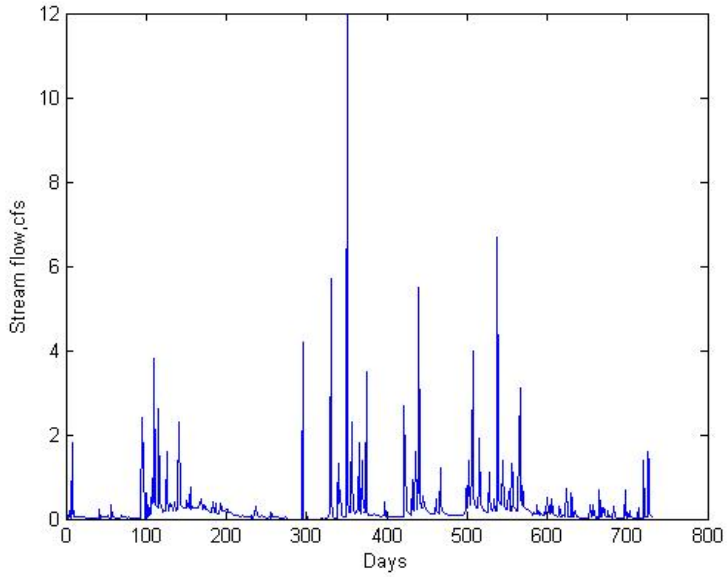


Figure B-18 Gage ID 1589180

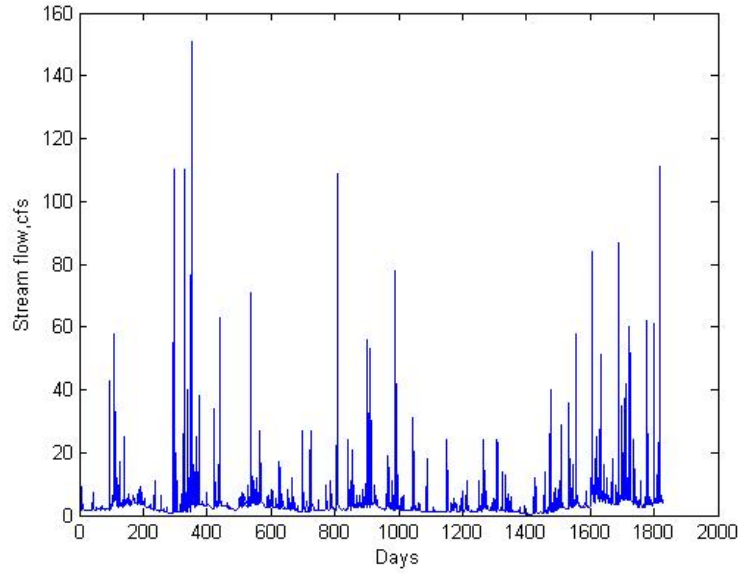


Figure B-19 Gage ID 1589197

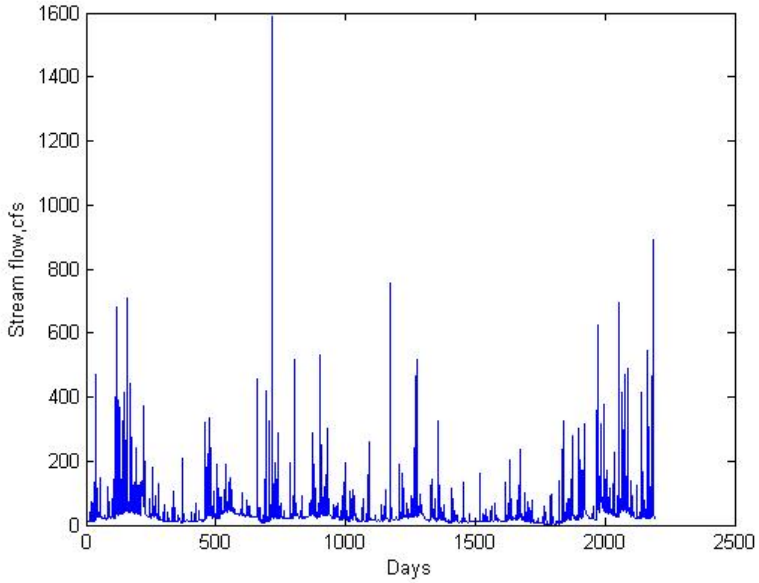


Figure B-20 Gage ID 1589300

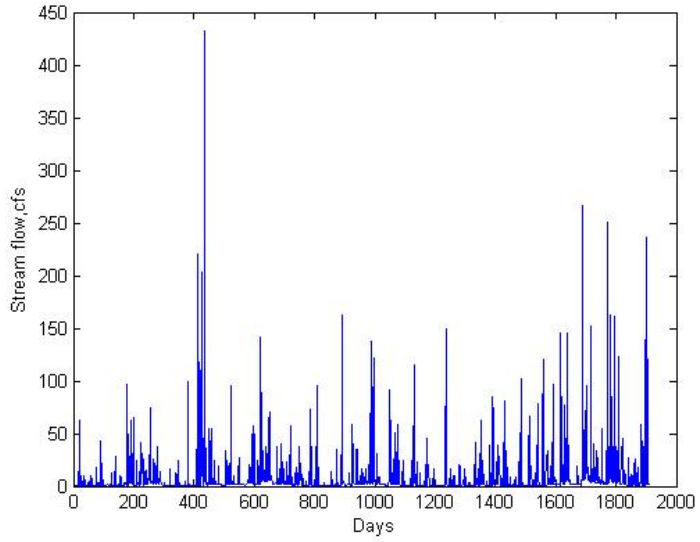


Figure B-21 Gage ID 1589330

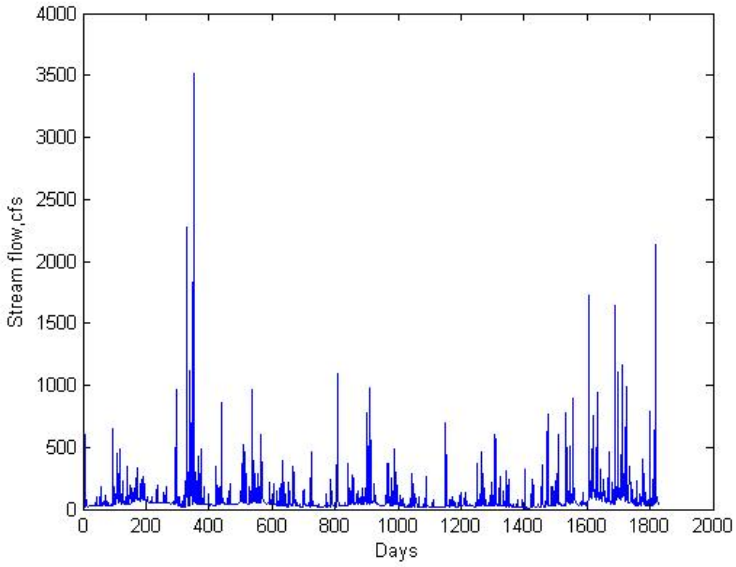


Figure B-22 Gage ID 1589352

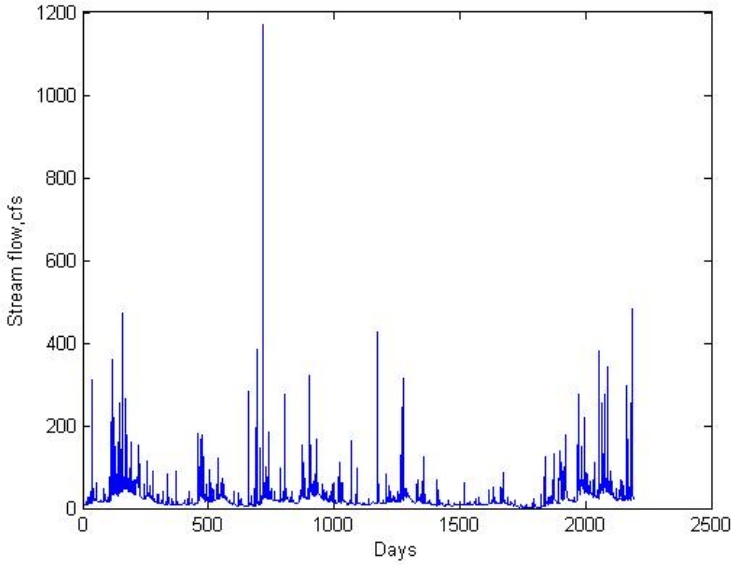


Figure B-23 Gage ID 1589440

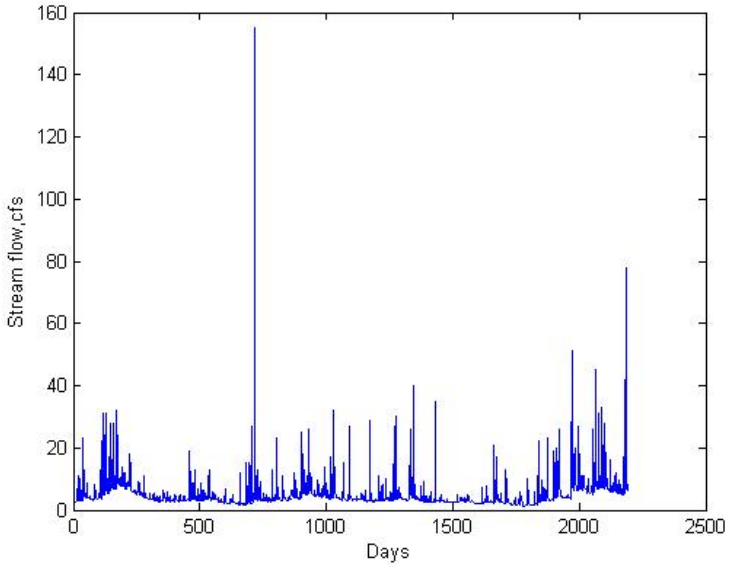


Figure B-24 Gage ID 1589500

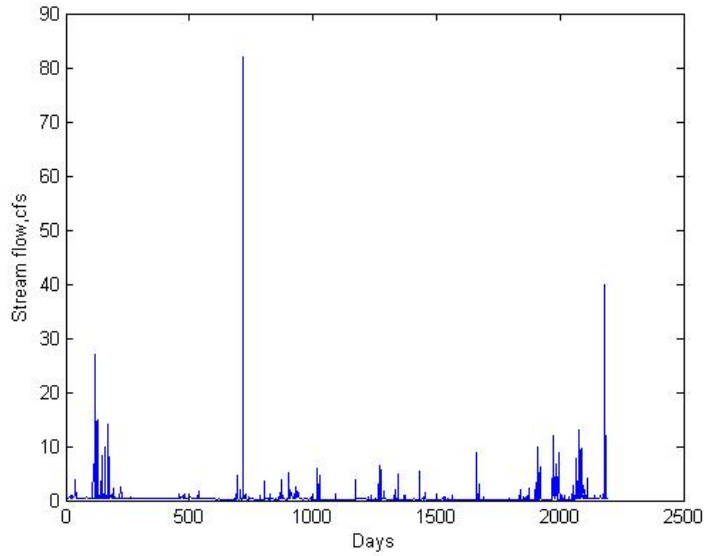


Figure B-25 Gage ID 1589795

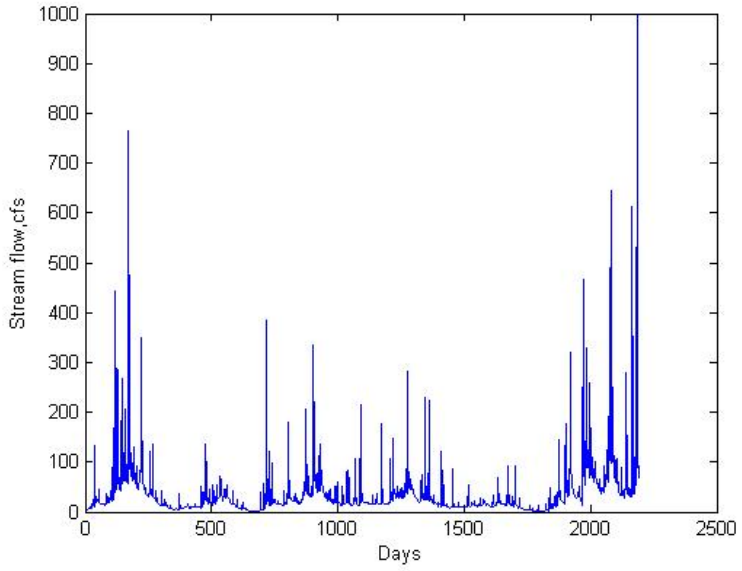


Figure B-26 Gage ID 1591000

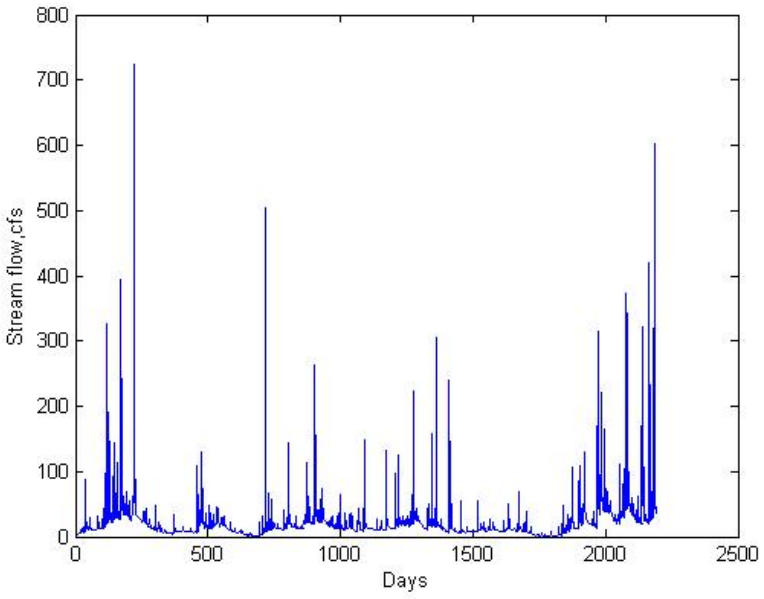


Figure B-27 Gage ID 1591400

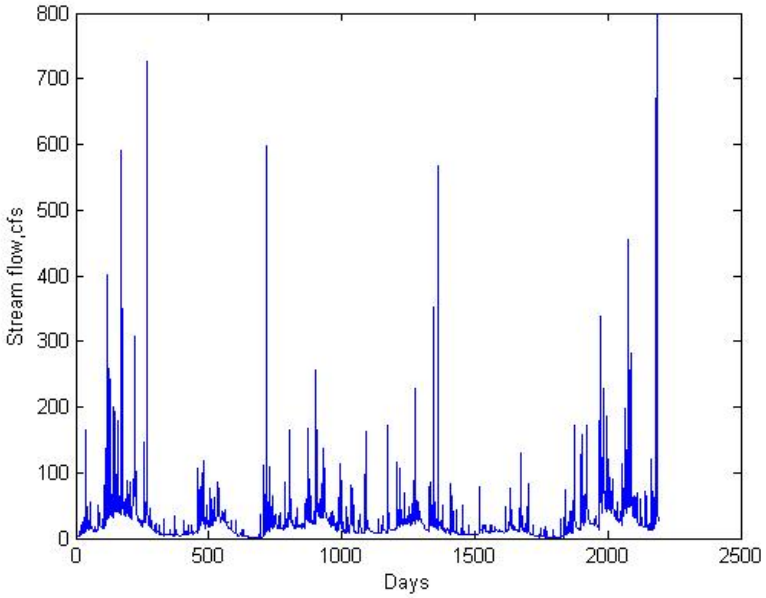


Figure B-28 Gage ID 1591700

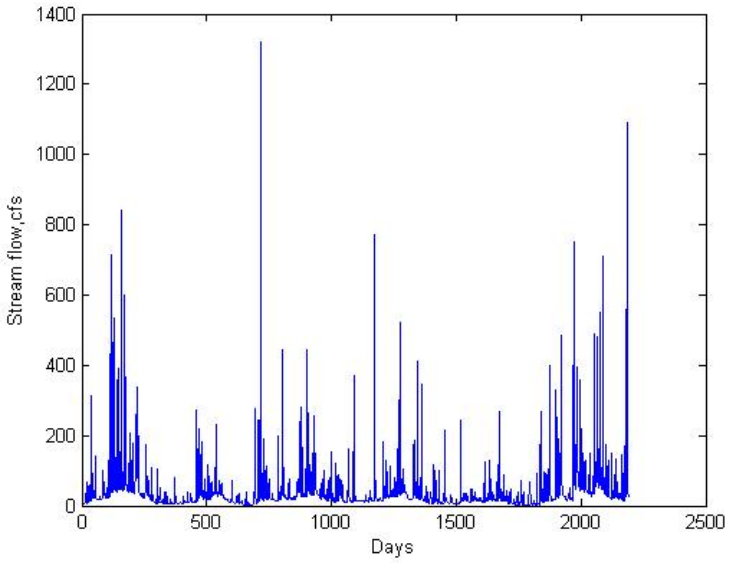


Figure B-29 Gage ID 1593500

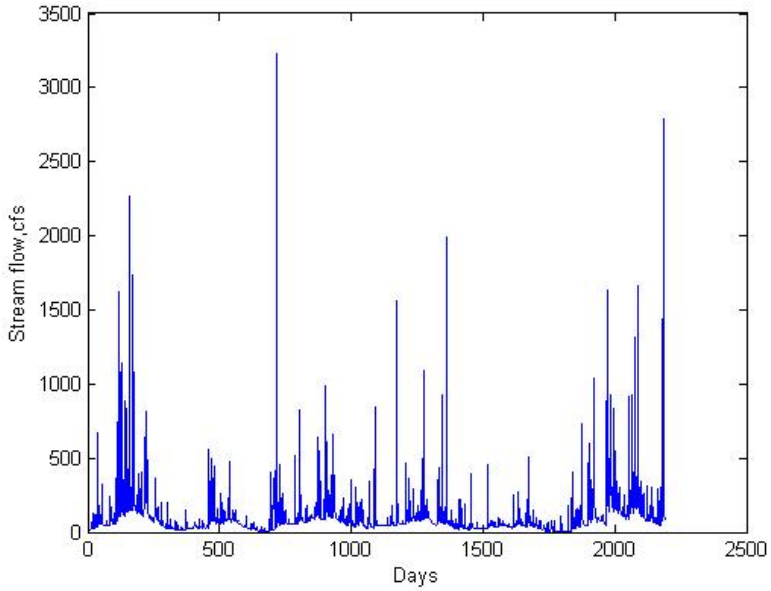


Figure B-30 Gage ID 1594000

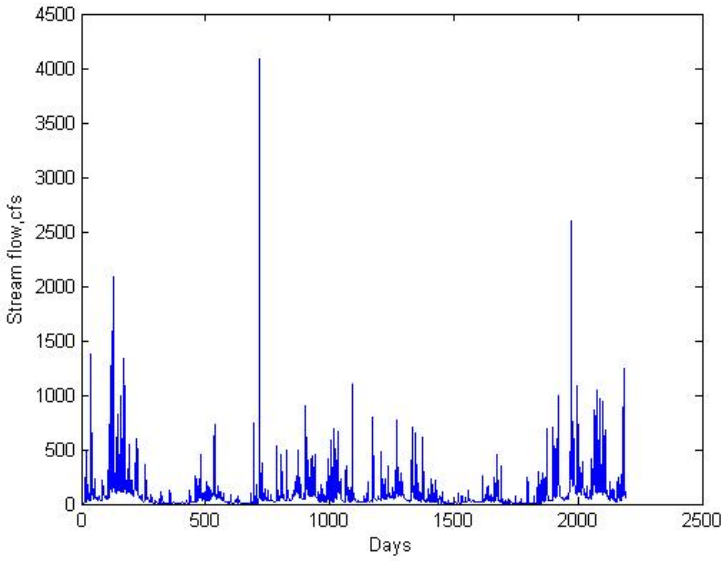


Figure B-31 Gage ID 1594526

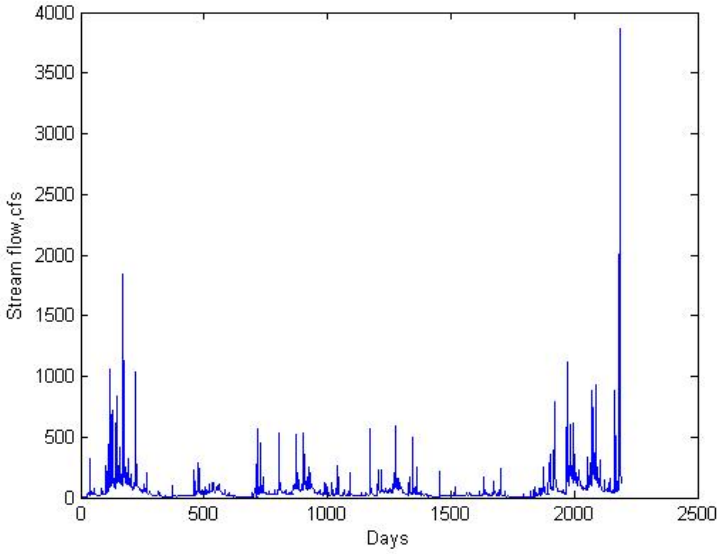


Figure B-32 Gage ID 1643500

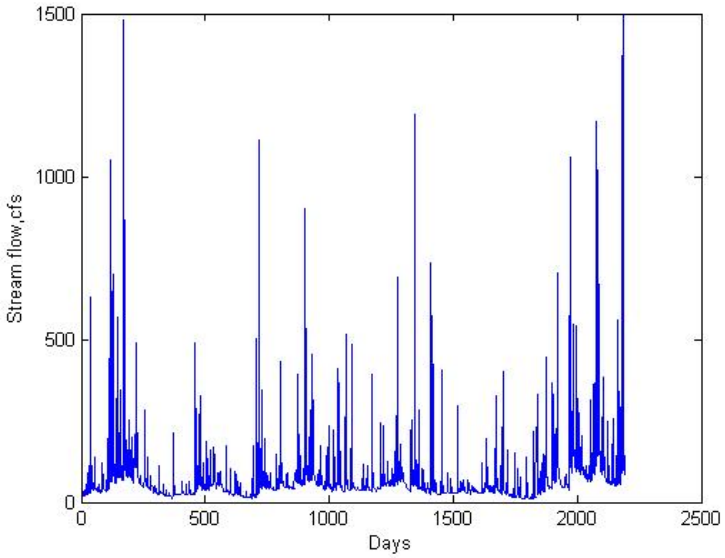


Figure B-33 Gage ID 1644600

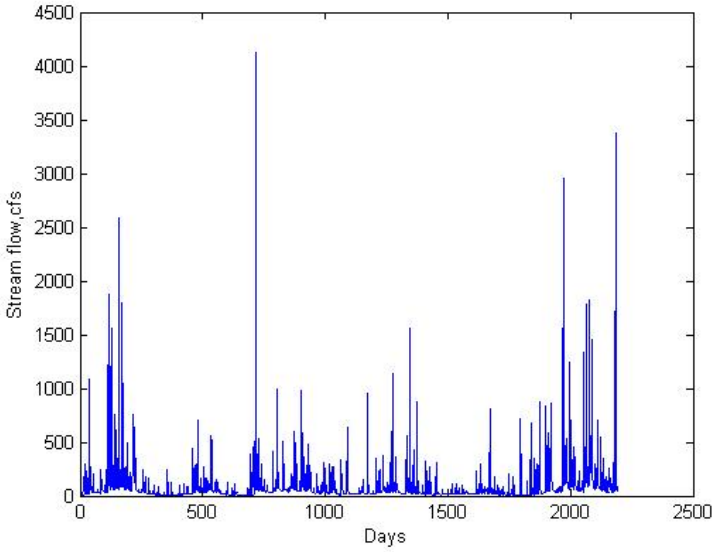


Figure B-34 Gage ID 1649500

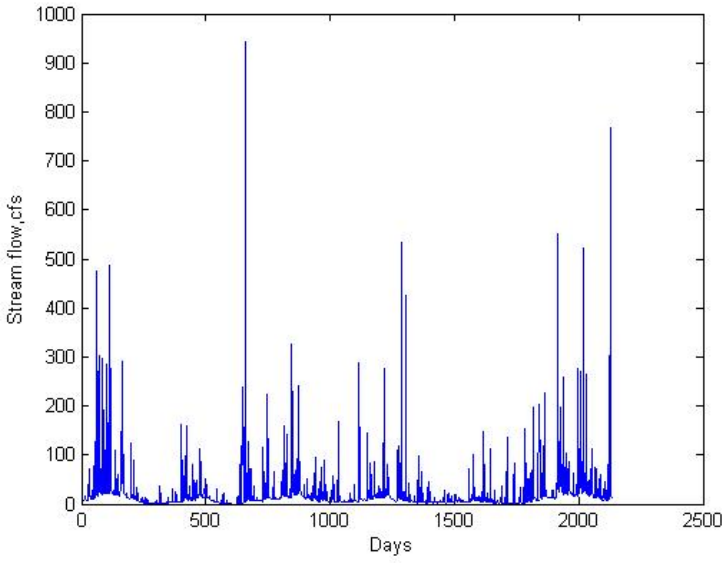


Figure B-35 Gage ID 1650500

# BIBLIOGRAPHY

Anderson, James R., Ernest E. Hardy, John T. Roach, and Richard E. Witmer, 1976. A land use and land cover classification system for use with remote sensor data. Washington, D.C.: U.S. Government Printing Office.

Arnold, Jr., C. L. and C. J. Gibbons, 1996. Impervious surface coverage: the emergence of a key environmental indicator. Journal of the American Planning Association 62(2):243-258.

Archer, David and Malcolm Newson, 2002. The use of indices of flow variability in assessing the hydrological and instream habitat impacts of upland afforestation and drainage. Journal of hydrology 268 (1):244-258.

Awasthi, K.D., B.K. Sitaula, B.R. Singh, and R.M.Bajacharaya, 2002. Land-use change in two Nepalese watersheds: GIS and geomorphometric analysis. Land Degradation & development 13:495-513.

Ayyub, Bilal and Richard McCuen, 2003. Probability, Statistics, and Reliability for Engineers and Scientists. CHAMPMAN and hall/CRC, A CRC Press Company, NY.

Baker, David B., R. Peter Richards, Timothy T. Loftus, and Jack W. Kramer, 2004. A new flashiness index: characteristics and applications to Midwestern rivers and streams. JAWRA 40(2):503-522.

Bartholow, J.M., 2000. Estimating cumulative effects of clearcutting on stream temperatures. Rivers 7(4):284-297.

Becciu, Gianfranco and Alessandro Paoletti, 2000. Moments of Runoff Coefficient and Peak Discharge Estimation in Urban Catchments. Journal of Hydrologic Engineering 5(2):197-205.

Beven, Keith J., 2001. Rainfall Runoff Modelling: The Primer. John Wiley & Sons, NY, USA.

Bhaduri, Budhendra, Marie Minner, Susan Tatalovich, and Jon Harbor, 2001. Long-term hydrologic impact of urbanization: a tale of two models. Journal of Water Resources Planning and Management 127(1) 13-19.

Bird, Sandra, Jim Harrison, Linda Exum, Stephen Alberty and Christine Perkins, 2002. Screening to Identify and Prevent Urban Storm Water Problems: Estimating Impervious Area Accurately and Inexpensively. In Proceedings for National Water Quality Monitoring Conference, May 20-23, 2002, Madison, WI.

Booth, Derek B., 1990. Stream-channel incision following drainage-basin urbanization. Water Resources Bulletin 26(3): 407-417.

Booth, Derek B., 2002. Forest cover, impervious-surface area, and the mitigation of stormwater impacts. Journal of the American Water Resources Association 38(3):835-845.

Brabec, Elizabeth, Stacey Schulte and Paul L. Richards, 2002. Impervious surfaces and water quality: A Review of current literature and its implications for watershed planning. Journal of Planning Literature 16(4):499-514.

Brun, S.E., L.E. Band, 2000. Simulating runoff behavior in an urbanizing watershed. Computers, Environment and Urban Systems. 24: 5-22.

Capiella, Karen and Kenneth Brown, 2001. Impervious cover and land use in the Chesapeake bay watershed. Center for Watershed Protection, Ellicot City, MD.

Carlson, Toby N. and S. Traci Arthur, 2000. The impact of land use-land cover changes due to urbanization on surface microclimate and hydrology: a satellite perspective. Global and Planetary Change 25:49-65.

Clausen, Bente, and Barry J.F.Biggs, 1997. Relationships between benthic biota and hydrological indices in New Zealand streams. Freshwater Biology 38:327-342.

Coutant, C., 1976. Thermal effects on fish ecology. Encyclopedia of environmental engineering, Vol. 2. W. & G. Baird, Ltd., Northern Ireland.

Corbett, Christopher W., Mattew Wahl, Dwayne E. Porter, Don Edwards, Claudia Moise, 1997. Nonpoint source runoff modeling a comparison of a forested watershed and an urban watershed on the South Carolina coast. Journal of Experimental Marine Biology and Ecology 213: 133-149.

Dougherty, Mark, Randel L. Dymond, Scott J. Goetz, and Normand Goulet, 2004. Evaluation of Impervious Surface Estimates in a Rapidly Urbanizing Watershed. Photogrammetric Engineering & Remote Sensing 70(11):1275-1284.

Dow, Charles L. and David R. DeWalle, 2000. Trend in evaporation and Bowen ratio on urbanizing watersheds in eastern United States. Water Resources Research 36(7): 1835-1843.

Finkenbine, J.K., J.W. Atwater, and D.S. Mavinic, 2000. Stream health after urbanization. Journal of the American Water Resources Association 36(5): 1149-1158.

Galli, J. 1990. Thermal impacts associated with urbanization and stormwater management best management practices. Mero. Wash. Counc. Gov., Maryland Dep. Environ. Washington, D.C. 188pp.

Goodrich, D. C. and W. G. Kepner, 2000. Landscape Indicator Interface with Hydrologic Models. EPA/600/R-00/042. U.S. Environmental Protection Agency, Office of Research and Development, Washington, D.C.

Hill, Joe. 2002. Evaluation of Rational Method "c" Values. San Diego County Hydrology Manual. Available at http://www.sdcounty.ca.gov/dpw/docs/evalcvalues.pdf

Homer, C., C. Huang, L. Yang, B. Wylie and M.Coan, 2004. Development of a 2001 national land-cover database for the United States. Photogrammetric Engineering and Remote Sensing 70 (7): 829-840.

James W. and Verspagen B.,1996. Thermal enhencement of stormwater by urban pavement. In Advances in Modelling the Management of Stormwater Impacts, vol5, ed. W. James. CHI, Canada.

Jennings, David, S.Taylor Jarnagin, 2002. Changes in anthropogenic impervious surfaces, precipitation and daily streamflow discharge: a historical perspective in a mid-Atlantic subwatershed. Landscape Ecology 17: 471-489.

Jennings, D., S.T. Jarnagin and D. Ebert. 2004. A modeling approach for determining watershed impervious surface area from National Land Cover Data 92. Photogrammetric Engineering and Remote Sensing 70(11):1295-1307.

Jenson, S.K. and J.O. Domingue, 1988. Extracting topographic structure from digital elevation data for geographic information system analysis. Photogrammetric Engineering and Remote Sensing 54(11):1593-1600.

Kauffman, Gerald J. and Tammy Brant, 2000. The Role of impervious cover as a watershed-based zoning tool to protect water quality in the Christina river basin of Delaware, Pennsylvania, and Maryland. Watershed Management Conference, Water Environment Federation.

Kaufman, Martin M. and William M. Marsh, 1997. Hydro-ecological implications of edge-cities. Landscape and Urban Planning 36:277-290.

Klein, R.D., 1979. Urbanization and stream quality impairment. Water Resources Bulletin. 15(4):948-963.

Krause, Colin W., Brendan Lockard, Tammy J. Newcomb, David Kibler, Vinod Lohani, and Donald J. Orth, 2004. Predicting influences of urban development on thermal habitat in a warm water stream. Journal of the American Water Resources Association 40(6): 1645-1658.

Larson, MG, DB Booth, and SA Morley, 2001. Effectiveness of large woody debris in stream rehabilitation projects in urban basins. Ecological Engineering 18(2):211-226.

Lee, Joong Gwang and James P. Heaney, 2003. Estimation of Urban Imperviousness and its Impacts on Storm Water Systems. Journal of Water Resources Planning and Management 129(5):419-426.

Limburg, Karin E. and Robert E. Schmidt, 1990. Patterns of fish spawning in Hudson river tributaries: Response to an urban gradient? Ecology 71(4):1238-1245.

McCuen, Richard H., 1993. Microcomputer applications in statistical hydrology. Prentice-Hall, New Jersey, U.S.A..

McCuen, Richard H., 1998. Hydrologic Analysis and Design, 2nd edition. Prentice Hall, New Jersey U.S.A.

McCuen, Richard H., 2003. Modeling Hydrologic Change: Statistical Methods. Lewis Publishers, NY, U.S.A.

MDP. Land use land cover. Maryland Department of Panning. Available at: http://www.mdp.state.md.us/zip_downloads_accept.htm. Accessed 2004.

Melesse, Assefa M., S.F.Shih, 2002. Spatially distributed storm runoff depth estimation using landsat images and GIS. Computers and Electronics in Agriculture 37: 173-183.

Melesse, Assefa M., Wendy D. Graham, Jonathan D. Jordan, 2003. Spatially distributed watershed mapping and modeling: GIS-based storm runoff response and hydrograph analysis: Part2 Journal of Spatial Hydrology 3(2).

Melesse, Assefa M., Wendy D. Graham, 2004. Storm Runoff Prediction Based on a Spatially Distributed Travel Time Method Utilizing Remote Sensing and GIS. Journal of the American Water Resources Association 40(4):863-879.

Mishra, Surendra Kumar, Vijay P. Singh, 1999. Another Look at SCS-CN Method, Journal of Hydrologic Engineering 4(3)257-264.

Mitchell, Sean, 1999. A simple model for estimating mean monthly stream temperatures after riparian canopy removal. Environmental Management 24(1):0077-0083.

Moglen, Glenn, 2000. Effect of orientation of spatially distributed curve numbers in runoff calculations. Journal of the American Water Resources Association 36(6) 1391-1400.

Moglen, Glenn, 2000. Urbanization, stream buffers, and stewardship in Maryland. Watershed protection Techniques, 3(2): 676-680.

Moglen, Glenn, and R.Edward Beighley, 2002. Spatially Explicit Hydrologic Modeling of Land Use Change. Journal of The American Water Resources Association 38(1) 241-253.

Moglen, Glenn, K.C. Nelson, M.A.Palmer, J.E. Pizzuto, C.E.Rogers, and M.I. Hejazi, 2004. "Hydro-Ecologic Responses to Land Use in Small Urbanizing Watersheds Within the Chesapeake Bay Watershed" in R.DeFries, G.Asner, and R.Houghton (eds.) Ecosystems and Land Use Change. Geophysical Monograph Series, American Geophysical Union, Washington, D.C. 153:41-60

Mohan, S., Madhav Narayan Shrestha, 2000. A GIS based integrated model for assessment of hydrological changes due to land use modifications. Proceedings of Restoration of Lakes and Wetlands Nov 27-29, Bangalore, India. Available at http://144.16.93.203/energy/water/proceed/section5/paper1/section5paper1.htm

Nelson, K.C., and M.A. Palmer, submitted. Stream temperature surges under urbanization and climate change: data, models, and response. JAWRA.

Newson, M.D. and C.L. Newson, 2000. Geomorphology, ecology, and river channel habitat: mesoscale approaches to basin-scale challenges. Prog. Phys. GEOGR. 24(2):195-217.

NRCS. NRI Information. Natural Resources Conservation Service. Available at: http://www.md.nrcs.usda.gov/technical/nritext.html Accessed 2004.

O'Brien Ed, 2005. Stormwater Management Manual for Western Washington: Volume I—Minimum Technical Requirements and Site Planning. Washington State Department of Ecology.

Old, Gareth H., Graham J.L. Leeks, John C. Packman, Barnaby P.G. Smith, Scott Lewis, Edward J. Hewitt, Matthew Holmes, and Andy Young, 2003. The impact of a convectional summer rainfall event on river flow and fine sediment transport in a highly urbanized catchment: Bradford, West Yorkshire. The Science of the Total Environment 314-316:495-512.

Palmer, M.A., G.E.Moglen, N.E. Bockstael, S. Brooks, J.E.Pizzuto, C.Weigand, and K.VanNess, 2002. The Ecological Consequences of Changing Land Use for Running Waters: the Suburban Maryland Case" in K.Krchnak (ed.) Human Population and Freshwater: Bulletin Series-Yale School of Foresty and Environmental Studies, Yale University Press 107:85-114.

Paul, Michael J. and Judy L. Meyer, 2001. Streams in the urban landscape. Annu. Rev. Ecol. Syst. 32:333-365.

Poff, N. LeRoy, David Allan, Mark B. Bain, James R. Karr, Karen L. Prestegaard, Brian D. Richter, Richard E. Sparks, and Julie C. Stromberg, 1997. The Natural flow regime. BioScience 47(11):769-784.

Rainis Ruslan, 2004. Estimating sediment yield using agricultural non-point sources (AGNPS) Model: the effects of slope information from different GIS software. Journal of Spatial Hydrology 4(2).

Richter, Brian D., Jeffrey V. Baumgartner, Jennifer Powell, and David P. Braun, 1996. A method for assessing hydrologic alteration within ecosystems. Conservation Biology. 10(4):1163-1174.

Rose, Seth and Norman E. Peters, 2001. Effects of urbanization on streamflow in the Atlanta area: a comprehensive hydrological approach. Hydrological processes 15:1441-1457.

Schueler, T.R., 1994. The importance of imperviousness. Watershed Protection Techniques 1(3):100-111.

Schueler, T.R., 1995. Site Planning for Urban Stream Protection, Chapter1: A Stream Protection Strategy. The Center for Watershed Protection. 18pp

Scholz, Jenna and Derek B. Booth, 2001. Monitoring urban streams: strategies and protocols for humid-region lowland systems. Environmental Monitoring and Assessment 71(2):143-64.

Scoggins, Matthew, 2000. Effects of hydrologic variability on biological assessments of streams in Austin, TX. Conference Proceedings, National Water Quality Monitoring Council.

SCS, 1985. National Engineering Handbook, Section 4: Hydrology. Soil Conservation Service, USDA.

SCS, 1986. Urban hydrology for small watersheds. USDA Soil Conservation Service Technical Release No. 55. Washington, D.C.

Shrestha, Madhav Narayan, 2003. Spatially distributed hydrological modelling considering land-use changes using remote sensing and GIS, Proceedings of Map Asia Conference.

Stewart, Patrick A, Michael T. Ritsche, and Douglas Krieger, 1999. Stormflow and Land Use Change: Low Density Development in the Ferson-Otter Creek Watershed. 1960-1996. American Farmland Trust Center for Agriculture in the Environment. DeKalb, Illinois. Working Paper CAE/WP99-3.

Stuebe, Miki, M., Johnston, Douglas M., 1990. Runoff volume estimation using GIS techniques. Water Resources Bulletin 26(4):611-620.
Sweeney, B.W., 1992. Streamside forests and the physical, chemical, and trophic characteristics of Piedment Streams in eastern North America. Water Science and Technology 26:2653-2673.

Sweeney, B.W., 1993. Effects of streamside vegetation on macroinvertebrat communities of White Clay Creek in Eastern North America. Proceedings of the Academy of Natural Sciences of Philadelphia 144:291-340.

Tan, C.H., A.M. Melesse, and S.S. Yeh, 2002. Remote Sensing and Geographic Information System in Runoff Coefficient Estimation in China Taipei. Proceedings of Asian Conference on Remote Sensing, November 25 – 29, Kathmandu, Nepal.

U.S. EPA, 1997. Urbanization and streams: studies of hydrologic impacts. EPA841-R-97-009, U.S. Environmental Protection Agency, Washington, D.C.

USGS (a). National Land Cover Dataset 2001(NLCD). U.S. Geological Survey. Available at: http://seamless.usgs.gov/website/seamless/products/nlcd01.asp Accessed 2004.

USGS (b). Daily streamflow for the Nation. U.S. Geological Survey. Available at http://nwis.waterdata.usgs.gov/usa/nwis/discharge. Accessed 2004.

Van Buren M.A., W.E.WATT, J. Marsalek, B.C. Anderson 2000. Thermal enhancement of stormwater runoff by paved surfaces. Wat. Res 34(4):1359-1371.

Vieux, Baxter, 2001. Water science and technology library: distributed hydrologic modeling using GIS. Kluwer Academic Publishers, Boston.

Vought, L.B.-M., A. Kullberg and R.C. Petersen, 1998. Effect of riparian structure, temperature and channel morphometry on Detritus processing in channelized and natural woodland steams in Southern Sweden. Aquatic Conservation: Marine and Freshwater Ecosystems 8:273-285.

Weng, Qihao, 2001. Modeling Urban Growth Effects on Surface Runoff with the Integration of Remote Sensing and GIS. Environmental Management 28(6): 737-748.

Wood, E. F., M. Sivapalan, K. Beven, and L. Band, 1988. Effects of spatial variability and scale with implications to hydrologic modeling. Journal of Hydrology, 102: 29-47.

Yang, Limin, Chengquan Huang, Collin G. Homer, Bruce K Wylie, Michael J. Coan, 2003. An approach for mapping large- area impervious surfaces: synergistic use of Landsat 7 ETM+ and high spatial resolution imagery. Canadian Journal of Remote Sensing 29(2);230-240.

Yeager, Matt and Xavier Swamikannu, 2001. Technical report: Mitigation of storm water impacts from new development in environmentally sensitive areas. California Regional Water Quality Control Board, Los Angeles Region, California.